ELSEVIER INSIGHTS

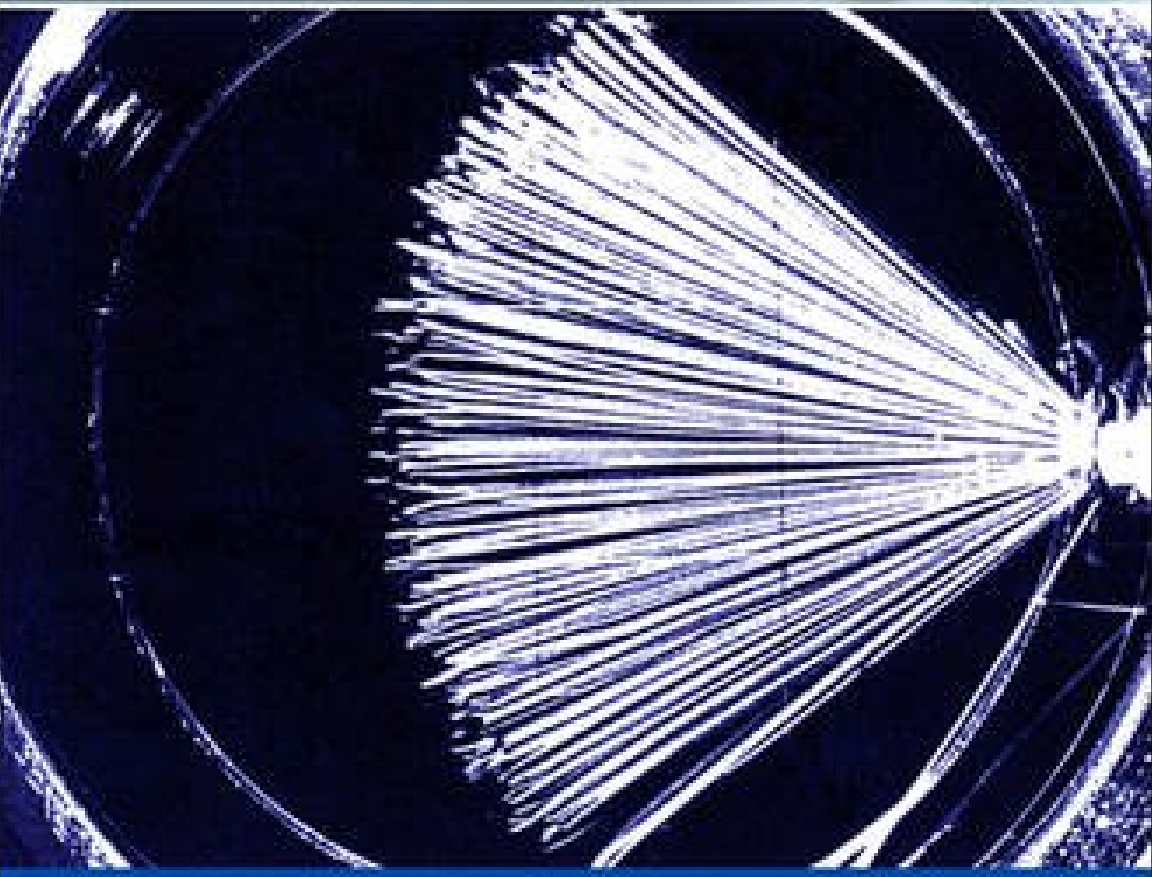

NUCLEAR AND RADIOCHEMISTRY

JÓZSEF KÓNYA • NOÉMI M. NAGY

Nuclear and Radiochemistry

Nuclear and Radiochemistry

József Kónya and Noémi M. Nagy
Isotope Laboratory, Department of Colloid and Environmental Chemistry
University of Debrecen
Debrecen, Hungary

AMSTERDAM • BOSTON • HEIDELBERG • LONDON • NEW YORK • OXFORD
PARIS • SAN DIEGO • SAN FRANCISCO • SINGAPORE • SYDNEY • TOKYO

Elsevier
32 Jamestown Road, London NW1 7BY
225 Wyman Street, Waltham, MA 02451, USA

First edition 2012

Notices
Knowledge and best practice in this field are constantly changing. As new research and experience broaden our understanding, changes in research methods, professional practices, or medical treatment may become necessary.

Practitioners and researchers must always rely on their own experience and knowledge in evaluating and using any information, methods, compounds, or experiments described herein. In using such information or methods they should be mindful of their own safety and the safety of others, including parties for whom they have a professional responsibility.

To the fullest extent of the law, neither the Publisher nor the authors, contributors, or editors, assume any liability for any injury and/or damage to persons or property as a matter of products liability, negligence or otherwise, or from any use or operation of any methods, products, instructions, or ideas contained in the material herein.

British Library Cataloguing-in-Publication Data
A catalogue record for this book is available from the British Library

Library of Congress Cataloging-in-Publication Data
A catalog record for this book is available from the Library of Congress

ISBN: 978-0-12-391430-9

Contents

Preface

This book aims to provide the reader with a detailed description of the basic principles and applications of nuclear and radiochemistry. Its content is based on the authors' more than 50 and 25 years of experience, respectively, as professors of nuclear and radiochemistry at both the B.Sc. and M.Sc. levels in the Isotope Laboratory of the Department of Colloid and Environmental Chemistry at the University of Debrecen, Hungary.

Although the book contains all modern aspects of nuclear and radiochemistry, it still has a characteristic local flavor. Special attention is paid to the thermodynamics of radioisotope tracer methods and to the very diluted systems (carrier-free radioactive isotopes), to the principles of chemical processes with unsealed radioactive sources, and to the physical and mathematical aspects of radiochemistry. This approach originates from the first professor of the Isotope Laboratory, Lajos Imre, who himself was Otto Hahn's disciple and coworker.

The material is divided into 14 chapters. Chapters 1−6 discuss the basic concepts of nuclear and radiochemistry and Chapters 7−14 deal with the applications of radioactivity and nuclear processes. There are separate chapters dedicated to the main branches of modern radiochemistry: nuclear medicine and nuclear power plants, including the problems of the disposal of nuclear wastes. One chapter (Chapter 10) deals with nuclear analysis (both bulk and surface analyses), including the analytical methods based on the interactions of radiation with matter.

As mentioned previously, the authors have extensive experience in teaching nuclear and radiochemistry. Therefore, we have had the chance to work with many exceptional students and excellent colleagues. Many thanks for their contributions. We are grateful for their assistance in the improvement of our educational work and the useful discussions that helped to advance our understanding in this field.

We thank our colleagues who have contributed to this book, namely, Dr. Lajos Baranyai (Chapter 11 and Section 8.7) and Dr. József Varga (Chapter 12). Many thanks to Dr. Szabolcs Vass and Dr. József Kónya (a physician and an associate professor) for their assistance in the fields of neutron diffraction and the biological effects of radiation, respectively. Thanks also to those colleagues, namely, Prof. László Bartha, Prof. Dezső Beke, Dr. István Csige, Prof. Julius Csikai, Prof. Béla Kanyár, Dr. Anikó Kerkápoly, Dr. Zsófia Kertész, Dr. Péter Kovács-Pálffy, Dr. László Kövér, Prof. Ernő Kuzmann, Boglárka Makai, Katalin Nagy, Zoltán Nemes, Dr. Katalin Papp, Dr. Péter Raics, Dr. Zsolt Révay, Dr. László Szentmiklósi, Dr. Edit Szilágyi, Dr. Nóra Vajda, who have provided excellent representative photographs, figures, data, and so on. Prof. Julius Csikai provided the beautiful photograph

on the book cover. Thanks to Zoltán Major for the improvement of the quality of the photograph.

We thank Dr. Klára Kónya for the critical reading of the manuscript and for her remarks and corrections.

The work is supported by the TÁMOP 4.2.1./B-09/1/KONV-2010-0007 project. The project is cofinanced by the European Union and the European Social Fund.

We recommend this book to students in chemistry, chemical engineering, environmental sciences, and specialists working with radiochemistry in industry, agriculture, geology, medicine, physics, analytics, and to those in other fields.

József Kónya and Noémi M. Nagy
December 2011, Debrecen (Hungary)

1 Introduction

From the dawn of natural sciences, scientists and philosophers have reflected on the nature of matter. In the end of the nineteenth century, the discoveries signed by Lavoisier, Dalton, and Avogadro (namely, the law of conservation of mass, the atomic theory, and the definition of a mole as a unit of the chemical quantity) led to a plausible model. This model was built on the principles of Dalton's atomic theory, which states that:

- all matter is composed of small particles called atoms,
- each element is composed of only one chemically distinct type of atom,
- that all atoms of an element are identical, with the same mass, size, and chemical behavior, and
- that atoms are tiny, indivisible, and indestructible particles.

In the same period, the basic laws of thermodynamics have been postulated. The first law of thermodynamics is an expression of the principle of conservation of energy.

This model of the matter has been challenged when it was discovered that the same element can have radioactive and stable forms (i.e., an element can have atoms of different mass). The discovery of the radioactivity is linked to Henri Becquerel's name and to the outcome of his experiments which were presented in 1896 at the conference of the French Academy and published in *Comptes Rendus e l'Académie des Sciences*.

Following his family tradition (his father and grandfather also studied fluorescence, and his father, Edmund Becquerel, studied the fluorescence of uranium salts), Becquerel examined the fluorescent properties of potassium uranyl sulfate [$K_2UO_2(SO_4)_2 \cdot 2H_2O$]. Since Wilhelm Röntgen's previous studies, it has been known that X-rays can be followed by phosphorescent light emitted by the wall of the X-ray tube, and Becquerel wanted to see if this process could be reversed, i.e., if phosphorescent light can produce X-rays. After exposing potassium uranyl sulfate to sunlight, he wrapped it in black paper, placed it on a photographic plate, and observed the "X-ray." He repeated the experiments with and without exposure to sunlight and obtained the same result: the blackening of the photographic plate. He has concluded that the blackening of the photographic plate was not caused by fluorescence induced by sunlight, but rather by an intrinsic property of the uranium salt. This property was first called Becquerel rays, and later it was termed

Nuclear and Radiochemistry. DOI: http://dx.doi.org/10.1016/B978-0-12-391430-9.00001-9

"radioactive radiation[1]." Becquerel also has observed that electroscope loses its charge under the effect of this radiation because the radiation induces charges in the air.

The same radiation was observed by Pierre Curie and Marie Curie, as well as G. Schmidt in Germany using thorium salts. They have found that the ores of uranium and thorium have more intense radiation than the pure salts: for example, pitchblende from Johanngeorgenstadt and Joachimstal has about five and four times more intense radiation, respectively, than black uranium oxide (U_3O_8). This more intense radiation originates from elements that were not present in the pure salts, which later were identified as the new radioactive elements polonium and radium, and which were separated from uranium ore in Joachimstal. The Curies presented the results at the French Academy in 1898 and published in *Comptes Rendus e l'Académie des Sciences.* As proposed by Marie Curie, the first new radioactive element, polonium, was named after her homeland of Poland. In the Curies' laboratory, radioactivity was detected by the ionization current produced by the radiation. In 1902, the Curies produced 100 mg of radium and determined the atomic mass, which they later corrected (226.5 g/mol). Marie Curie produced metallic radium by electrolysis of molten salts in 1910.

Rutherford has differentiated three types of radiation (alpha, beta, and gamma) by using absorption experiments in 1889. He also determined that the radiations had very high energy. In 1903, Rutherford and Soddy concluded that the radioactive elements are undergoing spontaneous transformation from one chemical atom into another and that the radioactive radiation was an accompaniment of these transitions. Radioactive elements were called radioelements. Since they were not known earlier, and therefore did not have names, some of them were named by adding letters to the name of the original (i.e., parent) element (e.g., UX, ThX). Others were given new names (such as radium, polonium, radium emanation-today radon).

The discovery of radium and polonium filled two empty places on the periodic table. Later studies, however, showed that some radioactive elements had the same chemical properties as known stable elements—they differed only in the amount of radioactivity. Therefore, they should be put in places in the periodic table that are already filled, which is impossible according to Dalton's atomic theory. For example, different types of thorium (thorium, UX1, iononium (Io), radioactinium, today Th-232, Th-234, Th-230, and Th-227, respectively) and radium (radium, mesothorium1, ThX, AcX, today Ra-226, Ra-228, Ra-224, or Ra-223, respectively) atoms have been recognized.

These experimental results presented serious contractions to the Daltonian model of matter and the principle of the conservation of mass and energy. Einstein

[1] In 1867, Niepce de Saint-Victor showed that uranium salts emit radiations in the dark, but Becquerel rejected this saying that "Niepce could not have observed the radiation from uranium because the author used plates that were not sensitive enough."

has solved part of these contradictions using the law of the equivalence of energy and mass:

$$E = mc^2 \tag{1.1}$$

where E is the energy of the system, m is the mass, and c means the velocity of light in a vacuum.

As the interpretation of the other part of the contradictions, Soddy defined the term "isotopes," neglecting the postulate in Dalton's theory on the identity of the atoms of an element. Accordingly, isotopes are atoms of the same element having different masses.

What kind of scientific and practical importance did these discoveries have? At first, they formed the basis of the modern atomic theory, resulting in the development of new fields and explaining some phenomena. For example, nucleogenesis, the formation of the elements in the universe, now can be explained based on the principles of natural sciences, attempting to give a philosophical significance of the "creation."

From the beginning, the practical importance has been underestimated. In 1898, however, radium found its role in cancer therapy. In 1933 in the Royal Society meeting, Rutherford said that "any talk of atomic energy" was "moonshine." Rutherford's statement inspired Leo Szilárd to devise the principle of the nuclear chain reaction, which was experimentally discovered by Otto Hahn in 1938. The chain reaction of uranium fission led to the production of nuclear power plants, and, unfortunately, nuclear weapons as well. However, in the future, the production of cheap, safe atomic energy can play a significant role in supplying energy.

As the practical applications of radioactivity, tracer methods, activation analysis, nuclear medicine, and radiation therapy can be mentioned. As mentioned previously, radioactivity has been discovered to be a natural process. Therefore, it is not an artificial product as believed by many. The environmental radioactive isotopes can be classified into three groups:

1. The members of three natural decay series starting with ^{238}U, ^{235}U, and ^{232}Th isotopes. From an environmental point of view, the members with relatively long half-lives are important, for example, ^{226}Ra and its daughter elements, ^{222}Rn, ^{210}Pb, ^{210}Bi, ^{210}Po from the decay series of ^{238}U and ^{220}Rn from the thorium series.
2. Long-life nuclei produced during nucleogenesis, for example, ^{40}K, ^{50}V, ^{87}Rb, ^{113}Cd, ^{115}In, ^{123}Te, ^{138}La, ^{144}Nd, ^{147,148}Sm, ^{152}Gd, ^{156}Dy, ^{174}Hf, ^{176}Lu, ^{186}Os, ^{187}Re, ^{190}Pt.
3. Natural radioactive isotopes continuously producing in the nuclear reactions of the atoms of air (nitrogen, oxygen, argon) with cosmic radiation, for example, ^{3}H, ^{7,10}Be, ^{14}C, ^{22}Na, ^{26}Al, ^{32,33}P, ^{35}S, ^{36}Cl, ^{39}Ar.

As previously discussed, many of these elements have naturally occurring radioactive isotopes.

The main stages of the history of nuclear science are summarized in Table 1.1, including the Nobel prizes gained by the scientists working in this field. In addition, the chapters of this book related to the given stages are also listed.

Table 1.1 History of Nuclear Science

Year	Discovery	Researcher(s)/county(ies)	Nobel Prize	In This Book
1895	X-ray	W. Röntgen	1901	This chapter
1896	Radioactivity by the radiation of uranium salt	H. Becquerel	1903	This chapter
1898	Polonium and radium	P. and M. Curie	1903	This chapter
1899	Radioactivity is caused by the decomposition of atoms	J. Elster and H. Geitel		This chapter
1900	Gamma radiation is considered as electromagnetic radiation	P. Villard and H. Becquerel, proved in 1914 by E. Rutherford and E. Andrade		Section 4.6 in Chapter 4
1900	Beta decay consists of electrons	H. Becquerel		Section 4.2 in Chapter 4
1902	Preparation of radium	P. and M. Curie, Debierne	1911	This chapter
1903	Alpha radiation consists of the ions of helium	E. Rutherford	1908	Section 4.1 in Chapter 4
1903	Radon (radium emanation)	W. Ramsay and F. Soddy	1904	Section 4.2, Section 8.5.1
1898−1902	Radiation has chemical and biological effects	P. Curie, A. Debierne, H. Becquerel, H. Danlos, and others		Section 13.4
1896−1905	Genetic relation of the radioelements	H. Becquerel, E. Rutherford, F. Soddy, B. Boltwood, and others		Section 4.2
1905	Equivalence of energy and mass	A. Einstein		This chapter
1907	Therapeutic application of radium	T. Stenbeck		Section 8.5.1
1909	Alpha scattering experiments: discovery of nucleus	H. Geiger and E. Mardsen		Section 5.2.2
1909	Terms of isotopes	F. Soddy	1921	Chapter 3

1910	Determination of atomic mass by deviation in electric and magnetic field	J.J. Thomson		Section 3.1.1
1911	Rutherford's atomic model	E. Rutherford		Section 2.1.1, Section 5.2.2
1912	Radioactive indication	G. Hevesy and F. Paneth	1943	Chapters 8–12
1912	Cloud chamber	C.T. Wilson	1927	Section 14.5.1
1913	Cosmic radiation	V.F. Hess	1936	Section 2.2, Section 13.4.3
1913	Interpretation of the decay series by using isotopes	K. Fajans and F. Soddy		Section 4.2
1913	Separation of neon isotopes using the deviation in electric and magnetic field	F.W. Aston	1922	Section 3.1.1
1913	Nucleus is surrounded by electrons moving on orbitals with well-determined energy	N. Bohr	1922	
1913	Determination of the size and charge of atomic nuclei	H. Geiger and E. Mardsen		Section 2.1.1, Section 5.2.2
1913	Counter for radioactivity measurement	H. Geiger		Section 14.1
1919	The first nuclear reaction: $^{4}He + {}^{14}N \rightarrow {}^{17}O + {}^{1}H$	E. Rutherford		Chapter 6
1919	Mass spectrometer	F.W. Aston	1922	Section 3.1.1
1921	Isomer nuclei: $^{234m}Pa(UX_2)^{234}Pa(UZ)$	O. Hahn		Section 4.4.6
1921	Separation of isotopes by distillation	J.N. Brönsted and G. Hevesy		Section 3.2
1923	Inelastic scattering of gamma photons	A.H. Compton	1927	Section 5.4.3
1924	Wave-particle duality of moving particles	L. De Broglie		Section 4.4.1, Section 5.5.3, Section 6.1, Section 10.2.2.4
1924	The radioactive tracer (Po) in biological research	A. Lacassagne and J.S. Lates		Section 8.5.1
1925	The exclusion principle	W. Pauli	1945	Section 2.3
1926	Wave mechanics in quantum theory	E. Schrödinger	1933	Section 4.4.1

(*Continued*)

Table 1.1 (Continued)

Year	Discovery	Researcher(s)/county(ies)	Nobel Prize	In This Book
1927	Experimental confirmation of the wave-particle duality	C.J. Davisson, L.H. Germer, and G.P. Thomson		Section 4.4.1
1927	The uncertainty principle	W. Heisenberg	1932	Section 2.1.1
1928	The Geiger–Müller counter	H. Geiger and W. Müller		Section 14.1
1931	A high-voltage generator for acceleration of ions	R.J. Van de Graaf		Section 6.2.3
1932	Cyclotron	E. Lawrence and M.S. Livingston		Section 6.2.3, Section 8.5.2
1932	Deuterium; isotope enrichment by evaporation of liquid hydrogen	H. Urey	1934	Chapter 3.2
1932	Neutron	J. Chadwick	1935	Section 2.1, Section 5.5.3
1932	Nucleus: protons + neutrons	W. Heisenberg		Section 2.1
1932	Positron	C.D. Andersson	1936	Section 4.2.2
1932	Nuclear reactions with accelerated charged particles	J.D. Cockcroft and E.D.S. Walton	1951	Section 6.2.3
1933	Isotopic effects in chemical reactions	H. Urey and D. Rittenberg		Sections 3.1.4 and 3.1.5
1933	Pair formation	I. Curie and F. Joliot-Curie		Section 5.4.5
1933	Magnetic momentum of proton	O. Stern	1943	Section 2.3
1931–1933	Nuclear studies by improved cloud chamber	P.M.S. Blackett	1948	Section 14.5.1
1931–1937	Symmetry principles of the nucleus	E.P. Wigner	1963	Section 2.3

1934	Annihilation	M. Thibaud and F. Joliot-Curie	Section 5.3.3
1934	Artificial radioactivity: $^{4}He + {}^{27}Al \rightarrow {}^{30}P + n$	F. Joliot-Curie and I. Curie	1935 Chapter 6
1934	Discovery of Cherenkov radiation	P.A. Cserenkov, I.M. Frank, and I.E. Tamm	1958 Section 5.3.2
1935	Postulation of mesons	H. Yukawa	1949 Section 2.2
1935	Semiempirical formula for the binding energy of nuclei	C.F. Weizsäcker	Section 2.5.1
1935–1936	Description of nuclear reactions with neutrons	E. Fermi	1938 Section 6.2.1
1936	Neutron activation analysis (NAA)	G. Hevesy and H. Levi	Section 10.2.2.1
1937	Principle of Cherenkov radiation	P.A. Cserenkov, I.M. Frank, and I.E. Tamm	1958 Section 5.3.2
1937	Technetium	G. Perrier and E. Segre	
1937	μ-Mesons in cosmic radiation	S. Neddermeyer and C.D. Andersson	Section 2.2
1938	Theory of nuclear fusion in stars	H.A. Bethe and C.F. Weizsäcker	1967 Section 6.2.5
1938	Fission of uranium using neutrons	O. Hahn and F. Strassman	1944 Section 6.2.1
1938	Photomultiplier	Z. Bay	Section 14.2.2
1930–1939	Magnetic properties of nucleus	I.I. Rabi	1944 Section 2.3
1940	First transuranium elements—neptunium and plutonium; chemistry of the transuranium elements; fission of plutonium-239 using neutrons	E.M. McMillan, G.T. Seaborg	1951 Section 6.2.6; the production of the additional transuranium elements are summarized in Table 6.3
1940	Fission of ^{235}U by thermal neutrons; ^{232}Th and ^{238}U by fast neutrons produce two to three new neutrons and release a high amount of energy		Section 6.2.1
1942	First nuclear reactor	E. Fermi and coworkers	Section 7.1.3
1944	Self-sustaining fission of uranium	Germany	Section 7.1

(*Continued*)

Table 1.1 (Continued)

Year	Discovery	Researcher(s)/county(ies)	Nobel Prize	In This Book
1945	Production of plutonium in kilograms. Application of nuclear weapons by the United States	Japan (Hiroshima, Nagasaki)		Section 7.5
1946−1948	Magnetic momentum of the nucleus	F. Bloch and E.M. Purcell	1952	Section 2.3
1949	Radiocarbon dating	W. Libby	1960	Section 4.3.6
1950	Shell model of nuclei	M.G. Mayer, O. Haxel, J.H.D. Jensen, and H.E. Suess	1963	Section 2.5.2
1951	First breeder and energy production reactor	Argonne National Laboratory (Idaho, USA)		Section 7.1
1951	Positronium atom	M. Deutsch		Section 5.3.3
1951	Application of Co-60 in therapy of cancer			Chapter 12
1951	Measurement of the time less than 10^{-6} s of the excited state in the nucleus by scintillation counter			
1952	Bubble chamber	D.A. Glaser	1960	Section 14.5.1
1952	The first uncontrolled fusion reaction (hydrogen bomb)	United States		Section 7.5
1952	The first atomic bomb experiment by Great Britain	Australia		Section 7.5
1953	Collective motion of the nucleons in the nucleus	A.N. Bohr, B.R. Mattelson, and L.J. Rainwater	1975	Section 2.5.3

1953	The first atomic bomb experiment by Soviet Union	Soviet Union		Section 7.5
1953	Establishment of European Organization of Nuclear Research (CERN)	Twelve countries		
1953–1955	Unified nuclear model	A. Bohr, B.R. Mottelson, and S.G. Nilsson		Section 2.5.3
1953–1960	Electron scattering on the nucleus	R. Hofstadter	1961	Section 10.2.1
1953–1960	Experimental detection of neutrinos	F. Reines	1995	Section 4.4.2
1954–1958	Electron spectroscopy	K.M. Siegbahn	1981	Section 10.2.1
1955	Nuclear-powered submarine (*Nautilus*)			
1954–1956	5 MWe energy production reactor in Obnyiszkban	Soviet Union		Chapter 7
1955–1960	Neutron spectroscopy and diffraction	B.N. Brockhouse C.G. Shull	1994	Section 5.5.3, Section 10.2.2.4
1956	45 MWe energy production reactor in Calder Hallban	Great Britain		Chapter 7
1956–1965	Nucleogenesis: formation of elements in the universe	S. Chandrasekhar W.A. Fowler	1983	Section 6.2
1958	Discovery of the Mössbauer effect	R. Mössbauer	1961	Section 5.4.7
1959	Radioimmunoassay (RIA): determination of peptide hormones	R.S. Yalow	1977	Section 12.3.1
1959	The first civilian nuclear-powered ship (the Lenin icebreaker)	Soviet Union		
1960	The first atomic bomb experiment by France	Algeria		Section 7.5
1960–1965	Classification of elementary particles	M. Gell-Mann	1969	Section 2.4
1961	Invention of ^{238}Pu-powered satellite (Transit-4A)			
1961	Semiconductor detectors			Section 14.3
1964	The first atomic bomb experiment by China	China		Section 7.5

(*Continued*)

Table 1.1 (Continued)

Year	Discovery	Researcher(s)/county(ies)	Nobel Prize	In This Book
1969	Plasma with high density in Tokamak fusion reactor	Soviet Union		Section 7.4
1974	The first atomic bomb experiment by India	India		Section 7.5
1974	Discovery of ancient natural nuclear reactor in Oklo (Gabon)	French scientists		Section 7.1.2
1976	SI-compatible-dose units (gray and sievert)	IUPAC		Section 13.4.1
1979	Accident at the Three Mile Island nuclear power plant	PA, USA		Section 7.2
1979?	The first atomic bomb experiment by Israel?			Section 7.5
1986	Accident at the Chernobyl nuclear power plant	Chernobyl, Soviet Union		Section 7.2
1998	The first atomic bomb experiment by Pakistan	Pakistan		Section 7.5
2006	The first atomic bomb experiment by North Korea	North Korea		Section 7.5
2011	Accident at the Fukushima nuclear power plant	Fukushima, Japan		Section 7.2

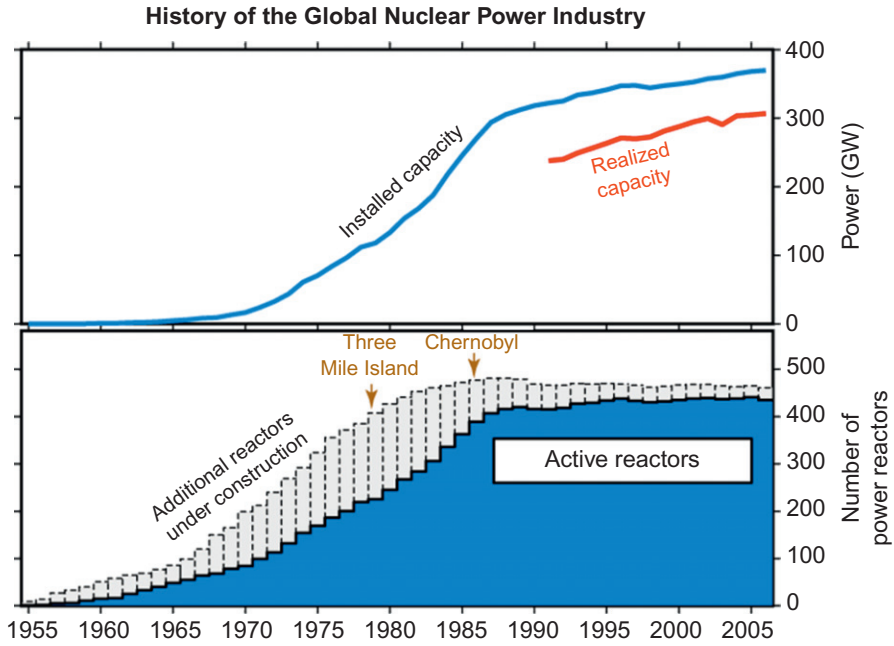

Figure 1.1 History of the use of nuclear power (top) and the number of active nuclear power plants (bottom).
Source: Free documentation from http://en.wikipedia.org/wiki/Nuclear_power.

In Table 1.1, the time of the experimental nuclear explosions by different countries is also mentioned. The useful applications of nuclear energy can be indicated by the increase in the capacity and number of nuclear power plants, as shown in Figure 1.1.

Further Reading

Becquerel, H. (1896). Sur les Radiations Invisibles Emises par les Corps Phosphorescents. *Comptes Rendus Acad. Sci. Paris* 122:501−503.
Curie, M. (1898). Rayons Émis par les Composes de l'Uranium et du Thorium. *Comptes Rendus Acad. Sci. Paris* 126:1101−1103.
Curie, P. and Sklodowska-Curie, M. (1898). Sur une Nouvelle Substance Radioactive Contenu dans la Pechblende. *Comptes Rendus Acad. Sci. Paris* 127:175−178.
Vroman, R., 2003. List of states with nuclear weapons. <http:/en.wikipedia.org/wiki/List_of_states_with_nuclear_weapons.> (accessed 28.03.12.)
Trelvis, 2002. Nuclear power. <http://en.wikipedia.org/wiki/Nuclear_power.> (accessed 28.03.12.).
Atomarchive.com, 1998−2011. <http://www.atomicarchive.com/Bios/Szilard.shtml.> (accessed 28.03.12.)
Hanh, O. (1962). *Vom Radiothor zur Uranspalzung*. Friedrich Vieweg & Sohn, Braunschweig.
Haissinsky, M. (1964). *Nuclear Chemistry and its Applications*. Addison-Wesley, Reading, MA.
Le Bon, G. (1912). *L'évolution de la matière*. Flammarion, Paris.
Stein, W. (1958). *Kulturfahrplan*. F.A. Herbig Verlangbuchhandlung, Berlin.

2 Basic Concepts

2.1 Atomic Nuclei

2.1.1 Components of Nuclei

The atomic nuclei were discovered by the English physicist Ernest Rutherford on the basis of Ernest Mardsen's experiments (Figure 2.1). In their experiments, Mardsen and Hans Geiger studied the backscattering of alpha rays (which were known to be positively charged) from a gold plate and observed that a very small portion of these particles (about 1 in 100,000) were scattered back at an angle of 180°. Since the backscattering of the positive alpha particles is directed by electrostatic forces, this is possible only if a very high portion of the positive charge of the atom is concentrated in very little volume. This small component of the atom is the atomic nucleus. The backscattered portion of the alpha particles indicates that the radius of the nucleus is about 10^5 times smaller than the radius of the atom.

In addition to the positive charge, the mass of the atom is concentrated in the nucleus. The radius of the atomic nuclei (R) can be expressed approximately by Eq. (2.1):

$$R = R_0 \times A^{1/3} \tag{2.1}$$

where A is the mass number and R_0 is the radius of the nucleus of the hydrogen atom ($\sim 1.3 \times 10^{-15}$ m). As a consequence of Eq. (2.1), the density of any atomic nucleus is approximately the same ($\rho = 2 \times 10^{17}$ kg/m^3), independent of the identity of the atoms. The mass of the nucleus is evenly distributed in the nucleus. This density then decreases quite abruptly to reach the density of the electron shell (which is very small—practically zero) at a distance of about 2.5×10^{-15} m from the nucleus. Similarly, the charge density surrounding the nucleus decreases over the same distance to reach the charge density of the electron shell, which is comparatively very small due to the relatively large size of the electron shell (about 10^{-10} m).

The alpha backscattering experiments proved that the atomic nuclei have mass, charge, and well-defined geometric size. At the time of the alpha backscattering experiments, not much was known about neutrons. It was conceptualized that in order to neutralize the positive charge of the protons, electrons must be present in the nucleus. This model is called J.J. Thomson's atomic model. According to this model, atomic

Nuclear and Radiochemistry. DOI: http://dx.doi.org/10.1016/B978-0-12-391430-9.00002-0

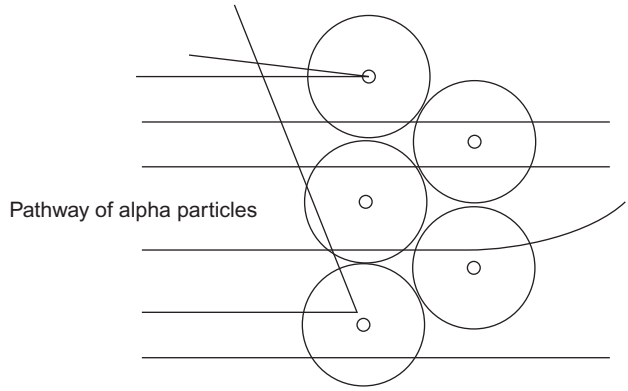

Figure 2.1 Backscattering of alpha particles.

nuclei should comprise protons and electrons. This model, however, can be disproved easily by the zero-point energy of the electron in the nucleus. Heisenberg's uncertainty principle says that

$$\Delta x \times \Delta v = \frac{h}{2\pi m} \tag{2.2}$$

where Δx and Δv are the uncertainty of the determination of the position and velocity, respectively; h is Planck's constant; and m is the mass of the particle. The radius of the nucleus (R) can be substituted for Δx in the equation; if $\Delta x > R$, then the electron is outside the nucleus. From Eq. (2.2), Δv, and from here the energy of the electron, can be expressed as follows:

$$\Delta v \approx \frac{h}{2\pi mR}, \quad E_{\text{kin}} = \frac{1}{2}mv^2 = \frac{h^2}{2mR^2} \tag{2.3}$$

These calculations for the nucleus show that the zero-point energy of the electron is two orders of magnitude greater than the binding energy of nucleons (7−8 MeV/nucleon). Thus, if the electrons were restricted in the nucleus, their energy would be so high that they would leave it instantly. So, it is clearly proved that electrons cannot be present in the nucleus. Subsequently, in 1920, Rutherford conceptualized that the nucleus contains neutral particles that explain the difference between the charge and the mass of the nucleus. These particles were called "neutrons," and they were experimentally demonstrated by James Chadwick in 1932 (Section 5.5.1).

Atomic nuclei consist of protons and neutrons. The number of protons is the atomic number (Z), and the sum of the number of protons (Z) and neutrons (N) is the mass number (A). The particles composing the nuclei are called "nucleons."

Table 2.1 The Masses of the Atomic Particles and Some Atoms Expressed in Different Units

Particle/nucleus	kg	a.m.u.[a]	MeV[b]
Proton (m_p)	1.6726×10^{-27}	1.0078	938.2
Neutron (m_n)	1.6749×10^{-27}	1.0086	939.5
Electron (m_e)	9.1072×10^{-31}	5.48×10^{-4}	0.511
^{1}H		1.0078	
^{2}H		2.0140	
^{4}He		4.0026	
^{14}N		14.00307	
^{16}O		15.99491	
^{17}O		17.0045	
^{24}Mg		23.98504	
^{35}Cl		34.9688	
^{37}Cl		36.9775	
^{40}Ca		39.9626	
^{64}Zn		63.9295	
^{206}Pb		205.9745	

[a] a.m.u., atomic mass unit.
[b] 1 a.m.u. = 931 MeV (million electron volts, Section 2.2).

2.2 Forces in the Nucleus

The mass of the charged particles (protons, nuclei, and electrons) can be determined by injecting them at a high speed into a magnetic field, where depending on their charge and mass, the path of particles deviates from a straight line. Neutrons, however, have no charges, so the mass of a neutron cannot be measured in this way; rather, its mass must be deduced. This can be achieved by the dissociation of the deuterium nucleus (one proton and one neutron) to a proton and neutron under the effect of gamma radiation.

The masses of free protons, neutrons, and electrons are listed in Table 2.1. When comparing the mass of the nucleus of an atom to the total mass of the free protons and neutrons, we can see that the sum of the mass of the free nucleons is always greater than the mass of the corresponding nucleus in the atom.

This difference will be equal to the binding energy of the nucleus (ΔE). [Note that Einstein's formula for the equivalence of mass and energy (shown in Eq. (1.1)) can be used to calculate the binding energy.] When the binding energy of the nucleus is divided by the mass number, the binding energy per nucleon is obtained ($\Delta E/A$):

$$\frac{\Delta E}{A} = \frac{(M - Z \times m_p - N \times m_n - Z \times m_e)c^2}{A} \tag{2.4}$$

where M is the mass of the atom (not the nucleus!).

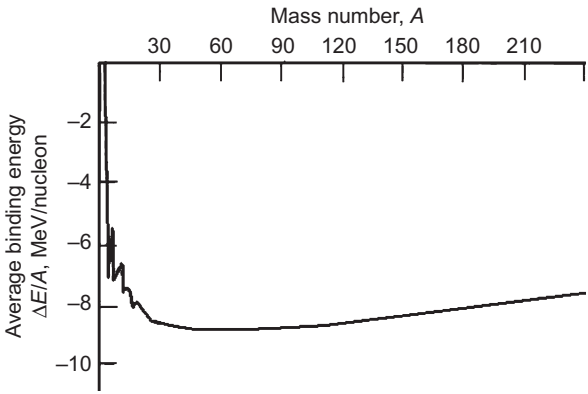

Figure 2.2 The binding energy per nucleon as a function of mass number.

The stability of a given nucleus can be characterized by the value of the binding energy per nucleon. The binding energy per nucleon as a function of atomic mass is shown in Figure 2.2.

The characteristic binding energy per nucleon for the most stable nuclei is in the range of 7−9 MeV. The absolute value of the binding energy per nucleon—the mass number function shows a maximum of about mass numbers 50−60. This mass represents the elements of the iron group; thus, these elements are the most stable ones in the periodic table. The smallest nucleus, where the term of the binding energy per nucleon can be defined, is the deuterium, which has the smallest binding energy per nucleon (around 1.8 MeV).

The binding energy is usually expressed in millions of electron volts. One electron volt is the amount of energy gained by an electron (elementary charge, 1.6×10^{-19} C) when it is accelerated through an electric potential of 1 V. Transferring the electron volt to the SI unit of energy (joule), $1\ \text{eV} = 1.6 \times 10^{-19}\ \text{C} \times 1\ \text{V} = 1.6 \times 10^{-19}$ J. For every 1 mol of electrons [found by multiplying by the Avogadro' number (6×10^{23} particles/mol)], about 10^5 J is obtained. The energy of an atomic mass unit (931 MeV), mentioned in Table 2.1, is $\sim 10^{13}$ J. The binding energy per nucleon (7−9 MeV) is about 10^{11} J that is 10^8 kJ. Therefore, the binding energy of the nuclei is about 10^8 kJ/mol.

Now let's compare the binding energy of the nuclei to the energy of chemical bonds. The energy of primary (ionic, covalent) chemical bonds is a few hundred kJ/mol (an amount of electron volts). Thus, the difference is about six orders of magnitude: the binding energy of the nuclei is about a million times higher than the energy of the chemical reactions.

In 1935, Yukawa provided an interpretation of the nature of the forces in the atomic nuclei using quantum mechanics. He constructed a model similar to the one for electrostatic forces, where two charged particles interact through the electromagnetic field. In Yukawa's model, the so-called meson field should be substituted for the electromagnetic field. In the case of the meson field, the range of the interaction is very short (about 10^{-15} m), while the electromagnetic field has a much bigger range. The potential between two particles in the nuclei, known as the

Yukawa potential (U), can be expressed as a function of the distance of the two particles (r):

$$U = -g^2 \frac{\exp(r/R)}{r} \tag{2.5}$$

In Eq. (2.5), the potential is negative, indicating that the force is attractive. The constant g is a real number; it is equal to the coupling constant between the meson field and the field of the protons and neutrons. R is the range of the nuclear forces, expressed as follows:

$$R = \frac{h}{2\pi m_\pi c} \tag{2.6}$$

where h is Planck's constant, c is the velocity of light in a vacuum, and m_π is the rest mass of the meson. Assuming that the meson field range is about 10^{-15} m, Yukawa suggested that there must be a particle with a rest mass of about 200 times that of an electron. In fact, this particle was observed in the cosmic ray in 1948. It is called π-meson, and its rest mass is 273 times higher than the rest mass of the electron. The meson is a kind of elementary particle (as discussed in Section 2.2).

The total nuclear binding energy (ΔE) can be given approximately on the basis of nuclear forces, by the summation of the interaction energies of the nucleon pairs ($U_{r,kl}$) at the distance r:

$$\Delta E = -\frac{1}{2} \sum_k \sum_l U_{r,kl} \tag{2.7}$$

where ΔE is the total nuclear binding energy and k and l are the number of protons and neutrons, respectively. The protons and neutrons are considered to be identical. The factor 1/2 is in Eq. (2.7) because of the two summations for protons and neutrons, so each nucleon appears twice. The total binding energy of the nucleus is proportional to the product of the number of protons and neutrons:

$$Z \times N = Z \times (A - Z) \tag{2.8}$$

The function of the total binding energy has a maximum of the atomic number expressed as follows:

$$\frac{\mathrm{d}(AZ - Z^2)}{\mathrm{d}Z} = 0 \tag{2.9}$$

From here

$$A = 2Z \tag{2.10}$$

In conclusion, those nuclei should be stable, such that the number of protons and neutrons are equal. This is indeed the case for light nuclei (e.g., ^{4}He, ^{12}C, ^{14}N, ^{16}O, ^{24}Mg). However, for heavier nuclei, the number of protons increases, so the electrostatic repulsion of the positively charged protons increases. For this reason, extra neutrons are needed for stability. So Eq. (2.10) is modified as:

$$A \geq 2Z \tag{2.10a}$$

which means that the nuclei with high atomic numbers are stable at the ratio of neutron/proton = 1.4. The nuclei with medium atomic numbers have a ratio of neutron/proton between two values (1−1.4), i.e., the ideal neutron/proton ratio of the stable nuclei continuously changes in the periodic table (Figure 2.3).

The energy of the electrostatic repulsion can be calculated as follows:

$$E_c = \frac{3}{5}\frac{Z(Z-1)\times e^2}{R_a} \tag{2.11}$$

where e is the elementary charge and R_a is the radius of the nucleus.

The nuclei are classified as isotope, isobar, isoton, or isodiaphere based on the number of nucleons (Table 2.2).

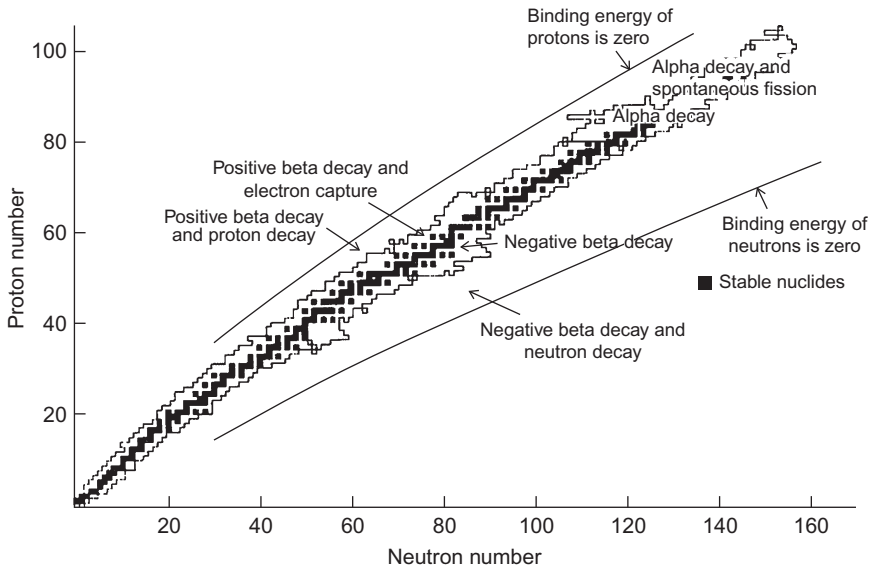

Figure 2.3 The stability of nuclei: atomic number as a function of the number of the neutrons.
Source: Conventional nuclear chart taken from Bes (1965) with permission from Elsevier.

2.3 Other Properties of Nuclei

The hyperfine structure observable in atomic spectra, including the interactions with nuclei, indicates that the nuclei have spin. The nuclear spin is a vector, and its absolute value is $\sqrt{I(I+1)}\frac{h}{2\pi}$, where I is the quantum number of the nuclear spin, simply called "nuclear spin." Nuclei with even mass numbers have $I = 0, 1, 2, 3\ldots$, whereas nuclei with odd mass numbers have $I = \frac{1}{2}, \frac{3}{2}, \frac{5}{2}\ldots\frac{11}{2}$. The nuclear spin is the sum of the spins of all protons and neutrons. In nuclear reactions, the conservation of spins also must occur.

Parity is related to the symmetry properties of nuclei. It expresses whether the wave function of a particle is even or odd (symmetrical or asymmetrical), depending on whether the wave function for the system changes sign when the spatial coordinates change their signs.

$$\text{Even parity:} \quad \Psi(-x, -y, -z) = \Psi(x, y, z) \tag{2.12}$$

$$\text{Odd parity:} \quad \Psi(-x, -y, -z) = -\Psi(x, y, z) \tag{2.13}$$

The conservation of parity also must occur for nuclear reactions.

The spin and the parity can be signed together: for nuclei with even parity, a + is written after the value of the spin, while for nuclei with odd parity, a − is written (e.g., 0+ or 7/2−).

The particles can be characterized by statistics describing the energies of single particles in a system comprising many identical particles, which has a close connection to the spin and parity of the particles. The particles with half-integral nuclear spin can be described using the Fermi−Dirac statistics. These particles obey the Pauli exclusion principle and have odd parity. These particles are called "fermions." The particles with zero or integral spin and even parity can be described using the Bose−Einstein statistics. These particles are called "bosons."

The movement of a charged particle causes magnetic momentum. The unit of measure for magnetic momentum is the Bohr magneton, which describes the magnetic momentum of an electron:

$$\mu_B = \frac{eh}{4\pi m_e} = 9.274 \times 10^{-24}\ \mathrm{J/T} \tag{2.14}$$

Table 2.2 Classification of Nuclei on the Basis of the Number of Nucleons

Term	*Z*, Atomic Number	*N*, Number of Neutrons	*A*, Number of Nucleons	*N*−*Z*, Number of Extra Neutrons
Isotope	Equal	Different	Different	
Isobar	Different	Different	Equal	
Isoton	Different	Equal	Different	
Isodiaphere				Same

For the nucleus, the mass of the proton can be substituted into Eq. (2.14) as follows:

$$\mu_N = \frac{eh}{4\pi m_p} = 5.050 \times 10^{-27}\ \mathrm{J/T} \tag{2.15}$$

where T is tesla. The quantity μ_N expresses the unit of nuclear magnetic momentum. The magnetic momentum of the different nuclei is in the range of $0-5\mu_N$. Surprisingly, the magnetic momentum of the proton is not equal to the value calculated from Eq. (2.15), but it is about 2.7926 times higher than the calculated value. Perhaps more surprising, the neutrons also have magnetic momentum, which is expressed by $-1.9135\mu_N$. This implies that the neutral neutron consists of smaller charged particles known as quarks, as discussed in Section 2.4. The negative sign of the magnetic momentum of the neutron indicates that the spin and magnetic momentums are in opposite directions.

Besides magnetic momentum, nuclei can have electric quadruple momentum too. The formation of quadruple momentum can be caused by the deviation of charge distribution from the spherical symmetry. Quadruple momentums have been determined for many nuclei by $I > 1/2$. Nuclei $I = 0$ or 1/2 cannot have quadruple momentums.

In conclusion, the characteristic properties of nuclei are listed as follows:

1. Rest mass
2. Electric charge
3. Spin
4. Parity
5. Statistics
6. Magnetic momentum
7. Electric quadruple momentum (not all nuclei).

2.4 Elementary Particles

The main constituents of atoms are protons, neutrons, and electrons. After the revision of Dalton's atomic theory, these particles were considered to be elementary particles, the basic constituents of matter. Later, Yukawa recognized that the nucleons interact with each other through the meson field, and a new elementary particle, the meson, had to be postulated. Moreover, several different kinds of mesons with different rest masses and charges have been discovered. In addition, new elementary particles have been observed in different nuclear and cosmic processes. Today, more than 300 elementary particles are known (this fact raises the ironic question: How can something be called elementary if there are hundreds of them?).

The elementary particles can be classified on the basis of rest mass: light and heavy elementary particles are called leptons and hadrons, respectively. Hadrons can be divided into two groups: mesons (with medium rest mass) and baryons (with large rest mass). They are characterized similarly to the nuclei; as listed at

the end of Section 2.3, they have rest mass, electric charge, spin, parity, statistics, magnetic moment, and electric quadruple moment. In addition, an important property of the elementary particle is the mean lifetime.

The heavy particles, hadrons, consist of more fundamental particles, which are called "quarks." Particles are referred to as fundamental if they exhibit no inner structure. Quarks can be experimentally demonstrated, for example, by irradiating protons with 50 GeV electrons. The magnetic momentum of neutrons implies the presence of charged particles inside the neutron as well.

The physics of the elementary particles postulate six types and three families of quarks (up−down, charm−strange, top−bottom). Within the atomic nucleus, the up and down quarks are the most important. The rest mass of up and down quarks is about 1/3 a.m.u. and their charge is +2/3 and −1/3, respectively. The proton consists of two up quarks and 1 down quark; the neutron contains one up quark and two down quarks. The sum of the rest masses of the three quarks gives 1 a.m.u. for both proton and neutron. In addition, the net charge of the nucleons (+1 for protons and 0 for neutrons) is the summation of the individual charges of the quarks. Table 2.3 illustrates the important properties of some elementary particles. The particles with half-integral spin (fermions) are the fundamental constituents of matter; the particles with integral spin (bosons) are the exchange particles between quarks, which are similar to the exchange of photons in the electromagnetic force between two charged particles.

Interactions in the last column of Table 2.3 can be ordered on the basis of their relative strength as follows:

Interaction	Relative Strength
Strong	1
Electromagnetic	10^{-2}
Weak	10^{-14}
Gravitation	10^{-39}

The range of the interactions is inversely proportional to their relative strength. In nuclear processes, strong interactions are dominant. The range of strong interactions is about 10^{-15} m.

The antiparticles of all the particles listed in Table 2.3 could and should exist. The electric charge of these antiparticles is the opposite of their corresponding particles. When the particle−antiparticle pairs interact with each other, they form other particles with lower or zero rest masses. As an example, the annihilation of positron and electron could be mentioned, which have a great practical importance (as discussed in Section 5.3.3).

2.5 Models of Nuclei

The structure of nuclei has been described by different models. At the moment, however, none of them alone explains all experimental observations. A useful review of 37 known models of the atomic nucleus is provided by Cook.

Table 2.3 Properties of Elementary (Fundamental) Particles

Fermions: Spin 1/2								Bosons: Spin 1				
Name	**Sign**	**Rest Mass (MeV)**	**Charge**	**Name**	**Sign**	**Rest Mass (MeV)**	**Charge**	**Name**	**Sign**	**Rest Mass (MeV)**	**Charge**	**Interaction**
Leptons				**Quarks**								
Electron	e	0.511	−1	Up	u	5.6	+2/3	Photon	γ	0	0	Electromagnetic
Electron neutrino	ν_e	0	0	Down	d	9.9	−1/3	W-boson	$W^{\pm}$	8.5×10^4	±1	Weak
Muon	μ^-	105.8	−1	Charm	c	1350	+2/3	Z^0-boson	Z^0	9.5×10^4	0	
Muon neutrino	ν_μ	0	0	Strange	s	199	−1/3	Gluon	g	0	0	Strong
Tauon	τ^-	1860	−1	Top	t	ca. 2×10^5	+2/3	**Boson: Spin 2**				
Tauon neutrino	ν_τ	0	0	Bottom	b	5000	−1/3	Graviton	G	0	0	Gravitation
				Heavy up	U	Existence						
				Heavy down	D	not proved						

The alpha model proposes the presence of alpha particles of great stability within the nuclei. This model has been suitable only for the interpretation of alpha decay.

2.5.1 The Liquid-Drop Model

The liquid-drop model is based on the constant density of nuclei, independent of the number and quality of nucleons. The phenomenon is analogous to a liquid drop in which the molecules are subjected to the same van der Waals forces, independent of the size of the drop.

According to the liquid-drop model, the nucleus can be imagined as a rather compact, spherical structure (similar to a liquid drop), the constituents of which are subjected to strong interactions acting in a very small range (about 10^{-15} m). Really, this is the nuclear force, the energy of which is approximately proportional to the mass number (A).

When the binding energy of a nucleus is calculated using this model, the nuclear energy has to be taken into account first. Let's suppose that the nuclear energy between two nucleons is U_0. In the closest geometric packing of spheres, one nucleon has 12 neighbors (the coordination number is 12). It should mean $-12U_0$, the total energy for one nucleon; however, each nucleon is considered twice (nucleon pairs are investigated), so only $-12U_0/2 = -6U_0$ is the nuclear energy for one nucleon. For a nucleus with a mass number of A, the total nuclear energy is $-6U_0A$. This energy is shown as volume energy in Figure 2.4.

Of course, the peripheral nucleons have only six neighbors, decreasing the nuclear energy. Considering the thickness of peripheral layer a, the volume of this layer is $4R^2\pi a$ (surface × thickness). Since the volume of one nucleus is $4R^3\pi/3$ and the number of nucleons is A, the volume of one nucleon is $4R^3\pi/3A$. The number of nucleons in the peripheral layer can be obtained by dividing the volume of the layer with the volume of one nucleon: $3aA/R$. Therefore, the surface energy (E_s) of the nucleus can be expressed as:

$$E_s = 9\frac{aAU_0}{R} \tag{2.16}$$

The nuclear energy corrected by the surface energy can also be seen in Figure 2.4.

Since the protons repulse each other, the energy of repulsion has to be taken into account. The energy of the electrostatic repulsion can be expressed as in Eq. (2.11). So, the binding energy per nucleon has to be corrected with the electrostatic repulsion too (Figure 2.4):

$$\frac{\Delta E}{A} = -6U_0 + 9\frac{a}{R}U_0 + \frac{3}{5}\frac{Z(Z-1)\,e^2}{AR} \tag{2.17}$$

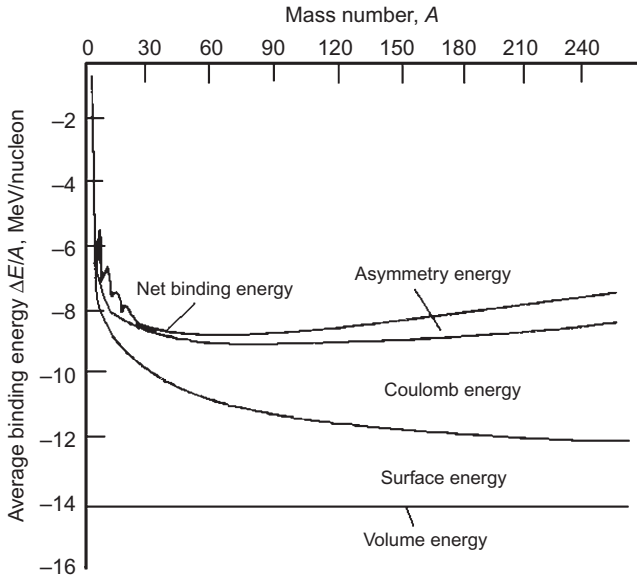

Figure 2.4 Factors influencing the binding energy by liquid drop.

The calculated binding energy per nucleon (Eq. (2.17)) is not accurately equal to the experimental value. The differences can be explained by two things. The first is that each value of A has a value of Z for which there is maximum stability (see Eqs. (2.10) and (2.10a)). When the ratio of the protons and neutrons is different from the maximum stability, a so-called asymmetry energy must also be taken into account because of the slightly different interaction energies of proton−proton, proton−neutron, and neutron−neutron pairs. The second is that the nuclei with even−even proton and neutron numbers are more stable than nuclei with odd−odd, even−odd, or odd−even nuclei. For even−odd and odd−even nuclei, this effect is taken to be zero, and for even−even nuclei, it is a negative number (increasing stability), whereas for odd−odd nuclei, it is a positive number (decreasing stability), and it will be discussed in Chapter 3.

The total semiempirical formula by Weizsäcker for the binding energy per nucleon is as follows:

$$\frac{\Delta E}{A} = -6U_0 + 9\frac{a}{R}U_0 + \frac{3}{5}\frac{Z(Z-1)e^2}{AR} + \frac{\varepsilon_4}{A} \pm \frac{\varepsilon_5}{A} \tag{2.18}$$

where

$$\frac{\varepsilon_4}{A} = \frac{\gamma}{A}\left(\frac{A}{2} - Z\right)^2 \tag{2.19}$$

and

$$\frac{\varepsilon_5}{A} = \pm\alpha_5 A^{3/4} \tag{2.20}$$

and γ and α_5 are constants. As seen in Figure 2.4, the binding energies calculated by Eq. (2.18) agree well with the experimental values.

2.5.2 The Shell Model

As seen in Section 2.5.1, the binding energy of nuclei can generally be expressed well by the liquid-drop model. However, this model cannot explain certain phenomena. For example, some nuclei with given mass numbers (2, 8, 20, 50, 82, 126, 184) are extremely stable. These numbers are called "magic numbers." Also, a very small difference in the nuclei results in a very great difference in stability. For example, ^{210}Po and ^{212}Po isotopes differ in only two neutrons, but their half-lives are 138.37 days and 10^{-7} s, respectively, a fact that indicates very different stabilities.

These phenomena can be explained by the shell model of nuclei. This model postulates that, similar to electrons, nucleons are arranged in shells in the nucleus. The closed shells result in the most stability, and the magic numbers indicate filled shells. The stability is indicated by the mass of the nuclei: within the isobar nuclei, the nucleus with the lower mass is stable. The radioactive nuclei have unfilled shells.

According to the shell model, there should be some transuranium elements with relatively great stability and "long" half-lives.

2.5.3 Unified and Collective Models

Other models of nuclei take into consideration the different collective properties of nuclei: the nonspherical shape of some nuclei, especially in excited state, and vibrational and rotational levels of nuclei; and these models are used to explain the hyperfine structure of nuclear spectra. The two names, unified and collective models, are mostly used interchangeably since both represent collective effects. The unified model is a hybrid of the liquid-drop model and the shell model: the closed shells are treated as a liquid drop, and the outer, unclosed shell is treated separately, similar to the shell model. The collective model postulates a core and an extra core in the nucleus, and the core is treated again as a liquid drop.

Further Reading

Bès, D.R. (1965). Nuclear structure away from the region of β-stability. *Nucl. Instrum. Methods* 38:277−281.

Cook, N.D. (2006). *Models of the Atomic Nucleus*. Springer, Berlin, ISBN 3540285695.

Choppin, G.R. and Rydberg, J. (1980). *Nuclear Chemistry, Theory and Applications*. Pergamon Press, Oxford.

Friedlander, G., Kennedy, J.W., Macias, E.S. and Miller, J.M. (1981). *Nuclear and Radiochemistry*. Wiley, New York, NY.

Haissinsky, M. (1964). *Nuclear Chemistry and its Applications.* Addison-Wesley, Reading, MA.

Lieser, K.H. (1997). *Nuclear and Radiochemistry*. Wiley-VCH, Berlin.

McKay, H.A.C. (1971). *Principles of Radiochemistry*. Butterworths, London.

3 Isotopes

The term "isotope" was coined by Soddy in 1910, who postulated that elements consist of atoms with the same number of protons but different numbers of neutrons.

If the ratio of the neutrons and protons is different from the optimal ratio associated with the stable state of an atom, the nucleus decomposes, emitting radiation. This process is known as "radioactive decay." The rest mass of the initial, parent nucleus is greater than the total rest mass of the produced, daughter nucleus and the emitted particle(s). The difference in the masses can be accounted for as the energy of the emitted radiation or particles. The radioactive decay is always exothermal; the emitted energy, however, is usually not released in the form of thermal energy but rather as the energy of the emitted radiation and high-energy particles.

For understanding the radioactive decay, the isobar nuclei (i.e., nuclei that have the same mass number) is a good starting point. The isobars can have odd and even values. The binding energy per nucleon as a function of the mass number gives one parabola for the odd (Figure 3.1A) and two parabolas for the even isobar nuclei (Figure 3.1B–E). In the case of even isobars, the upper and lower parabolas refer to the binding energy of nuclei containing odd or even numbers of protons and neutrons, respectively (the fifth member in Eq. (2.18) can be positive or negative). Thus, the upper parabola is defined by nuclei with odd numbers of protons and neutrons (odd–odd) and the lower parabola by nuclei with even numbers of protons and neutrons (even–even).

In the case of odd isobars, one stable nucleus is at the minimum of the parabola (Figure 3.1A). For this nucleus, the ratio of protons and neutrons is optimal. On the left side of the parabola, the number of neutrons is too high, initiating a radioactive decay in which the number of the neutrons decreases and the number of the protons increases. This process is negative beta decay. On the right side of the parabola, the number of protons is too high, initiating a radioactive decay in which the number of the protons decreases and the number of the neutrons increases. This process is positive beta decay and/or electron capture.

For even isobars, the odd–odd parabolas contain one stable nucleus (Figure 3.1C), whereas the even–even parabolas have one (Figure 3.1B), two (Figure 3.1D), or three (Figure 3.1E) stable nuclei, depending on the relative position of the odd–odd and even–even parabolas. Similar to odd isobars, the nuclei

Nuclear and Radiochemistry. DOI: http://dx.doi.org/10.1016/B978-0-12-391430-9.00003-2

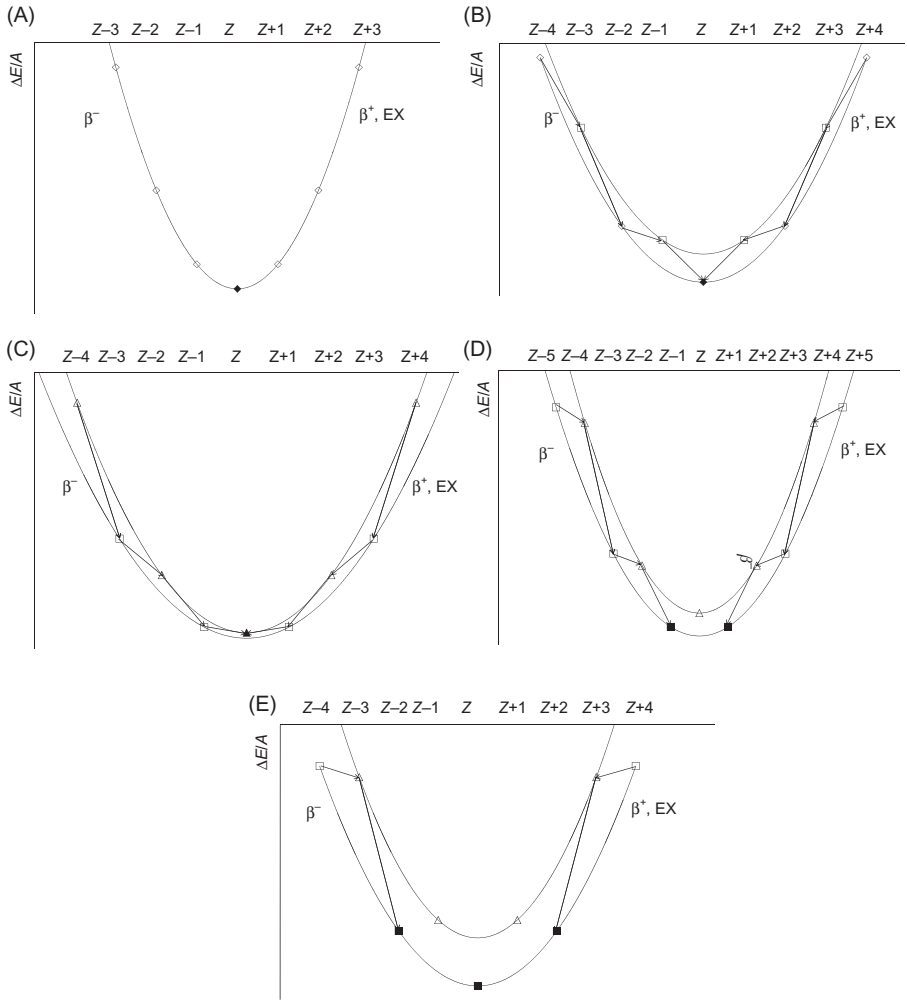

Figure 3.1 Isobar parabolas for odd (A) and even (B−E) mass numbers. Stable nuclei are signified with filled dots. For the even mass numbers, the upper parabola means the odd proton and neutron numbers, whereas the lower parabola refers to the even proton and neutron numbers.

on the sides of the parabolas decompose by negative and positive beta decays or electron capture; as a result of the decays, however, the nuclei go from the even−even parabola to the odd−odd parabola and vice versa. Since the odd−odd parabola is in the upper position, nuclei with odd numbers of protons and neutrons are stable only when they are located in the minimum of the upper parabola and the energy level of this minimum is below the energy level of adjacent even−even nuclei on the lower parabola (Figure 3.1C). This is only the case for four odd−odd light nuclei (^{2}H, ^{6}Li, ^{10}Li, and ^{14}N).

Table 3.1 A Classification of Stable Nuclei

Type	Number of Nuclei	Mass Number	Spin	Parity	Statistics
Even−even	162	A = 2*k*, even	0	Even	Bose−Einstein
Odd−odd	4		1,2,3,4...	Even	
Even−odd	56	A = 2*k* + 1, odd	$\frac{1}{2}, \frac{3}{2}, \frac{5}{2}, \ldots$	Odd	Fermi−Dirac
Odd−even	52			Odd	

k means an integer.

These occurrences of the stable nuclei are summarized by Mattauch's rule, which states that odd isobars have one stable nucleus, whereas even isobars have two or more stable nuclei, and the atomic numbers of these latter items differ by two. Consequently, if two adjacent elements have nuclides of the same mass, then at least one of them must be radioactive. This rule provides an explanation, for example, why technetium (atomic number 43) does not have stable isotopes.

The parabolas show, too, that the number of radioactive nuclides is much more than that of stable nuclides. Today, we know of approximately 270 stable nuclides and 2000 radioactive nuclides, but the number of radioactive nuclides may reach about 6000. The stable nuclides are listed and classified in Table 3.1.

It can be stated that even−even nuclei are the most frequently stable. The most abundant nuclei of the Earth's crust are even−even nuclei (^{16}O, ^{24}Mg, ^{28}Si, ^{40}Ca, ^{48}Ti, ^{56}Fe).

3.1 Isotopic Effects

Isotope atoms may have some different physical, chemical, geological, and biological properties. In addition, the isotopes are usually present not as free atoms, but in compounds, participating in chemical bonds. This means that there are isotope compounds or isotope molecules in which one atom (or perhaps more atoms) is substituted by another isotope. For example, the very simple hydrogen molecule represents six different isotope molecules, which can be written using two different symbolisms:

$$^{1}H_2, {}^{1}H{}^{2}H, {}^{1}H{}^{3}H$$
$$^{2}H_2, {}^{2}H{}^{3}H$$
$$^{3}H_2$$

and

$$H_2, HD, HT$$
$$D_2, DT$$
$$T_2$$

where D and T mean the isotope of hydrogen with mass number 2 and 3, namely, deuterium and tritium, respectively.

A similar situation exists for oxygen molecules, as follows:

$^{16}O_2, {}^{16}O^{17}O, {}^{16}O^{18}O$
$^{17}O_2, {}^{17}O^{18}O$
$^{18}O_2$

The compound of these elements, water, may have 18 different isotope molecules. Of course, the relative amount of the isotope molecules is very different, determined by the natural abundance of the isotopes.

The thermodynamic properties of the substances can be characterized by the partition function, combining translation, rotation, vibration, and electron excitation. At a constant temperature, the translation energy of the isotope atoms or molecules is the same.

The rotation energy (E_r) of a diatomic molecule can be expressed by the Schrödinger equation for a rigid rotor:

$$\frac{\partial^2\Psi}{\partial x^2} + \frac{\partial^2\Psi}{\partial y^2} + \frac{\partial^2\Psi}{\partial z^2} + \frac{8\pi^2\mu}{h^2}E_r\Psi = 0 \tag{3.1}$$

The solution of Eq. (3.1) is:

$$E_r = \frac{1}{2}I\varpi^2 = \frac{1}{2}\frac{L^2}{I} = J(J+1)\frac{h^3}{8\pi^2 c(I_x I_y I_z)} \tag{3.2}$$

where Ψ is the wave function, I is the moment of inertia, ω is the angular speed, L is the moment of impulse, and J is the rotation quantum number. The moment of inertia of a diatomic molecule is expressed as follows:

$$I = m_1 r_1^2 + m_2 r_2^2 = \mu r_0^2 \tag{3.3}$$

where r_1 and r_2 are the distance of the center of mass from the atoms with m_1 and m_2 mass and μ is the reduced mass, i.e.,

$$\mu = \frac{m_1 m_2}{m_1 + m_2} \tag{3.4}$$

The reduced mass can be very different for the isotope molecules, and this difference will affect the chemical properties. For example, the masses of the TH and D_2 molecules are very similar, but the reduced masses are rather different: 3/4 and 1 for TH and D_2, respectively.

The vibration energy of a diatomic molecule (E_v) can be expressed by the Schrödinger equation of a harmonic oscillator:

$$\frac{\partial^2 \Psi}{\partial x^2} + \frac{8\pi^2 \mu}{h^2}\left(E_v - \frac{1}{2}kx^2\right)\Psi = 0 \tag{3.5}$$

where

$$E_v = \left(v + \frac{1}{2}\right)hc\omega \tag{3.6}$$

where ν is the vibration quantum number, ω can be defined as:

$$\omega = \frac{1}{2\pi c}\sqrt{\frac{k}{\mu}} \tag{3.7}$$

In this equation, k is a constant (a spring constant in classical physics), $x = r - r_e$, and r and r_e are the mean and the shortest distance between the two atoms, respectively.

When comparing the ratio of the vibration energies for two isotope molecules, look at the following equation:

$$\frac{E_{v1}}{E_{v2}} = \sqrt{\frac{\mu_2}{\mu_1}} \tag{3.8}$$

The electronic excitation can be characterized by the wave number (ν^*) of spectrum lines. It can be described by Moseley's law. For the hydrogen atom, it is:

$$\nu^* = \frac{2\pi^2 e^4}{h^3 c}\frac{M_a m_e}{M_a + m_e}\left(\frac{1}{n_1^2} - \frac{1}{n_2^2}\right) = Ry\left(\frac{1}{n_1^2} - \frac{1}{n_2^2}\right) \tag{3.9}$$

where M_a and m_e are the masses of the nucleus and the electron, n_1 and n_2 are the main quantum numbers of the electron shells involved in the excitation process, and Ry is the Rydberg constant. As seen, the reduced mass of the atom appears in Eq. (3.9), which may be different when the isotope is not the same because of the different masses of the nuclei.

All expressions of the rotation, vibration, and electronic excitation energies contain the reduced masses, which are different for isotope atoms and molecules. This difference in the reduced masses is responsible for the isotopic effects, namely, the different physical, chemical, and other properties of the isotopes and isotope molecules.

3.1.1 Physical Isotope Effects

At a given temperature, the thermal (kinetic) energy of ideal gases is the same, independent of the chemical identity of the gas. So, the kinetic energy (E_{kin}) of the different molecules of hydrogen isotopes (H,D,T) is:

$$E_{kin} = \frac{3}{2}RT = \frac{1}{2}m_H v_H^2 = \frac{1}{2}m_D v_D^2 = \frac{1}{2}m_T v_T^2 \tag{3.10}$$

Since the ratio of the masses of the isotopes is $m_H{:}m_D{:}m_T = 1{:}2{:}3$,

$$v_H : v_D : v_T = 1 : \frac{1}{\sqrt{2}} : \frac{1}{\sqrt{3}} \tag{3.11}$$

This difference in the velocity of the isotope molecules influences all the properties involving the movement of gases, for example, diffusion and viscosity.

In gas columns, such as the atmosphere, the isotopes separate because of their different masses. This separation can be calculated by the following barometric formula:

$$p_h = p_0 \, e^{-\frac{Mgh}{RT}} \tag{3.12}$$

where p_0 and p_h are the pressure at the level of a reference level (zero level) and at the height h, respectively, M is the molar mass of the gas, g is the gravitational constant, h is the height related to the reference level, R is the gas constant, and T is the temperature (in kelvin).

For two isotopes/isotope molecules with different mass numbers (M_1 and M_2):

$$\frac{p_2}{p_1} = \frac{p_{20}}{p_{10}} e^{-\frac{(M_2 - M_1)gh}{RT}} \tag{3.13}$$

The partial pressures, of course, are proportional to the concentrations of the isotopes/isotope molecules.

A similar expression can be deduced for the centrifugation of the isotope molecules, substituting $g \times h$ with $(\omega r)^2$, where ω is the angular speed and r is the distance from the rotation axis:

$$\frac{p_2}{p_1} = \frac{p_{20}}{p_{10}} e^{-\frac{(M_2 - M_1)(\omega r)^2}{RT}} \tag{3.14}$$

As seen in Eqs. (3.13) and (3.14), the degree of the isotope effects is determined by the difference of the masses. It means that these effects are observed for all isotopes, including heavy elements. Therefore, the centrifugation can be applied to the separation of isotopes of heavy elements, for example, ^{235}U and ^{238}U.

In electric and magnetic fields, the charged particles move along a curved path. The deviation from the initial direction is proportional to the specific charge of the moving particle.

In electric fields,

$$X = k\frac{E}{v^2}\frac{e}{m} \tag{3.15}$$

where X is the deviation, k is a constant, E is the strength of the electric field, v, e, and m are the speed, the charge, and the mass of the particle, and e/m is the specific charge (mass-to-charge ratio).

In magnetic fields,

$$Y = K_{\mathrm{m}}\frac{H}{v}\frac{e}{m} \tag{3.16}$$

where Y is the deviation, K_{m} is a constant, and H is the strength of the magnetic field.

The specific charge of isotopes with different masses and the same charge is different; therefore, they move along differently curved paths in the same electric or magnetic field. The mass spectrometers utilize this process for determining the mass of particles. Isotopes can also be separated in macroscopic quantities using the deviation from the straight line in electric and magnetic fields.

3.1.2 Spectroscopic Isotope Effects

The different reduced mass of the molecules that contain isotope atoms may also have an effect on the optical spectra of the isotope molecules. The phenomenon is called the spectroscopic isotope effect, and it can be observed in both atomic and molecular spectra.

Light emission is the result of the change of the energy of a particle from a greater level (E') to a lower level (E''). In light absorption, the reversed process takes place. The energy levels mean rotation, vibration, and electron energies. The change in the rotation and vibration energies produces the molecular spectra, whereas the change of the electron energies gives the atomic spectra. As seen in Section 3.1, all the rotation, vibration, and electron energies depend on the reduced mass of the molecule (Eqs. (3.2) and (3.6)) or the atom (Eq. (3.9)), so the spectra of the isotope molecules and atoms are different. For example, the reduced mass of the $H^{35}Cl$ is $\mu = 0.9722$ and that of the $H^{37}Cl$ molecule is $\mu = 0.9737$. As can be calculated by Eq. (3.8), the ratio of the vibration energies of the two molecules is 1.00076. This value is very close to 1, so the difference of the spectra can be observed only by very high resolution spectrometers.

The spectroscopic isotope effects can be observed in some atomic spectra too. However, the difference in the reduced masses of the isotope atoms is very small. As a result, only hydrogen−deuterium spectroscopic isotope effects can be detected easily. The wave number of the hydrogen isotopes can be calculated by Eq. (3.9).

The wave number of a H_α line is 15,233 cm^{-1} and that of a D_α line is 15,237 cm^{-1}. The difference is 4 cm^{-1}, which can be observed by traditional spectrometers. As seen in Eq. (3.9), the reduced masses determine the Rydberg constant (Ry), the ratio of which for deuterium and hydrogen is:

$$\frac{Ry(\mathrm{D})}{Ry(\mathrm{H})} = \frac{M_\mathrm{D} m_\mathrm{e}}{M_\mathrm{D} + m_\mathrm{e}} \times \frac{M_\mathrm{H} + m_\mathrm{e}}{M_\mathrm{H} m_\mathrm{e}} = \frac{0.9997283}{0.9994568} = 1.0002717 \tag{3.17}$$

This value is about three times less than the ratio for the vibration energies of the HCl isotope molecules (1.00076). The natural isotope ratio of hydrogen to deuterium was determined on the spectral line intensities of hydrogen in 1939.

3.1.3 Phase Equilibrium Isotope Effects

The distribution of the isotope molecules is different in phases that are in thermodynamic equilibrium, including the liquid/gas, liquid/solid, and solid/gas phases. Similarly, the solubility of the isotope molecules is also different.

The isotope effects in the liquid/gas phases have been well studied. The effect can be characterized by the partial pressure of the isotope molecules:

$$\frac{p' - p}{p} = \frac{p'}{p} - 1 \approx \ln\frac{p'}{p} = \varepsilon \tag{3.18}$$

where p and p' are the partial pressure of the lighter and the heavier molecule, respectively, and ε is the relative partial pressure. The degree of the isotope effect is usually low: $\varepsilon \ll 1$. Of course, the different partial pressures result in different boiling points (Table 3.2).

Usually, the partial pressure of the lighter molecules is greater. If not, an inverse isotope effect exists. Among the molecules in Table 3.2, methane shows an inverse isotope effect.

A well-known isotope effect in the solid/liquid phase is the ice/water system. The boiling point of ^2H_2O and ^1H_2O is different. As a result, the deuterium content of the icy seas is greater than the average deuterium content of the oceans.

The adsorption of the isotope molecules can also be different, a fact that is used in adsorption chromatography to separate isotopes. As the pressure and temperature decrease, the isotope effects increase, resulting in increased separation factors.

The different solubility of the isotope molecules have mainly been studied during the dissolution of light and heavy water in organic solvents. The inorganic salts and some organic compounds dissolve differently in light and heavy water.

3.1.4 Isotope Effects in the Kinetics of Chemical Reactions

The reaction rate of the isotope molecules may be different. This effect is determined by the reaction mechanism, including thermodynamic properties of the transition state, so the kinetic isotope effects can be applied for the study of the mechanism of the chemical reactions.

Table 3.2 Relative Tension of Some Isotope Molecules

	Relative Partial Pressure	
	At Triple Point	**At Boiling Point (1 bar)**
H_2(*ortho*)/HD	3.61	1.81
$(NH_3/ND_3)^{1/3}$	1.080	1.036
$(H_2O/D_2O)^{1/2}$	1.120	1.026
CH_4/CH_3D	1.0016	0.9965
$^3He/^4He$	7.0	
$^{20}Ne/^{22}Ne$	1.043	
$^{128}Xe/^{136}Xe$	1.006	
$^{12}CO/^{13}CO$	1.01	
$^{14}NH_3/^{15}NH_3$	1.0055	1.0025
$H_2{}^{16}O/H_2{}^{18}O$	1.01	1.0046
$^{11}BF_3/^{10}BF_3$		≈1.01

The kinetic effects are significant in the case of light elements since the mass of the isotopes of these elements has the greatest differences, resulting in relatively great differences in the rotation, vibration, and electron energies of the isotope molecules and the transition state. The reactions of the molecules containing different H, C, N, O, and S isotopes are important. Obviously, the reactions of such molecules are interesting mainly in organic chemistry.

The kinetic isotope effects can be classified as primary and secondary effects. In the primary effects, the bond that contains the isotope atoms breaks or forms in the rate-determining step. The primary kinetic isotope effects can be divided further in intermolecular and intramolecular effects. In the intermolecular effect, two molecules react with different rates. In the intramolecular effect, the equivalent sites within the same molecules show different rates because the sites have different isotopes.

A primary intermolecular isotope effect is as follows:

$$AX + BY \xrightarrow{k_1} BX + AY \tag{3.19}$$

$$AX' + BY \xrightarrow{k_2} BX' + AY \tag{3.20}$$

In Eqs. (3.19) and (3.20), two identical molecules (AX and AX′) contain different isotopes of the same element (X and X′). When the reaction constants are different ($k_1 \neq k_2$), the reaction of the two isotope molecules (AX and AX′) with the molecule BY shows a primary intermolecular isotope effect.

A primary intramolecular isotope effect can be observed in the following process:

$$\begin{array}{l} AXX' + 2BY \rightarrow \underset{\uparrow}{BX'} + \underset{\uparrow}{BX} + AYY \\ \qquad\qquad\quad\ \ k_3 \qquad\ k_4 \end{array} \tag{3.21}$$

where k_3 and k_4 are the rate of the production of BX′ and BX, respectively. An isotope effect occurs when $k_3 \neq k_4$.

In the secondary isotope effects, the isotope atom does not directly take part in the reaction. For example,

$$AXX + BY \xrightarrow{k_5} BX + AXY \tag{3.22}$$

$$AXX' + BY \xrightarrow{k_6} BX + AX'Y \tag{3.23}$$

where $k_5 \neq k_6$.

A primary isotope effect can be observed in the thermal decarboxilation of oxalic acid if one or both carbon atoms are substituted by the ^{13}C isotope:

$$\begin{array}{l} {}^{12}COOH \quad k_1 \\ | \qquad\qquad \longrightarrow {}^{12}CO_2 + H_2O + {}^{12}CO \\ {}^{12}COOH \end{array} \tag{3.24}$$

$$\begin{array}{lll} {}^{12}COOH & & {}^{12}CO_2 + H_2O + {}^{13}CO \\ | & \overset{k_2}{\nearrow} & \\ | & \underset{k_3}{\searrow} & \\ {}^{13}COOH & & {}^{13}CO_2 + H_2O + {}^{12}CO \end{array} \tag{3.25}$$

$$\begin{array}{l} {}^{13}COOH \\ | \qquad\qquad \xrightarrow{k_4} {}^{13}CO_2 + H_2O + {}^{13}CO \\ {}^{13}COOH \end{array} \tag{3.26}$$

An intramolecular isotope effect is found when k_2/k_3, whereas intermolecular isotope effects can be observed in case of $k_1/(k_2 + k_3)$, k_1/k_4, and $(k_2 + k_3)/k_4$, respectively.

As a secondary isotope effect, the reaction of carboxyl groups of malonic acid is mentioned when deuterium is substituted for the hydrogen bonded to the β-carbon atom. The maximum values of the kinetic isotope effects (shown in Table 3.3) are determined using the thermodynamic properties of the isotope molecules.

The study of the isotope effects can be used to elucidate the reaction mechanism, as the following example shows. The oxidation of alcohols to carboxylic acid by bromine is made up of two steps:

$$CH_3 - CH_2 - OH + Br_2 \xrightarrow{\text{slow}} CH_3 - CHO + 2HBr \tag{3.27}$$

$$CH_3 - CHO + Br_2 + H_2O \xrightarrow{\text{fast}} CH_3 - COOH + 2HBr \tag{3.28}$$

The rate-determining step is the oxidation of the alcohol, which results in the formation of aldehyde (Eq.(3.27)), a first-order reaction both for alcohol and

Table 3.3 Maximum Values of Isotope Effects in the Kinetics of Chemical Reactions

Isotope Substitution		Bond	Ratio of Rate Constants
Maximum Primary Isotope Effects at 25°C			
H	D		18
H	T		60
^{10}B	^{11}B		1.3
^{12}C	^{13}C		1.25
^{12}C	^{14}C		1.5
^{14}N	^{15}N		1.14
^{16}O	^{18}O		1.19
^{19}F	^{18}F		1.25
^{31}P	^{32}P		1.02
^{32}S	^{35}S		1.05
Cl natural	^{38}Cl		1.14
^{127}I	^{131}I		1.02
Maximum Secondary Isotope Effects at 25°C			
H	D	C–H	1.74
H	T	C–H	2.20
H	D	O–H	2.02
H	T	O–H	2.74
^{12}C	^{13}C	C–C	1.012
^{12}C	^{14}C	C–C	1.023

bromine. There are two mechanistic possibilities. The first is that bromine reacts with the hydrogen in the hydroxide group and in a rate-determining step:

$$CH_3 - CH_2OH + Br_2 \xrightarrow{\text{slow}} CH_3 - CH_2 - OBr + HBr \tag{3.29}$$

$$CH_3 - CH_2 - OBr \xrightarrow{\text{fast}} CH_3 - CHO + HBr \tag{3.30}$$

This support for this mechanism is that it resembles the fast reaction of alkyl hypochlorites. If this is the right mechanism, secondary isotope effects should be observed if the alcohol CH_2 group is labeled by an isotope of the hydrogen. In the case of H–T substitution, this mechanism can decrease the reaction rate by 2.2 times (Table 3.3).

The second possibility is that bromine reacts with the carbon atom of the alcohol CH_2, which would result in a much higher (i.e., primary) isotope effect when substituting one of the hydrogen atoms of alcohol CH_2 by tritium. In this case, two types of aldehyde would form, an unlabeled and a labeled molecule:

$$CH_3 - CHT - OH + Br_2 \begin{cases} \xrightarrow{k_{T1}} CH_3 + CHO + TBr + HBr \\ \xrightarrow{k_{T2}} CH_3 + CTO + HBr \end{cases} \tag{3.31}$$

$$CH_3 - CH_2 - OH + Br_2 \xrightarrow{k_H} CH_3CHO + 2HBR \tag{3.32}$$

Because of the two product molecules of the labeled alcohol, the value of the isotope effect has to be calculated as:

$$\frac{2k_H}{k_{T1} + k_{T2}} = 8 \tag{3.33}$$

Thus, examining the relative rates, it can be determined if the reaction starts with the reaction of CH_2 and Br_2, or if it proceeds via a hypobromite intermediare.

3.1.5 The Isotope Effect in a Chemical Equilibrium

The equilibrium constants of the reactions involving isotope molecules may also be different:

$$AX + BY \Leftrightarrow AY + BX \tag{3.34}$$

$$AX' + BY \Leftrightarrow AY + BX' \tag{3.35}$$

Both X and X′ mean the isotopes of the same element. The equilibrium constants are as follows:

$$K = \frac{[AY][BX]}{[AX][BY]} \tag{3.36}$$

$$K' = \frac{[AY][BX']}{[AX'][BY]} \tag{3.37}$$

The ratio of the two equilibrium constants is:

$$\frac{K}{K'} = \overline{K} = = \frac{[BX][AX']}{[BX'][AX]} \tag{3.38}$$

This ratio gives the equilibrium constant of the isotope exchange reaction:

$$AX + BX' \Leftrightarrow AX' + BX \tag{3.39}$$

When the equilibrium constant of the isotope exchange is equal to 1, there is no isotope effect—the distribution of the isotopes is the same in both compounds.

The equilibrium constants of some isotope exchange reactions are listed in Table 3.4. The calculated values were obtained from the thermodynamic properties.

As seen in Table 3.4, the equilibrium constants of isotope exchange reactions are close to 1 but frequently not equal to 1. These small differences from 1 have, however, a great theoretical and practical importance because they provide a way to separate isotopes and give important geological information (discussed further in Section 3.4).

Table 3.4 Equilibrium Constants of Some Isotope Exchange Reactions

Isotope Exchange Reaction	Temperature (K)	Equilibrium Constant	
		Experimental	Calculated
$0.5C^{16}O_2 + H_2{}^{18}O_{aq} \Leftrightarrow 0.5C^{18}O_2 + H_2{}^{16}O_{aq}$	273	1.044	1.044
$^{15}NH_3 + {}^{14}NH_{3aq} \Leftrightarrow {}^{15}NH_{3aq} + {}^{14}NH_3$	298	1.026	
$H^{12}CN + {}^{13}CN^-_{aq} \Leftrightarrow H^{13}CN + {}^{12}CN^-_{aq}$	295	1.026	1.030
$HC^{14}N + CN^-_{aq} \Leftrightarrow HC^{15}N + CN^-_{aq}$	295	1	1.002
$^{12}CO_3^{2-} + {}^{13}CO_2 \Leftrightarrow {}^{13}CO_3^{2-} + {}^{12}CO_2$	273	1.017	1.016
$H^{12}CO_3^- + {}^{13}CO_2 \Leftrightarrow H^{13}CO_3^- + {}^{12}CO_2$	298	1.014	
$^{34}SO_2 + H^{32}SO_3^- \Leftrightarrow {}^{32}SO_2 + H^{34}SO_3^-$	298	1.019	
$^{36}SO_2 + H^{32}SO_3^- \Leftrightarrow {}^{32}SO_2 + H^{36}SO_3^-$	298	1.043	
$^7Li(Hg) + {}^6LiCl \Leftrightarrow {}^6Li(Hg) + {}^7LiCl$	295	1.025	
$H_2{}^{18}O + 1/3C^{16}O_3^{2-} \Leftrightarrow H_2{}^{16}O + 1/3C^{18}O_3^{2-}$	273	1.022	
	298	1.0176	
$H_2{}^{18}O + 1/4Si^{16}O_4^{2-} \Leftrightarrow H_2{}^{16}O + 1/4Si^{18}O_4^{2-}$	273	1.0204	
	298	1.0157	
$H_2{}^{18}O + 1/4S^{16}O_4^{2-} \Leftrightarrow H_2{}^{16}O + 1/4S^{18}O_4^{2-}$	288	1.03	
	413	1.014	
$H_2{}^{18}O + 1/4S^{16}O_4^{3-} \Leftrightarrow H_2{}^{16}O + 1/4S^{18}O_4^{3-}$	273	1.0104	
	298	1.0037	

3.1.6 Biological Isotope Effects

Living organisms can react with the isotope molecules in different ways. As discussed in previous chapters, the cause of the physical and chemical isotope effects can be easily understood, but the biological effects are much more complicated. The most important isotope effects occur in the case of the isotope of hydrogen since the hydrogen bond plays a very important role in the secondary and tertiary structures of the proteins and nucleic acids. When substituting deuterium for hydrogen, the strength of the hydrogen bond increases, i.e., the cleavage of a deuterium bond requires more energy. This increase is similar to the differences in the partial pressure of water under the effect of hydrogen−deuterium substitution. Heavy water (D_2O) inhibits or can stop the proliferation of cells. The experience shows that living organism may die when the deuterium−hydrogen substitution happens quickly. However, when the deuterium−hydrogen substitution is slow, the living organisms can adapt to the heavy water. During the adaptation phase, cell destruction or cell proliferation may be observed. After the adaptation, the cells develop as usual.

Recently, there have been some reports claiming that drinking deuterium-free water has desirable physiological effects, such as reducing the risk of cancer. This effect may have been observed *in vitro*. However, because of the fast isotope exchange of deuterium and hydrogen in the environment (air, nutrients, etc.), deuterium concentration of the human body cannot be lowered in this manner.

3.2 Separation of Isotopes

Any of the above-mentioned isotope effects can be used to separate the isotopes. Distillation, gas diffusion, centrifugation, electromagnetic separation, electrolysis, and chemical isotope exchange are widely used methods for isotope separation. A newer, novel method of doing this is laser isotope separation (LIS).

The LIS technique was originally developed in the 1970s as a cost-effective, environmentally friendly way of supplying enriched uranium. The method is based on the fact that different isotopes of the same element absorb different wavelengths of laser light. Therefore, a laser can be precisely tuned to ionize only atoms of the desired isotope, which are then drawn to electrically charged collector plates.

The isotope separation is characterized by the separation factor. In a two-component system, the separation factor (α) is defined as:

$$\alpha = \frac{X_1(1 - X_0)}{(1 - X_1)X_0} = \frac{R_1}{R_0} \tag{3.40}$$

where X_0 and X_1 are the molar fraction of one of the isotopes before and after separation, respectively.

$$R_0 = \frac{X_0}{1 - X_0} \quad \text{and} \quad R_1 = \frac{X_1}{1 - X_1} \tag{3.41}$$

In addition, $1-\alpha$ is called the enrichment factor.

Since the degree of the isotope effects is usually small, one separation step is frequently not enough to reach a high enough enrichment. In this case, a multistage process in cascade can be applied. The enrichment factor of a separation cascade (A) is proportional to the number of stages (n):

$$A = \alpha^n = \frac{R_1}{R_0} \tag{3.42}$$

By increasing n, the enrichment increases proportionally.

The enriched isotopes are used for the production of fuels and moderators of nuclear reactors and nuclear weapons, for analytical purposes (e.g., NMR, Mössbauer spectroscopy), and for the preparation of targets in the production of radioactive isotopes. In Table 3.5, the most important enriched isotopes are listed. Beside enrichment, the depletion of the isotopes can be important for special applications. Depleted ^{64}Zn is used in nuclear industry. The addition of zinc to the cooling water inhibits the corrosion and the formation of ^{60}Co (discussed in Section 7.3) from the steel of the reactor, decreasing the workers' radiation exposure. Natural zinc contains 48% ^{64}Zn; however, the gamma emitter ^{65}Zn isotope is produced by (n,γ) nuclear reaction of ^{64}Zn (discussed in Section 6.3). To avoid the production of ^{65}Zn, depleted ^{64}Zn (<1%) is produced by centrifugation and applied in nuclear reactors.

Table 3.5 Most Important Enriched (and Depleted) Isotopes

Isotope	Separation Method	Application
^{2}H	Electrolysis, fractionation, distillation, chemical exchange	Moderator in heavy water, nuclear reactors, nuclear weapons, NMR spectroscopy
^{6}Li	Electrolysis of LiOH, transfer of lithium ions from an aqueous solution to a lithium amalgam	Production of tritium for nuclear weapons and fusion reactor experiments
^{10}B	Distillation of BF_3, exchange with distillation	Neutron absorber in nuclear reactors, neutron detection, boron cancer therapy
^{13}C	Distillation of CO	Tracer studies, especially in organic chemistry, NMR spectroscopy
^{15}N	Distillation of NO, exchange between $NH_{3(g)}$ and NH_4^+	Tracer studies
^{18}O	Exchange between CO_2 and H_2O	Tracer studies, production of ^{18}F isotope for positron emission tomography (PET)
^{20}Ne	Thermal diffusion	Tracer studies
^{67}Zn, ^{68}Zn ^{112}Cd ^{124}Xe	Electromagnetic separation	Production of PET isotopes: ^{67}Ga ^{111}In ^{123}I
^{191}Ir ^{124}Xe ^{186}W Depleted ^{46}Ti	Electromagnetic separation	Production of isotopes for radiation therapy: ^{192}Ir ^{125}I ^{188}Re ^{46}Sc
^{74}Se	Electromagnetic separation	Production of ^{75}Se for gamma cameras
depleted ^{64}Zn	Centrifugation	Corrosion inhibitor in the cooling water of nuclear reactors
^{57}Fe ^{119}Sn	Electromagnetic separation	Mössbauer spectroscopy
^{235}U	Gas diffusion of UF_6, electromagnetic separation, centrifugation of UF_6, LIS	Nuclear reactors, nuclear weapons

3.3 Isotope Composition in Nature

As a result of the isotope effects, isotopes are fractionated in nature. The amount of natural isotope fractionation, however, is usually smaller than would be expected from the isotope effects because the cyclic processes characteristic in nature tend to compensate for the fractionation caused by isotope effects. Only the isotope

Table 3.6 International Standard of Isotope Ratios

Isotopes	Name of Standard	Notation of Standard	$R_{standard}$
$D/^{1}H$	Vienna Standard Mean Ocean Water	VSMOW	0.00015575
$^{18}O/^{16}O$	Vienna Standard Mean Ocean Water	VSMOW	0.0020052
$^{13}C/^{12}C$	Vienna Pee Dee Belemnite (carbonate rock)	VPDB	0.0112372
$^{15}N/^{14}N$	Air (free of all anthropogenic impurities)	AIR	0.003676
$^{34}S/^{32}S$	Canyon Diablo Troilite (meteorite)	CDT	0.045005

fractionation of the light elements can be easily observed. Thus, the heaviest element showing isotope separation in nature is germanium. Besides the isotope effects, the fractionation of the radioactive isotopes is also influenced by the radioactive decay.

The stable isotope concentrations of the substances are presented as the molar ratio of the heavy-to-light isotopes. Since this ratio is small, stable isotope abundances are usually presented relative to an international standard:

$$\delta = \left(\frac{R_{\text{sample}}}{R_{\text{standard}}} - 1 \right) \times 1000 \tag{3.43}$$

where δ is expressed in ‰. In Eq. (3.43), R_{sample} and R_{standard} are the ratio of heavy-to-light isotopes in the sample and the standard, respectively. For example, the value of δ for the stable isotopes of hydrogen is:

$$\delta = \left(\frac{(\text{D}/\text{H})_{\text{sample}}}{(\text{D}/\text{H})_{\text{standard}}} - 1 \right) \times 1000 \tag{3.44}$$

Traditionally, the isotope ratios of five elements (namely, hydrogen, carbon, nitrogen, oxygen, and sulfur) are used for practical, especially geochemical, purposes. The standard of the isotope ratios of these elements is summarized in Table 3.6. Standard materials are available from the International Atomic Energy Agency (IAEA) and the National Institute of Standards and Technology (NIST) to ensure accurate measurement and reporting of isotope ratios for unknown samples and to facilitate cross-lab comparability.

3.4 Study of Geological Formations and Processes by Stable Isotope Ratios

As mentioned previously, the isotope ratios of five elements, hydrogen, carbon, nitrogen, oxygen, and sulfur, are widely applied because

- they have small atomic mass, so their isotope effects are relatively high;
- they typically form covalent bonds. The strong covalent bond inhibits the equalizing effect of cyclic processes;

- they can form many compounds;
- the abundance of the heavier isotope is relatively high;
- the isotope ratios can be measured using the same technique.

The isotope ratios are routinely determined by mass spectrometers that have been improved especially for the measurements of isotope ratio, where the isotope ratios are measured in H_2, CO_2, N_2, and SO_2 gases. In addition, other spectroscopic techniques, such as infrared spectroscopy, ion microprobe, diode laser spectroscopy, and hollow cathode spectroscopy, are used in some cases.

The ratios of the stable isotopes give information on changes of the composition of the Earth's mantle, climate (paleoclimatology), major extinction events, hydrological processes, and so on. In addition, stable isotope ratios can give useful tools for other disciplines connected to geological formations (archeology, criminology, environmental science, etc.). In addition, interesting information is obtained by studying the isotope ratios of other planets. For example, in the rocks from Mars and meteorites, the D/H ratio can be much higher than on the Earth (up to 4000‰). This shows that the high portion of the light isotope, ^1H, evaporated from Mars. In the following sections, some example for the utilization of stable isotope ratios in geology and related disciplines will be shown.

3.4.1 Study of the Temperature and Age of Geological Formations

During the slow formation of any other sedimentary rock from natural water, heterogeneous isotope exchange takes place between the oxygen in water and the surface layers of the rock. For example, in case of carbonate rock, the exchange can be described as:

$$H_2{}^{18}O + 1/3C^{16}O_3^{2-} \Leftrightarrow H_2{}^{16}O + 1/3C^{18}O_3^{2-} \tag{3.45}$$

The equilibrium constant of the reaction (3.45) depends on the temperature as postulated by the van't Hoff equation. This temperature dependence can be measured in laboratory conditions. Thus, the formation temperature of the rocks can be estimated, assuming that the oxygen isotopes inside particles that are more than 10 μm in diameter do not exchange with the oxygen isotopes of water. Similarly, the temperature of the formation of sulfate, phosphate, and silicate rocks can be estimated. The disadvantage of this method is that the isotope ratio of ancient water is not known; it is usually estimated by modeling $\delta^{18}O$ gradients in marine sediment pore waters.

Another novel method for the determination of the formation temperature of carbonate rocks is based on the simultaneous measurement of $^{18}O/^{16}O$ and $^{13}C/^{12}C$ isotope ratios. Since a carbonate ion consists of one carbon and three oxygen atoms, it has 20 different versions depending on the isotope composition, and these versions are in chemical equilibrium with each other. The most abundant equilibrium is:

$$^{13}C^{16}O_3^{2-} + {}^{12}C^{18}O^{16}O_2^{2-} \Leftrightarrow {}^{13}C^{18}O^{16}O_2^{2-} + {}^{12}C^{16}O_3^{2-} \tag{3.45a}$$

For the determination of the formation temperature, the quantity of $^{13}C^{18}O^{16}O_2^{2-}$ has to be measured, and the quantity of the other isotopologues can be considered constant. By digestion of the carbonate rock by phosphorous acid, the quantity of $^{13}C^{18}O^{16}O$ is proportional to the quantity of $^{13}C^{18}O^{16}O_2^{2-}$ therefore, the mass spectrometry of the CO_2 gives this value, and from there, the temperature of rock formation can be estimated.

The stable isotope ratios can give information on the age of rocks, too, assuming that the ratio of sulfur isotopes was the same at the time of the formation of the Earth. When the biological processes start, the biological isotope effects change the ratio of the sulfur isotopes: they become different in seawater and rocks. The ratio of $^{34}S/^{32}S$ increases in seawater and proportionally decreases in rocks. Since the biological activity started for about 700−800 million years ago, the ages of the geological samples from this period can be determined using $^{34}S/^{32}S$ isotope ratios.

3.4.2 Study of the Hydrological Process by Measuring the Ratio of Oxygen and Hydrogen Isotopes

In hydrogeology, the ratios of hydrogen and oxygen isotopes are frequently used. Hydrogen and oxygen are connected by covalent bonds; therefore, the ratios of $^{18}O/^{16}O$ and D/H are evaluated together. Since a portion of the subsurface water is originated from rainwater, the rate and degree of the accumulation of subsurface water can be determined using the isotope ratios. The IAEA measures the isotope ratios of rainwater monthly for some ten years. These measurements show the geographical distribution of the D/H and $^{18}O/^{16}O$ and the factors affecting the isotope ratios in water. In the following section, these factors and the related isotope effects are summarized. It is important to note that more than one isotope effect can influence the isotope ratios. The different partial pressure of the isotope molecules, for example, plays a role in all cases when evaporation takes place.

- The effect of height: the ratio of $^{18}O/^{16}O$ and D/H in the water vapor decreases with the height as postulated by the barometric formula (Eqs. (3.12) and (3.13)). The decrease of $\delta^{18}O$ and δD is about -0.12 to -0.5‰/100 m and -1.5 to -4‰/100 m, respectively.
- The effect of meridians is related to the centrifugation of the isotopes: the $\delta^{18}O$ and δD of the water vapor and rain decreases into the direction of the poles because of the decrease in the radius of the meridian (r in Eq. (3.14)).
- The continental effect: the diffusion rate of the lighter isotope molecules of the water vapor evaporated from the oceans is higher, so the ratios of $^{18}O/^{16}O$ and D/H decreases from the sea side to the inland area of the continents.
- The effect of temperature is associated with the change of the partial pressure of the isotope molecules, as shown in Eq. (3.18). When the temperature increases by 1°C, the $\delta^{18}O$ of water vapor increases by 0.5‰. It results in several effects. Seasonal effects are observed: in winter, the $^{18}O/^{16}O$ and D/H ratios decrease. The difference of $^{18}O/^{16}O$ isotope ratios can reach 10‰. The effect of temperature is shown in the isotope ratio of the rainwater, i.e., in Central Europe, warm, Mediterranean rainwater originating from the south usually contains more heavier isotopes than rainwater coming from the north.

- There is a linear relationship between the $\delta^{18}O$ and δD values. The function is called the Global Meteoric Water Line—GMWL:

$$\delta D = 8\delta^{18}O + \delta \tag{3.46}$$

The slope of the straight line is 8, while the intercept, which is the mean value of δ, is 10. $\delta^{18}O = 0$ represents the Standard Mean Ocean Water, in which the abundance ($R_{standard}$) of hydrogen isotopes is about 10 times lower than that of oxygen isotopes. It should be noted that the mean value (10) includes fairly high differences: in North America, this value is +6‰, while in Mediterranean areas, it is +22‰. The difference comes from the partial pressure of the isotope molecules. The slope of the GMWL, however, is independent of geographical location, except that when water evaporation is significant, the slope is in the range of 3−6. As before, this fact can be explained by the effect of the temperature: when the temperature increases, the heavier isotope molecules evaporate more quickly.

- At high temperatures, isotope exchanges can take place between water and rocks (Eq. (3.45)). This is a chemical isotope effect, which causes the increase of the $^{18}O/^{16}O$ ratio in water and simultaneously the decrease of this ratio in the rocks. Since the oxygen content of the rocks is much higher than the hydrogen content, the change of the hydrogen isotopes can be neglected.
- The isotope ratio allows for the possibility of finding the leakages in the aquifers. The δ values are additive, so they can be used to study the communication between the aquifers when the composition of water is very similar, but the isotope ratios are different. Because of the additive character of $\delta^{18}O$ and δD ratios, the degree of mixing, if any, can be calculated.

3.4.3 Changes in the Isotope Ratio of Nitrogen

The main source of nitrogen is the air; the $^{15}N/^{14}N$ isotope ratio of the air (free of anthropogenic pollutants) has been chosen as the standard (see Table 3.6 earlier in this chapter). In addition, the biosphere also contains a significant amount of nitrogen. Nitrogen is not frequently observed in the rocks because the nitrates usually dissolve in water. The nitrate in water, however, is toxic. The $\delta^{15}N$ value can give information on the origin of the polluting sources of nitrate, assuming that the nitrogen isotope ratios are different and that neither isotope exchanges nor chemical reactions take place between the different sources of nitrate.

The sources of nitrate can include the following:

- The nitrogen content of soils, including all nitrogen compounds. The characteristic value of $\delta^{15}N$ soils is in the range of +5‰ to +9‰.
- The nitrate content of the soil, $\delta^{15}N$ is +2‰ to +9‰. This value shows that the abundance of ^{15}N of the nitrate in soil can be lower than the mean value of $\delta^{15}N$.
- The fresh excrement of animals typically has $\delta^{15}N$ in the range of +1 and +6‰; however, for example, penguin excrement shows $\delta^{15}N \approx +8$‰. When aging, ammonia, with the

lighter isotope (^{14}N), evaporates because the partial pressure of ammonia containing the lighter isotope is higher. Therefore, $\delta^{15}N$ increases up to +10‰ to +23‰. In the soil of the rookeries, $\delta^{15}N$ is even higher, and in the soil of a penguin rookery, it can reach more than +30‰.

- Synthetic fertilizers have $\delta^{15}N = +2‰$ to +7‰. This value can be explained by the fact that the fertilizers are synthesized from air ($\delta^{15}N = 0$) and mineral nitrogen sources with much higher $\delta^{15}N$. In addition, the chemical isotope effects during the production (i.e., the contact catalytic synthesis of ammonia) can also influence the isotope ratio.
- When the nitrate content of the fertilizers (including organic and synthetic) by the evaporation of ammonia decreases by 20%, the $\delta^{15}N$ increases by 5‰. Since the nitrogen isotope ratios are different in the original organic and inorganic fertilizers, a given value of $\delta^{15}N$ can relate to different polluting sources. For example, in sandy soil, $\delta^{15}N = +4‰$ to +5‰ may show that the polluting source is synthetic fertilizer, while in clayey soil, the same value can mean that the pollution originates from organic fertilizer. Therefore, the nitrogen isotope ratio alone gives no definite information on the polluting sources.

The ratio of $^{15}N/^{14}N$ presents a characteristic distinction between herbivores and carnivores, as the ^{15}N isotope tends to be concentrated by 3−4‰ with each step of the food chain (terrestrial plants, with the exception of legumes, has the isotopic ratio 2−6‰ of N). Measuring the nitrogen isotope ratio in hair, for example, can give archeological information on alimentary habits.

3.4.4 Isotope Ratios of Carbon

Since carbon compounds are present in any sphere of the Earth (atmosphere, hydrosphere, lithosphere, or biosphere), the determination of the carbon isotope ratios obviously plays an important role in the study of the global carbon cycle. In addition, the isotope analysis of other planets provides important information. For example, the $\delta^{18}O$ is the same in the rocks of the upper parts of the Earth's crust and the Moon ($\delta^{18}O = 5.5 \pm 0.2‰$), proving that the Earth and Moon share the same origin.

An important question in the global carbon cycle is the carbon isotope ratio of the Earth's mantle. Because of the very high temperature, even isotope composition should be expected; however, there are significant differences in the isotope ratio of different minerals. Diamond and SiC mineral, for example, contain more ^{12}C isotopes than magmatic minerals.

Deviation from the mean carbon isotope ratios refers to the major extinction event. Since the $^{13}C/^{12}C$ ratio of the biomass is lower than that of the sedimentary carbonate rocks, the sediments forming during the extinction events from the biomass show lower $^{13}C/^{12}C$ ratio than the mean value of the carbonate rocks. The $^{13}C/^{12}C$ can continue to decrease via the release of methane-hydrate bound to the deep-sea sediments, which is due to bacterial activity that prefers the light carbon isotope. During global warming, the methane-hydrate releases as carbon dioxide, increasing the carbon dioxide content of the atmosphere. The industrial carbon dioxide emission also decreases the $^{13}C/^{12}C$ ratio because of the burning of fossil fuel. All the above processes are in fact the consequence of biological isotope effects.

3.4.5 Stable Isotope Ratios in Ecological Studies

The stable isotope ratios provide information on the presence and magnitude of important ecological processes. Many ecological processes produce characteristic isotope ratios. The stable isotope ratio value relative to known background values may indicate the presence or absence of such processes. The exact values of the isotope ratios make it possible to determine the magnitude of these processes, if any.

As mentioned previously, in the case of carbon isotope ratios, the climatic changes can influence the stable isotope ratios. In addition, the change of other environmental conditions can also affect the isotope ratios. Environmental changes can be studied using some substances (tree rings, hair, and ice cubes) that preserve a record of the isotope ratios for a long time.

The isotope ratios remain the same during the movement of different elements and compounds. As a result, the source of essential elements, resources, or pollutions is easily traced using isotope ratios. The isotope ratios can be very different depending on geographic location. This provides a way to trace the movement or origin of a substance or component in the landscape to continental scales. The origins of environmental pollutions can be identified in this way. For example, the origin of waste deposits by paint factories can be identified using the lead isotope ratios of the raw material. Lead has four stable isotopes: ^{204}Pb, ^{206}Pb, ^{207}Pb, and ^{208}Pb. ^{204}Pb is a primordial isotope, and the other ones are the final stable members of the radioactive decay series (as discussed in Section 4.2). Since the quantity of ^{204}Pb isotope remains constant and the quantity of ^{206}Pb, ^{207}Pb, and ^{208}Pb changes over time and depends on the uranium and thorium concentrations, the isotope composition of lead strongly depends on its origin, which can then easily be identified. As will be discussed in Section 4.3.1, the isotope ratios of lead can also be used to date rocks.

Further Reading

Choppin, G.R. and Rydberg, J. (1980). *Nuclear Chemistry, Theory and Applications*. Pergamon Press, Oxford.

Demény, A. (2004). *Stabilizotóp-geokémia (Stable isotope geochemistry)*. Magyar Kémiai Folyóirat 109−110:192−198.

Friedlander, G., Kennedy, J.W., Macias, E.S. and Miller, J.M. (1981). *Nuclear and Radiochemistry*. John Wiley and Sons, New York, NY.

Ghosh, P., Adkins, J., Affek, H., Balta, B., Guo, W., Schauble, E.A., et al. (2006). ^{13}C−^{18}O bonds in carbonate minerals: a new kind of paleothermometer. *Geochim. Cosmochim. Acta* 70:1439−1456.

Haissinsky, M. (1964). *Nuclear Chemistry and its Applications*. Addison-Wesley Publishing Company, Inc., Reading, MA.

University of Wyoming, USA. <http://www.uwyo.edu/sif/stable-isotopes/index.html.> (accessed 24.03.12.)

Lieser, K.H. (1997). *Nuclear and Radiochemistry*. Wiley-VCH, Berlin.

McKay, H.A.C. (1971). *Principles of Radiochemistry*. Butterworths, London.

4 Radioactive Decay

As mentioned earlier (Section 2.1.1), the stability of a nucleus (as characterized by the binding energy) is determined by the ratio of protons to neutrons (see Eq. (2.10)). The binding energy of isobar nuclei as a function of proton−neutron ratio forms a parabola or parabolas (see Figure 3.1), where those nuclei close to the minimum are stable while those farther away are undergoing radioactive decay in order to reach the optimal proton/neutron ratio. The radioactive decay is a random process for the individual nucleus so as to describe the kinetics of radioactive decay, a statistical approach has to be applied.

4.1 Kinetics of Radioactive Decay

4.1.1 Statistics of Simple Radioactive Decay

Let us consider that the probability of the decomposition of a radioactive nuclide in a Δt time interval is p:

$$p = \lambda \Delta t \tag{4.1}$$

where λ is a factor of proportionality. The probability of the process that the nuclide does not decompose in Δt is:

$$1 - p = 1 - \lambda \Delta t \tag{4.2}$$

The probability that the nuclide does not decompose in another second, third, or more Δt interval can also be defined by Eq. (4.2). The probability that the nuclide does not decompose in the $2 \times \Delta t$ interval is:

$$(1 - p)^2 = (1 - \lambda \Delta t)^2 \tag{4.3}$$

The probability that the nuclide does not decompose in $n \times \Delta t$ is:

$$(1 - p)^n = (1 - \lambda \Delta t)^n \tag{4.4}$$

Let us divide the total time of the observation (t) into n intervals:

$$\frac{t}{n} = \Delta t \tag{4.5}$$

Nuclear and Radiochemistry. DOI: http://dx.doi.org/10.1016/B978-0-12-391430-9.00004-4

Substituting Eq. (4.5) into Eq. (4.4), we obtain:

$$(1-p)^n = \left(1 - \lambda\frac{t}{n}\right)^n \tag{4.6}$$

At $n \to \infty$:

$$\lim_{n\to\infty}(1-p)^n = \lim_{n\to\infty}\left(1 - \lambda\frac{t}{n}\right)^n = \mathrm{e}^{-\lambda t} \tag{4.7}$$

When the initial number of the radioactive nuclides is N_0, the number of nuclides that do not undergo radioactive decomposing during t time (N) is:

$$N = N_0\,\mathrm{e}^{-\lambda t} \tag{4.8}$$

Equation (4.8) describes the kinetics of the simple radioactive decay, i.e., the radioactive decay law, where λ is the decay constant. The value of the decay constant characterizes the radionuclide; thus, it is independent of physical and chemical conditions (pressure, temperature, chemical environment, etc.).

As seen in Eq. (4.8), the radioactive decay has first-order kinetics, having all characteristics of first-order reactions. It has a well-defined half-life ($t_{1/2}$), i.e., the time needed to reduce the number of the radioactive nuclides to half:

$$\frac{N_0}{2} = N_0\,\mathrm{e}^{-\lambda t_{1/2}} \tag{4.9}$$

and from here,

$$\lambda = \frac{\ln 2}{t_{1/2}} \tag{4.10}$$

Half-life performance 7 and 10 times over gives the interval when the number of radionuclides decreases below 1% and 0.1% of the initial number, respectively.

The reciprocal of the decay constant (λ) is the average lifetime (τ) of the radionuclides, which is the time when the number of the radionuclides decreases by a factor of e (i.e., Euler's constant). This amount of time should be required for the decomposition of all radionuclides if the rate of decay remains constant.

$$\tau = \int_0^\infty \frac{t\lambda N\,\mathrm{d}t}{N_0} = \int_0^\infty t\lambda\,\mathrm{e}^{-\lambda t}\,\mathrm{d}t = \lambda\left[\frac{\mathrm{e}^{-\lambda t}}{\lambda^2}(-\lambda t - 1)\right]_0^\infty = \frac{1}{\lambda} \tag{4.11}$$

4.1.2 Activity and Intensity

Radioactivity (A, also known "absolute activity") is defined as the number of decompositions in a unit time. Radioactivity is in proportion to the initial quantity of the radioactive nuclei:

$$A = -\frac{\mathrm{d}N}{\mathrm{d}t} = \lambda N = \lambda N_0 \, \mathrm{e}^{-\lambda t} = A_0 \, \mathrm{e}^{-\lambda t} \tag{4.12}$$

It is important to note that the activity−time function (Figure 4.12) is analogous to the number of the radioactive nuclei−time function (Eq. (4.8)).

The unit of radioactivity is the becquerel (Bq), which describes the number of decomposition/disintegrations that take place in 1 s (1 Bq = 1 dps = 1 disintegrations per second). An earlier unit of radioactivity was the curie (Ci), which is the number of decompositions in 1 g of radium in 1 s. The relation between the two activity units is $1\ \mathrm{Ci} = 3.7 \times 10^{10}$ Bq. Besides these two, dpm (which means "disintegrations per minute") is frequently used for practical purposes.

Radioactivity is usually measured not by identifying the radioactive nuclei but by counting the emitted particles. In theory, to achieve accurate activity measurement, all particles emitted in 4π spatial angles should be taken into consideration. In practical applications, however, it is more common that the radioactive intensity (I), a quantity proportional to the radioactivity, is measured. The proportionality factor is the measuring efficiency (k):

$$I = kA = k\lambda N \tag{4.13}$$

The intensity−time function, of course, is similar to the activity−time function (shown in Eq. (4.12)):

$$I = I_0 \, \mathrm{e}^{-\lambda t} \tag{4.14}$$

Obviously, this relation is valid so long as the measuring efficiency (k) stays constant for all measurements.

The units of intensity are as follows:

- cpm means counted particles per minute,
- cps is counted particles per second.

4.1.3 Decay of Independent (Mixed) Nuclei

There are cases when more than one radionuclide is present at the same time. The radioactivity, as well as the activity−time function, depends on all the radionuclides that are present. The identification of each nuclide requires the mathematical decomposition of the activity−time function into components. Then, the identification of the radionuclides present can be done on the basis of the type of decay, the energy, and the half-life of the emitted particles.

When the decays of the radioactive nuclei present are independent, the radioactivities of the mixed nuclides are the sum of the radioactivities of all nuclides. Consequently, the activity−time function cannot be described by the kinetic of the simple radioactive decay (Eq. (4.8)). This means that the radioactivity−time curve must be decomposed. In principle, the decomposition could be done easily by using computing techniques. However, since the functions have to be fitted to the experimental activity−time function, it has some limitations; for example, the activity/intensity and the half-life of the individual isotopes can be determined only by the decomposition of the activity/intensity−time function if there is at least one order of magnitude difference in the half-lives, and if the isotope mixture does contain only a limited number of different radioactive isotopes. If these conditions are not met, adding or neglecting additional nuclides does not improve the accuracy of the mathematical decomposition of the activity−time function.

4.1.4 Branching Decay

A radioactive decay is described as branching when one parent element decomposes to two daughter nuclides. This type of decay can be characterized by two decay constants and half-lives as follows:

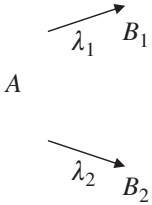

where A is the parent nuclide, B_1 and B_2 are the daughter nuclides, and λ_1 and λ_2 are the decay constants for the production of B_1 and B_2, respectively. Examples of such decay are the decomposition of the ^{212}Pb isotope into ^{212}Po and ^{212}Tl, the decay of ^{64}Cu isotope to ^{64}Zn and ^{64}Ni, and the disintegration of the ^{40}K isotope into ^{40}Ca and ^{40}Ar isotopes.

Since during branching decay, the quantity of the parent element decreases via two independent processes, the rate of decay of the parent element can be defined by the sum of the two decay constants:

$$-\frac{\mathrm{d}N}{\mathrm{d}t} = (\lambda_1 + \lambda_2)N \tag{4.15}$$

From here,

$$\frac{\mathrm{d}N}{N} = -(\lambda_1 + \lambda_2)\mathrm{d}t \tag{4.16}$$

By the integration of Eq. (4.16):

$$\ln N = -(\lambda_1 + \lambda_2)t + \text{constant} \tag{4.17}$$

Assuming that at $t = 0$, $N = N_0$:

$$N = N_0 \, \mathrm{e}^{-(\lambda_1+\lambda_2)t} \tag{4.18}$$

Equation (4.18) is similar to the kinetics of the simple radioactive decay (Eq. (4.8)), except that the sum of the individual constants is used as the decay constant. In those cases, when the daughter elements formed through different decay mechanisms or the energy of the emitted radiation is sufficiently different, the values of the decay constants can be determined separately. The proportion of the decay constants will determine the relative quantity of the daughter nuclides formed.

In most cases, however, both daughter elements are formed via beta decay, the spectra of which is continuous (see Section 4.4.2), and the decays are very difficult or impossible to separate. In this case, the ratio of the quantity of the daughter elements can be calculated as follows.

The sum of the quantities of the two daughter elements is equal to the quantity of the decomposed parent element at any time:

$$B_1 + B_2 = N_0 - N = N_0(1 - \mathrm{e}^{-(\lambda_1+\lambda_2)t}) \tag{4.19}$$

The rate of the formation of the daughter elements is:

$$\frac{\mathrm{d}B_1}{\mathrm{d}t} = \lambda_1 N = \lambda_1 N_0 \, \mathrm{e}^{-(\lambda_1+\lambda_2)t} \tag{4.20}$$

$$\frac{\mathrm{d}B_2}{\mathrm{d}t} = \lambda_2 N = \lambda_2 N_0 \, \mathrm{e}^{-(\lambda_1+\lambda_2)t} \tag{4.21}$$

By integrating Eqs. (4.20) and (4.21) from $t = 0$ to ∞:

$$B_1 = \left[-\frac{\lambda_1}{\lambda_1+\lambda_2} N_0 \, \mathrm{e}^{-(\lambda_1+\lambda_2)t} \right]_0^{\infty} \tag{4.22}$$

$$B_2 = \left[-\frac{\lambda_2}{\lambda_1+\lambda_2} N_0 \, \mathrm{e}^{-(\lambda_1+\lambda_2)t} \right]_0^{\infty} \tag{4.23}$$

we obtain:

$$B_1 = \frac{\lambda_1}{\lambda_1 + \lambda_2} N_0 \tag{4.24}$$

$$B_2 = \frac{\lambda_2}{\lambda_1 + \lambda_2} N_0 \tag{4.25}$$

The ratio of Eqs. (4.24) and (4.25) is:

$$\frac{B_1}{B_2} = \frac{\lambda_1}{\lambda_2} \tag{4.26}$$

Therefore, in branching decay, the ratio of the quantities of the daughter elements is equal to the ratio of the decay constants. By determining the quantities of the daughter elements, the ratio of the decay constants can be calculated.

Equations (4.20) and (4.21) have been integrated from $t = 0$ to ∞, but the same results are obtained by the integration over any time interval.

4.1.5 Kinetics of Successive Decay

When the daughter element of a parent element is also radioactive and decays further, we describe this as a successive decay series. It means that there are genetic relations between the radionuclides. There are some similar decay series in the products of uranium fission initiated by neutrons. For example, ^{90}Sr isotope decomposes by negative beta decay to ^{90}Y, which also decomposes by negative beta decay to stable ^{90}Zr. In this series, there are two successive decays; however, there are series with more than two successive decays. Three natural radioactive decay series where alpha and beta decays form long decay series are known. Their starting parent nuclides are ^{235}U, ^{238}U, and ^{232}Th isotopes, and the last, stable nuclides are different lead isotopes, namely, ^{207}Pb, ^{206}Pb, and ^{208}Pb. These natural radioactive decay series are shown in Figures 4.4–4.6.

For simplicity, the kinetics of the radioactive decay series are demonstrated for the two-member decay series (a parent nuclide and one radioactive daughter nuclide). The total radioactivity (A) is the sum of the radioactivities of the parent (A_1) and daughter (A_2) nuclides:

$$A = A_1 + A_2 \tag{4.27}$$

The kinetics of the radioactive decay of the parent nuclide can be described using the kinetics of the simple decay, as discussed previously:

$$A_1 = \lambda_1 N_1 = \lambda_1 N_0 \, \mathrm{e}^{-\lambda_1 t} \tag{4.28}$$

The radioactivity of the daughter nuclides depends on two factors: it continuously forms from the parent nuclide and decays. Therefore, the quantity of the daughter nuclide is determined both by the rate of its formation and by its decay:

$$\frac{\mathrm{d}N_2}{\mathrm{d}t} = \lambda_1 N_1 - \lambda_2 N_2 \tag{4.29}$$

In Eqs. (4.28) and (4.29), N_1 and N_2 are the number of the parent and daughter nuclides, respectively; λ_1 and λ_2 are their decay constants.

For the solution of Eq. (4.29), the next substitutions are applied:

$$N_2 = u \times v \tag{4.30}$$

and

$$v = \mathrm{e}^{-\lambda_2 t} \tag{4.31}$$

The total derivative with respect to t of the function in Eq. (4.30) is:

$$\frac{\mathrm{d}N_2}{\mathrm{d}t} = \frac{\mathrm{d}(uv)}{\mathrm{d}t} = uv' + u'v = -u\lambda_2 \, \mathrm{e}^{-\lambda_2 t} + \mathrm{d}u \, \mathrm{e}^{-\lambda_2 t} \tag{4.32}$$

From Eqs. (4.29) and (4.32):

$$-u\lambda_2 \, \mathrm{e}^{-\lambda_2 t} + \mathrm{d}u \, \mathrm{e}^{-\lambda_2 t} = \lambda_1 N_1 - \lambda_2 N_2 \tag{4.33}$$

By substituting Eqs. (4.28) and (4.30) into Eq. (4.33), we obtain:

$$-u\lambda_2 \, \mathrm{e}^{-\lambda_2 t} + \mathrm{d}u \, \mathrm{e}^{\lambda_2 t} + u\lambda_2 \, \mathrm{e}^{-\lambda_2 t} - \lambda_1 N_{10} \, \mathrm{e}^{-\lambda_1 t} = 0 \tag{4.34}$$

After mathematical simplification:

$$\mathrm{d}u \, \mathrm{e}^{-\lambda_2 t} - \lambda_1 N_{10} \, \mathrm{e}^{-\lambda_1 t} = 0 \tag{4.35}$$

The solution of Eq. (4.35) is:

$$\int \mathrm{d}u = \int \lambda_1 N_{10} \, \mathrm{e}^{(\lambda_2 - \lambda)t} \tag{4.36}$$

$$u = \frac{\lambda_1}{\lambda_2 - \lambda_1} N_{10} \, \mathrm{e}^{(\lambda_2 - \lambda_1)t} + C \tag{4.37}$$

where C is a constant. By substituting Eq. (4.37) into Eq. (4.30):

$$N_2 = \frac{\lambda_1}{\lambda_2 - \lambda_1} N_{10} \, \mathrm{e}^{-\lambda_1 t} + C \, \mathrm{e}^{-\lambda_2 t} \tag{4.38}$$

When at $t = 0$, $N_2 = N_{20}$, then from Eq. (4.38):

$$N_{20} = \frac{\lambda_1}{\lambda_2 - \lambda_1} N_{10} + C \tag{4.39}$$

By expressing C and substituting into Eq. (4.38), we obtain:

$$N_2 = \frac{\lambda_1}{\lambda_2 - \lambda_1} N_{10} \, \mathrm{e}^{-\lambda_1 t} + \left(N_{20} - \frac{\lambda_1}{\lambda_2 - \lambda_1} N_{10} \right) \mathrm{e}^{-\lambda_2 t} \tag{4.40}$$

After equivalent mathematical transformation:

$$N_2 = \frac{\lambda_1}{\lambda_2 - \lambda_1} N_{10}\, \mathrm{e}^{-\lambda_1 t}\left[1 - \mathrm{e}^{(\lambda_1 - \lambda_2)t}\right] + N_{20}\, \mathrm{e}^{-\lambda_2 t} \tag{4.41}$$

or

$$N_2 = \frac{\lambda_1}{\lambda_2 - \lambda_1} N_{10}\left[\mathrm{e}^{-\lambda_1 t} - \mathrm{e}^{-\lambda_2 t}\right] + N_{20}\, \mathrm{e}^{-\lambda_2 t} \tag{4.42}$$

Instead of the number of the radioactive nuclides, radioactivities can be written using $A_2 = N_2\lambda_2$ and $A_1 = N_1\lambda_1$:

$$A_2 = \frac{\lambda_2}{\lambda_2 - \lambda_1} A_{10}\, \mathrm{e}^{-\lambda_1 t}\left[1 - \mathrm{e}^{(\lambda_1 - \lambda_2)t}\right] + A_{20}\, \mathrm{e}^{-\lambda_2 t} \tag{4.43}$$

This equation of the activity can be transformed directly to intensities only if the measuring efficiency for both the parent and daughter nuclides is the same. If not, intensity can be measured only after reaching radioactive equilibrium (see Section 4.1.6).

The first and second members in Eq. (4.41) express, respectively, the increase and decay of the quantity of the daughter nuclide compared to its quantity at $t = 0$. The maximum quantity of the daughter nuclide can be determined by the differentiation of Eq. (4.41): the quantity of the daughter nuclide is maximized when Eq. (4.41) has an extremum. For the sake of simplicity, suppose that, at $t = 0$, $N_2 = 0$:

$$\frac{\mathrm{d}N_2}{\mathrm{d}t} = -\frac{\lambda_1\lambda_1}{\lambda_2 - \lambda_1} N_{10}\, \mathrm{e}^{-\lambda_1 t} + \frac{\lambda_1\lambda_2}{\lambda_2 - \lambda_1} N_{10}\, \mathrm{e}^{-\lambda_2 t} = 0 \tag{4.44}$$

From here:

$$t_{\max} = \frac{1}{\lambda_1 - \lambda_2} \ln \frac{\lambda_1}{\lambda_2} \tag{4.45}$$

At $t = 0$, $N_2 \neq 0$, the equation has an additional member (which is not discussed here).

For radioactive decay series having more than two members, the formation and decay rates can be defined for the third to nth members, similar to Eq. (4.29):

$$\frac{\mathrm{d}N_3}{\mathrm{d}t} = \lambda_2 N_2 - \lambda_3 N_3$$

$$\frac{\mathrm{d}N_n}{\mathrm{d}t} = \lambda_{n-1} N_{n-1} - \lambda_n N_n \tag{4.46}$$

The solution of the rate equations can be given as follows:

$$N_n = \sum_{i=1}^{n} c_i^n \, \mathrm{e}^{-\lambda_i t} \tag{4.47}$$

where

$$c_i^n = N_{10} \frac{\prod_{k=1}^{n-1} \lambda_k}{\prod_{\substack{k=1 \\ k \neq i}}^{n} (\lambda_k - \lambda_i)} \tag{4.48}$$

For three members:

$$N_3 = N_{10} \left[\frac{\lambda_1 \lambda_2 \, \mathrm{e}^{-\lambda_1 t}}{(\lambda_2 - \lambda_1)(\lambda_3 - \lambda_1)} + \frac{\lambda_1 \lambda_2 \, \mathrm{e}^{-\lambda_2 t}}{(\lambda_1 - \lambda_2)(\lambda_3 - \lambda_2)} + \frac{\lambda_1 \lambda_2 \, \mathrm{e}^{-\lambda_3 t}}{(\lambda_1 - \lambda_3)(\lambda_2 - \lambda_3)} \right] \tag{4.49}$$

4.1.6 Radioactive Equilibria

The properties of the radioactive decay series depend on the ratio of the decay constants of the isotopes in genetic relations. Four different scenarios can occur:

1. $\lambda_1 < \lambda_2$: the parent nuclide decays more slowly than the daughter nuclide.
2. $\lambda_1 \ll \lambda_2$: the parent nuclide decays much more slowly than the daughter nuclide.
3. $\lambda_1 > \lambda_2$: the parent nuclide decays faster than the daughter nuclide.
4. $\lambda_1 \approx \lambda_2$: the decay rates are approximately the same.

Depending on the ratio of the decay constants, radioactive equilibria of the isotopes in genetic relations can (or cannot) be reached:

1. When the parent nuclide decays more slowly than the daughter nuclide ($\lambda_1 < \lambda_2$), the exponential function $\mathrm{e}^{(\lambda_1 - \lambda_2)t}$ in Eq. (4.41) tends to become zero after a sufficient length of time. Supposing that no daughter nuclide is present at $t = 0$ (at $t = 0$, $N_2 = 0$), Eq. (4.41) becomes:

$$N_2 = \frac{\lambda_1}{\lambda_2 - \lambda_1} N_{10} \, \mathrm{e}^{-\lambda_1 t} \tag{4.50}$$

that is,

$$N_2 = \frac{\lambda_1}{\lambda_2 - \lambda_1} N_1 \tag{4.51}$$

Expressing radioactivities, assuming that $N_2 = A_2/\lambda_2$ and $N_1 = A_1/\lambda_1$, we obtain:

$$A_2 = \frac{\lambda_2}{\lambda_2 - \lambda_1} A_1 \tag{4.52}$$

An equivalent mathematical transformation of Eq. (4.51) results in:

$$\frac{\lambda_1 N_1}{\lambda_2 N_2} = 1 - \frac{\lambda_1}{\lambda_2} \tag{4.53}$$

On the right side of Eq. (4.53), only constant values are present. This means that the right side itself is also constant. Since $\lambda_1 < \lambda_2$, its value is between 0 and 1. Consequently, the left side of Eq. (4.53) is also constant, which assumes that the ratio of the radioactivities of the parent and daughter nuclides is constant. This is a form of the radioactive equilibria of isotopes in genetic relation, called a transient or current equilibrium. In a transient equilibrium, the radioactivity of the daughter nuclide is always higher. In Figure 4.1, the radioactivities of the parent and daughter nuclides and the total activity are both plotted as a function of time.

As seen in Figure 4.1, the slope of the activity−time functions becomes the same (λ_1) after reaching the transient equilibrium, which means that the radioactivity of the daughter nuclide can be described by the decay constant (or the half-life) of the parent nuclide. The radioactivity can be measured correctly after reaching the transient equilibrium. The time needed to reach the transient equilibrium can be determined by the maximum quantity of the daughter nuclide (Eq. (4.45)) when $t = 0$, $N_2 = 0$; if not, an extended equation has to be used which is not discussed here.

2. When the parent nuclide decays much more slowly than the daughter nuclide, $\lambda_1 \ll \lambda_2$, and $t = 0$, $N_2 = 0$, Eq. (4.41) becomes:

$$N_2 = \frac{\lambda_1}{\lambda_2} N_{10}\, \mathrm{e}^{-\lambda_1 t}\left[1 - \mathrm{e}^{-\lambda_2 t}\right] \tag{4.54}$$

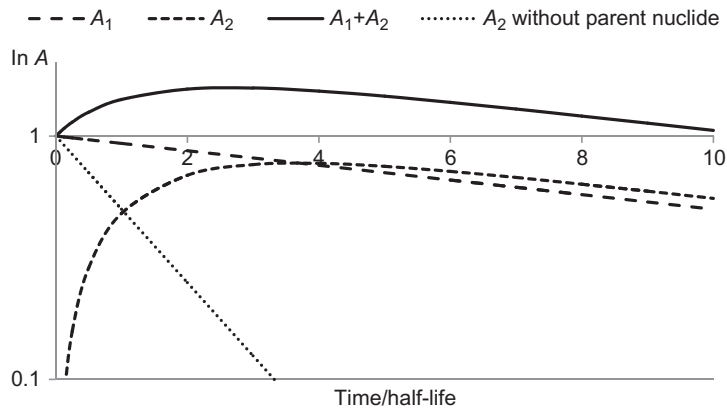

Figure 4.1 Transient equilibrium: activities of the parent nuclide (A_1), the daughter nuclide (A_2), the total activity ($A_1 + A_2$), and the activity of the daughter nuclide when not produced from the parent nuclide as a function of time. Time is expressed compared to the half-life of the daughter nuclide. The ratio of the half-life of parent nuclide:daughter nuclide is 10:1.

Since the parent nuclide decays very slowly (i.e., $e^{-\lambda_1 t} \approx 1$):

$$N_2 = \frac{\lambda_1}{\lambda_2} N_{10} \left[1 - e^{-\lambda_2 t}\right] \tag{4.55}$$

This is expressed in activities as follows:

$$A_2 = A_{10}[1 - e^{-\lambda_2 t}] \tag{4.56}$$

After about 10 half-lives of the daughter nuclide, $e^{-\lambda_2 t} \approx 0$; so, from Eq. (4.56), we obtain:

$$N_2 = \frac{\lambda_1}{\lambda_2} N_{10} \tag{4.57}$$

and from here,

$$N_2 \lambda_2 = N_{10} \lambda_1 \tag{4.58}$$

When the decay series composes more than two members, Eq. (4.58) applies to all members:

$$N_1 \lambda_1 = N_2 \lambda_2 = \cdots = N_n \lambda_n = A_1 = A_2 = \cdots = A_n \tag{4.59}$$

Equation (4.59) means that in equilibrium, the radioactivity of all nuclides is the same. This type of radioactive equilibria is called "secular equilibrium." In Figure 4.2, the activities of the parent and daughter nuclides are plotted as a function of time under the conditions of the secular equilibrium.

In a secular equilibrium, the short or very long half-lives of the members can be determined if the quantity of the nuclides and the half-life or decay constant of one of the nuclides is known. For example, the second member in the decay series of ^{238}U is the ^{234}Th isotope. The half-lives are 24.1 days for ^{234}Th and 4.5×10^9 years for ^{238}U. The very long half-life of ^{238}U can be determined by the quantitative separation and activity measurement of ^{234}Th. The quantity of ^{238}U can be determined by any chemical analytical method (the chemical analysis and the activity measurements are independent methods). From these data, the half-life or the decay constant of ^{238}U can be calculated using Eq. (4.59) when ^{238}U and ^{234}Th are in secular equilibrium.

3. When $\lambda_1 > \lambda_2$, the parent nuclide decays faster than the daughter nuclide. This is important in the production of radioactive isotopes when the parent nuclide can be produced easily or a carrier-free daughter nuclide is required. Since the decay of the parent nuclide occurs faster, decomposition of the parent nuclide yields a pure daughter nuclide. The optimal conditions of the yield of the daughter nuclide (the time of the maximum activity) can be determined by Eq. (4.45). This time shows the time of the so-called ideal equilibrium, when the activities of the

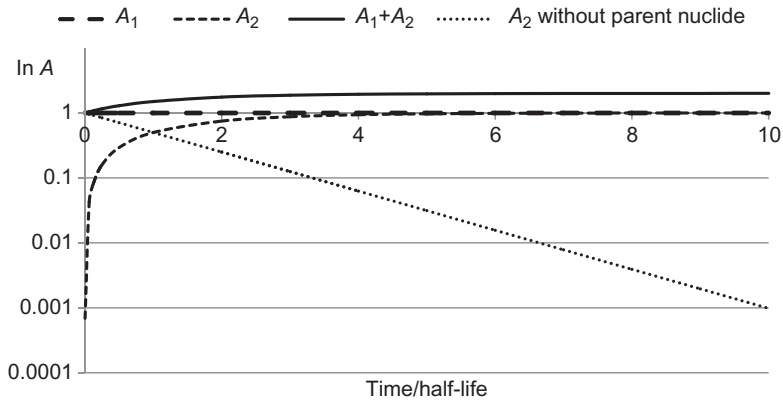

Figure 4.2 Secular equilibrium: activities of the parent nuclide (A_1), the daughter nuclide (A_2), the total activity ($A_1 + A_2$), and the activity of the daughter nuclide when not produced from the parent nuclide as a function of time. Time is expressed compared to the half-life of the daughter nuclide.

parent and daughter nuclides are the same. This means when the parent nuclide decays faster than the daughter nuclides, they are in equilibrium for one moment (at t_{max}, $A_1 = A_2$). The kinetics of the decay of the daughter nuclide is described by Eqs. (4.41) and (4.42). In Figure 4.3, the activities of the parent and daughter nuclide are shown as a function of time.

As an example of the isotope production when $\lambda_1 > \lambda_2$, the production of ^{131}I from tellurium is mentioned:

$$^{130}\text{Te}(n,\gamma)^{131}\text{Te} \xrightarrow{\beta^-} {}^{131}\text{I} \tag{4.60}$$

4. When $\lambda_1 \approx \lambda_2$ (i.e., the decay rates of the parent and daughter nuclides are approximately the same), Eq. (4.41) cannot be solved because of the zero value of the denominator ($\lambda_2 - \lambda_1 \approx 0$). So, the limit of the function is expressed as follows:

$$\lim_{\lambda_1 \to \lambda_2} N_2 = \lambda t N_{10}\, e^{-\lambda t} = \lambda t N_1 \tag{4.61}$$

In Eq. (4.61), the decay constant has no index because equality is assumed. The quantity of the daughter nuclide depends on the quantity of the parent nuclide and the time:

$$N_2 = N_1 \lambda t \tag{4.62}$$

Among the decay products of ^{222}Rn, ^{214}Pb and ^{214}Bi have similar half-lives, 19.9 and 26.8 min, respectively. By measuring the half-lives, these two isotopes

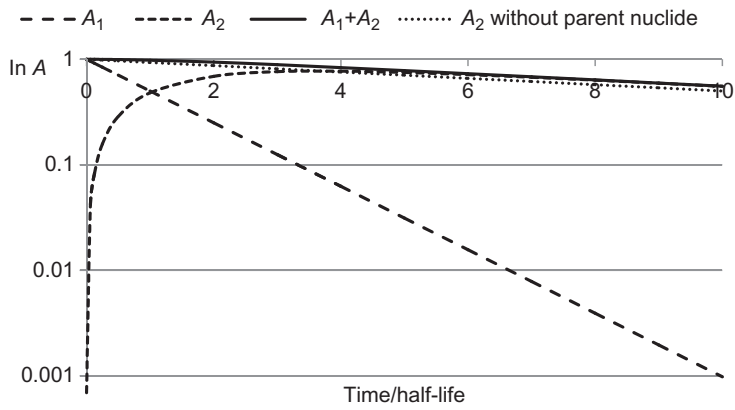

Figure 4.3 Activities of the parent nuclide (A_1), the daughter nuclide (A_2), the total activity ($A_1 + A_2$), and the activity of the daughter nuclide when not produced from the parent nuclide as a function of time. Time is expressed compared to the half-life of the parent nuclide. The ratio of the half-life of parent nuclide:daughter nuclide is 1:10.

cannot be separated. When they are present together, from the activity−time function, about 40 min is given for the half-life.

4.2 Radioactive Decay Series

There are three natural decay series that include the heavy elements, from thallium to uranium; their initial nuclides are ^{238}U, ^{235}U, and ^{232}Th isotopes, and via alpha and beta decays, they end up as lead isotopes (^{206}Pb, ^{207}Pb, and ^{208}Pb, respectively) (see Figures 4.4−4.6). The half-lives of the initial nuclides are about billion years, which is similar to the age of the Earth (as discussed in Section 6.2.5). The mass number of the members can be given as $4n$ in the thorium series, $4n + 2$ in the ^{238}U series, and $4n + 3$ in the ^{235}U series. The decay series characterized by $4n + 1$ starts with the ^{237}Np isotope, it can be produced artificially (see Section 6.2.6). Since the half-life of ^{237}Np is 2.2 million years, even if it was present at the time of the formation of the Earth, it has since decomposed.

4.3 Radioactive Dating

As discussed in Section 3.4, stable isotope ratios can be applied for different geological, ecological, and environmental studies, including the dating of different geological formations and groundwater. Besides stable isotopes, radioactive

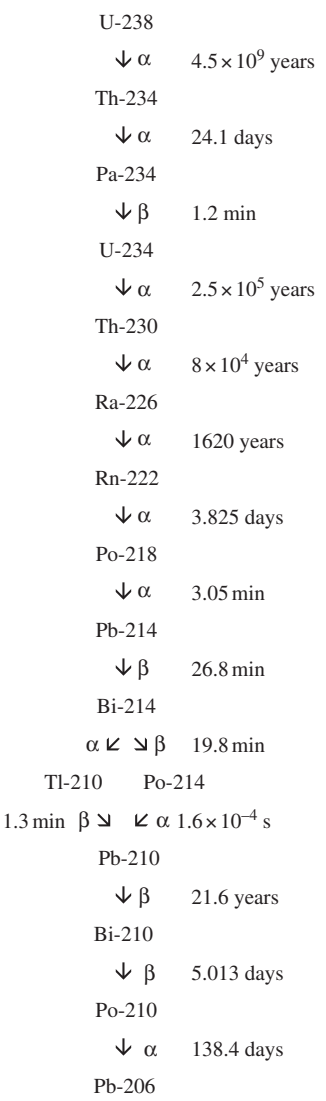

Figure 4.4 The main isotopes of the ^{238}U radioactive decay series.

isotopes or the stable products of different radioactive decays can be used for dating. In these studies, the half-lives of the radioactive isotopes play an important role; the interval, which can be determined by any radioactive dating method, depends on the half-life of the applied radioactive decay. For example, the age of the Earth and the Earth's crust can be estimated by radioactive dating to be about 5 and 3.6 billion years, respectively. These determinations are based on the fact that the half-lives of different radioactive isotopes are in the range of the age of the Earth and the Earth's crust. In this chapter, the main methods of radioactive dating will be discussed.

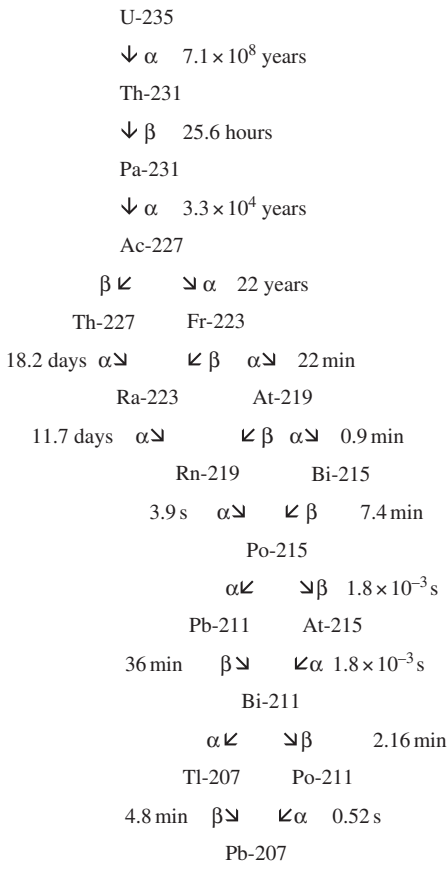

Figure 4.5 The main isotopes of the ^{235}U radioactive decay series.

4.3.1 Radioactive Dating by Lead Isotope Ratios

The age of rocks can be estimated by means of the radioactive decay series. Let us suppose that at the time of the rock formation, only the initial isotopes of the decay series had been produced, and the lead isotopes at the end of the decay series had been formed only from the initial uranium and thorium isotopes. As a result, the concentration of the lead isotopes (with 206, 207, and 208 mass numbers) in the rock is determined by the age. To derive the relationship between the ratio of the lead isotopes and the age of the rock, the ^{238}U decay series is used. According to the kinetics of the simple radioactive decay:

$$^{238}N = {}^{238}N_0 \, \mathrm{e}^{-\lambda_{238} t} \tag{4.63}$$

where ^{238}N and $^{238}N_0$ are the quantity of the ^{238}U isotope at the time of the measurement and at the time of the rock formation ($t = 0$), respectively, λ_{238} is the

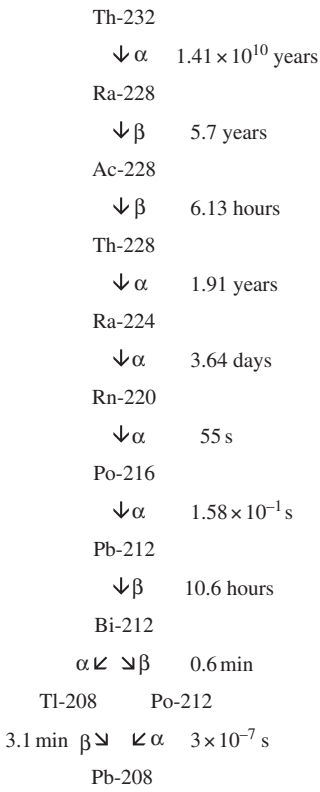

Figure 4.6 The main isotopes of the ^{232}Th radioactive decay series.

decay constant of ^{238}U, and t is the age of the rock. As the quantity of ^{238}U isotope decreases, the quantity of the stable nuclide (^{206}N), the ^{206}Pb isotope, increases:

$$^{206}N = {}^{238}N_0 - {}^{238}N = {}^{238}N_0(1 - e^{-\lambda_{238}t}) \tag{4.64}$$

Equation (4.64), however, cannot be used directly because the quantity of the ^{238}U at $t = 0$ is not known. This unknown quantity can be neglected if the ratio of the quantities of the first (^{238}U) and last (^{206}Pb) members of the decay series is expressed by dividing Eq. (4.64) by Eq. (4.63):

$$\frac{^{206}N}{^{238}N} = \frac{^{238}N_0(1 - e^{-\lambda_{238}t})}{^{238}N_0\, e^{-\lambda_{238}t}} = \frac{1 - e^{-\lambda_{238}t}}{e^{-\lambda_{238}t}} = e^{\lambda_{238}t} - 1 \tag{4.65}$$

Similar equations can be described for the other decay series, namely, for the ratio of the ^{207}Pb/^{235}U and the ^{208}Pb/^{232}Th isotopes:

$$\frac{^{208}N}{^{232}N} = e^{\lambda_{232}t} - 1 \tag{4.66}$$

$$\frac{^{207}N}{^{235}N} = e^{\lambda_{235}t} - 1 \tag{4.67}$$

where the Ns are the quantities of the isotopes (the mass numbers of which are signed in the upper indices), and the λs are the decay constants.

By measuring these ratios, the age of the geological formations can be determined. However, the chemical behavior of uranium, thorium, and lead, as well as the intermediate members of the decay series, is different, so they may have been leached from the rock differently. So, in this form, Eq. (4.65) can be applied only when the loss of the members of the uranium or thorium decay series can be neglected. If not, the different leaching of the uranium and lead can be neglected if the ratio of the lead isotopes is taken into consideration. The ratio of the uranium isotopes in nature is ^{235}U:$^{238}U = 1{:}139$, determined as follows:

$$^{238}N = 139^{235}N \tag{4.68}$$

When Eq. (4.67) is divided by Eq. (4.65) and Eq. (4.68) is substituted, we obtain:

$$\frac{^{207}N}{^{206}N} = \frac{1}{139}\frac{(e^{\lambda_{235}t} - 1)}{(e^{\lambda_{238}t} - 1)} \tag{4.69}$$

As a conclusion, the age of rocks can be estimated by means of Eq. (4.69) from the ratio of lead isotopes determined by mass spectrometry since the decay constants are known and thus t can be calculated. The advantage of this method is that it gives the right results even if the lead has been leached from the rock because the leaching does not change the ratio of the lead isotopes.

With these dating methods, the quantity of ^{206}Pb, ^{207}Pb, and ^{208}Pb are measured by mass spectrometry. For more accurate measurements, these quantities are related to the quantity of the ^{204}Pb isotope as a reference nuclide, which is not radiogenic.

4.3.2 Radioactive Dating by Helium Concentration

As seen in Figures 4.4–4.6, there are alpha decays in all decay series. The numbers of alpha decays are eight, seven, or six in the series of ^{238}U, ^{235}U, and ^{232}Th isotopes, respectively. Since the alpha particles are the nuclei of helium, the quantity of the helium gas accumulated inside the rocks can be applied to estimate age. Of course, this method can give the right ages only if the helium gas has not escaped from the rock.

From 1 g of uranium or thorium, 1.195×10^{-4} mm^3 or 2.9×10^{-5} mm^3 of helium gas is formed in a year. Therefore, this method requires the accurate determination of small volumes of helium gas. For this purpose, the rock is dissolved in a mixture of $H_2SO_4 + K_2S_2O_8$ or in an acidic oxidizing solution containing $CuCl_2$ and KCl, avoiding the formation of hydrogen gas in significant volumes. The few hydrogen and nitrogen molecules that form are oxidized by palladium or barium

catalysts, respectively. The noble gases are separated by activated carbon in a chromatographic procedure performed at the temperature of liquid nitrogen. In this way, the quantity of helium can be determined with an accuracy of about 2×10^{-7} cm^3.

4.3.3 Radioactive Dating by Fission of Uranium

By spontaneous fission of uranium (discussed in Section 4.4.5), different xenon isotopes ($^{129,\ 131,\ 132,\ 133,\ 136}$Xe) are formed. The age of uranium-containing rocks or ores can be determined from the quantity of the xenon accumulated in the rocks.

Besides spontaneous fission, the neutrons coming from the cosmic ray also induce the fission of uranium in the silicates. The fission products destroy the silicate lattice. The fission tracks can be etched (e.g., by hydrogen fluoride) so that they can become visible through a microscope. The age can be estimated from the density of the fission tracks.

4.3.4 Radioactive Dating by Argon Concentration

The only source of ^{40}Ar isotopes is branching decay (discussed in Section 4.1.4) of ^{40}K isotopes:

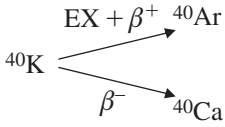

If all the argon gas stays trapped in the rock, the age of a potassium-containing rock can be estimated from the argon concentration:

$$^{Ar\text{-}40}N = {}^{K\text{-}40}N \frac{\lambda_{EX+\beta^+}}{\lambda_{EX+\beta^+ +\beta^-}} (e^{\lambda_{EX+\beta^+ +\beta^- t}} - 1) \tag{4.71}$$

where $\lambda_{EX+\beta^+}$ and $\lambda_{EX+\beta^+ +\beta^-}$ are the decay constants of ^{40}K for the production of ^{40}Ar and for the total decay, independent of the daughter nuclides, respectively. Since ^{40}Ca may form via other routes, the quantity of ^{40}Ca cannot be used for dating.

4.3.5 Radioactive Dating by ^{87}Rb–^{87}Sr, Parent–Daughter Pairs

The ^{87}Rb isotope has a long half-life (4.88×10^{10} years). This isotope emits negative beta radiation (as discussed in Section 4.4.2), producing an ^{87}Sr isotope. Similarly to the ratio of ^{40}K/^{40}Ar, the age of geological formations can be determined by the ratio of ^{87}Rb/^{87}Sr. The problem with this approach, however, is that the source of an ^{87}Sr isotope is not the decay of ^{87}Rb alone; it was present at the time of the rock formation ($t = 0$). Thus, the quantity of ^{87}Sr ($^{Sr\text{-}87}N$) can be expressed as:

$$^{Sr\text{-}87}N = {}^{Sr\text{-}87}N_{t=0} + {}^{Rb\text{-}87}N(e^{\lambda_{Rb\text{-}87} t} - 1) \tag{4.72}$$

where $^{Sr\text{-}87}N_{t=0}$ is the quantity of Sr-87 at the time of the formation of the rock (at $t = 0$), $^{Rb\text{-}87}N$ is the quantity of Rb-87, $\lambda_{Rb\text{-}87}$ is the decay constant of Rb-87,

and t is the age of the rock. Since the initial quantity of the Sr-87 is not known, for dating purposes, it also has to be determined. This problem is solved by incorporating the quantity of Sr-86 into Eq. (4.72). Sr-86 is a stable isotope, the quantity of which does not change over time. By dividing Eq. (4.72) by the constant quantity of Sr-86 ($^{\text{Sr-86}}N$), we obtain:

$$\frac{^{\text{Sr-87}}N}{^{\text{Sr-86}}N} = \frac{^{\text{Sr-87}}N_{t=0}}{^{\text{Sr-86}}N} + \frac{^{\text{Rb-87}}N}{^{\text{Sr-86}}N}\left(e^{\lambda_{\text{Rb-87}}t} - 1\right) \tag{4.73}$$

When the quantities of Sr-86, Sr-87, and Rb-87 are determined in different rocks or minerals with the same genetics, and the ratio of $^{\text{Sr-87}}N/^{\text{Sr-86}}N$ is plotted as a function of $^{\text{Rb-87}}N/^{\text{Sr-86}}N$, a straight line is obtained. The slope of this straight line is $(e^{\lambda_{\text{Rb-87}}t} - 1)$, and the intercept is $^{\text{Sr-87}}N_{t=0}/^{\text{Sr-86}}N$, which shows the initial ratio of the strontium isotopes. The age can be determined from the slope of the straight line. The line is called an "isochron," which means "similar age." The method has been used to determine the age of igneous, metamorphic, and sedimentary rocks, and it is used frequently to date meteorites.

4.3.6 Radiocarbon Dating

Libby discovered that the radioactive isotope of carbon, ^{14}C isotope, is formed from the nitrogen that is present in air under the effect of neutrons from the cosmic ray. The nuclear reaction is $^{14}N(n,p)^{14}C$. (Nuclear reactions will be discussed in Chapter 6.) If the flux of the neutrons is assumed to be constant, the formation and subsequent decay of ^{14}C result in a constant concentration of ^{14}C. Since the living organisms continuously incorporate ^{14}C of the carbon dioxide in the air, the ^{14}C concentration of the living organism (i.e., the ratio of $^{14}C/^{12}C$) is the same. When the living organism dies, the continuous uptake of ^{14}C ends, and only the radioactive decay of ^{14}C continues. Thus, the concentration and the radioactivity of ^{14}C decrease. From the $^{14}C/^{12}C$ ratio, the time elapsed from the death of the living organism can be estimated. In radiocarbon dating, 5570 years is traditionally used as the half-life of ^{14}C (the actual half-life is 5736 years). This means that dating is feasible if the living organism lived between 250 and 35,000 years ago. The activity of ^{14}C in the carbon dioxide of the air and the living organisms is 16 dpm/g carbon. However, more accurate results can be obtained using modern mass spectrometry equipments to determine the $^{14}C/^{12}C$ isotope ratio.

An interesting application of the $^{14}C/^{12}C$ ratio of tooth enamel for the estimation of the age of individuals born after 1943 was published. Tooth enamel is formed at well-determined times of childhood and contains 0.4% carbon. After the formation, there is no exchange between the carbon in the enamel and the carbon dioxide in the air. Thus, the $^{14}C/^{12}C$ of the tooth enamel reflects the ratio in the air at the time of the enamel formation. The $^{14}C/^{12}C$ ratio in the air was nearly constant until 1955, when aboveground nuclear bomb tests raised it signifiantly. After the Limited Test Ban Treaty in 1963, atmospheric ^{14}C began to drop exponentially,

and it did not return to the level before 1955 until recently. Thus, if the $^{14}C/^{12}C$ ratio of the tooth enamel is determined, the time of the enamel formation, and from here the age of the individuals, can be estimated.

Besides radiocarbon, tritium is also formed of nitrogen in the air and neutrons in the nuclear reactions $^{14}N(n,3\ ^{4}He)T$ and $^{14}N(n,T)^{12}C$. Similar to ^{14}C, tritium isotopes can participate in continuous exchanges between the hydrogen in the air and living organisms. The half-life of tritium is 12.35 years, so it should be suitable for dating in the interval of 10−80 years (e.g., for the dating of wine in bottles). However, thermonuclear explosions in the atmosphere significantly increased the natural tritium concentration, so the dating on the basis of tritium concentration has become quite limited. Tritium activity can be used for the dating of glacier and polar ice in layers, however, because in these cases, the effect of the nuclear explosions is neglible.

4.4 Mechanism of Radioactive Decay

4.4.1 Alpha Decay

Alpha decay was discovered by Rutherford, who placed an isotope-emitting alpha radiation into a thin glass foil and put the foil into a glass vessel closed at the bottom with mercury. The alpha particles have great energy, so they can penetrate the foil into the glass vessel and transform to helium by reacting with two electrons. The gas, of course, shows helium spectrum under excitation. Helium gas, however, cannot penetrate the foil because of the low energy of the atoms, so helium cannot be detected outside the foil.

Apha decay is characteristic for nuclei with great atomic and mass numbers. Thermodynamically, alpha decay can take place at $A > 150$, but it is only common at $A > 210$, except for samarium and neodymium, which have isotopes emitting alpha radiation. Alpha decay is possible when the mass decreases in Eq. (4.75).

Alpha particles consist of two protons and two neutrons. By emitting an alpha particle, the ratio of protons to neutrons changes and the atomic and mass number decreases by 2 or 4, respectively.

$$^{A}_{Z}M \rightarrow {}^{A-4}_{Z-2}M + \alpha \tag{4.74}$$

The alpha particle, consisting of two protons and two neutrons, is very stable because of the filled energy levels for protons and neutrons.

The energy of the alpha radiation is in the range of 4−9 MeV. The energy can be calculated from the difference of the rest masses between the parent nuclide and the daughter nuclide, the alpha particle, and the emitting electrons:

$$\Delta m = M_A - M_{A\text{-}4} - m_\alpha - 2m_e \tag{4.75}$$

where M_A, $M_{A\text{-}4}$, m_α, and m_e are the rest masses of the parent nuclide, daughter nuclide, alpha particle, and electron, respectively. Since 1 a.m.u. is equivalent to 931 MeV energy, the energy of the alpha particle can be expressed as:

$$\Delta E = 931 \text{ MeV} \times \Delta m \tag{4.76}$$

The energy of the alpha particle, however, is smaller than the value calculated by Eq. (4.76) because a portion of the energy recoil the daughter nuclide. The energy of the recoiling can be calculated on the basis of the law of conservation of linear momentum:

$$m_\alpha v_\alpha + Mv = 0 \tag{4.77}$$

where m_α and M are the masses of the alpha particle and the daughter nuclide, and v_α and v are the rates of the alpha particle and the daughter nuclide, respectively. The rate of the daughter nuclide is expressed from Eq. (4.77):

$$v = \frac{m_\alpha v_\alpha}{M} \tag{4.78}$$

The total energy emitted in alpha decay is the sum of the energies of the daughter nuclide and the alpha particle:

$$E = \frac{1}{2}Mv^2 + \frac{1}{2}m_\alpha v_\alpha^2 \tag{4.79}$$

By substituting Eq. (4.79) into Eq. (4.78), you get the following:

$$E = \frac{1}{2}M\frac{m_\alpha^2 v_\alpha^2}{M^2} + \frac{1}{2}m_\alpha v_\alpha^2 = \frac{1}{2}m_\alpha v_\alpha^2\left(\frac{m_\alpha}{M} + 1\right) \tag{4.80}$$

The energy of alpha radiation can be measured in a calorimeter, so the kinetics of the alpha decay can be studied by calorimetry.

In the case of alpha decay, the decay constants of alpha emitters (λ) in a decay series correlate to the radiation energy (E) and the range R of the alpha particles in air. This relation can be expressed by the Geiger−Nuttall rule:

$$\log \lambda = a + b \times \log R \tag{4.81}$$

$$\log \lambda = a' + b' \times \log E \tag{4.82}$$

where a, b, a', and b' are constants in a decay series.

The $\log \lambda - \log E$ function for the alpha-emitting members of the ^{238}U decay series is shown in Figure 4.7.

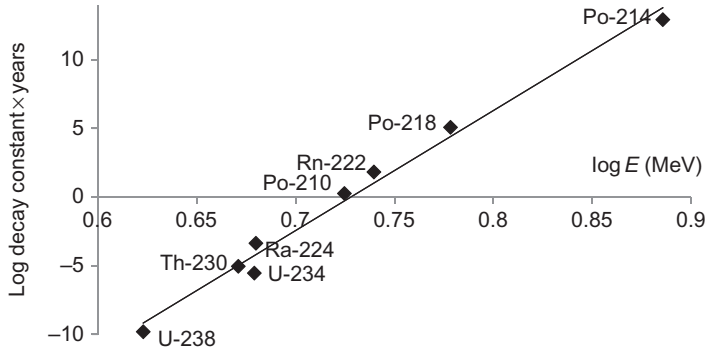

Figure 4.7 Log λ−log E function for the alpha-emitting members of the ^{238}U decay series, illustrating the Geiger−Nuttall rule.

The alpha particles have well-determined, discrete energies. An alpha emitter, however, can produce alpha particles with different energies. This phenomenon can be interpreted by the shell model of nuclei: after the decay, the nucleus is in an excited energy state. The energy of the alpha particles is lower than the value calculated from the differences of the rest masses (Eq. (4.75)), and the difference corresponds to the excitation energy of the nucleus. The excited nucleus may return to a lower excited state or ground state, emitting photons with a characteristic energy. These photons are called gamma photons (described in Section 4.4.6). Since the nucleus may return to the ground state via excited states, the emission of an alpha particle can be followed by more than one gamma photon. In the case of intermediate members of decay series, the energy of a small number of alpha particles may be greater than the value calculated from the differences of the rest masses if the parent nuclide has been in an excited state at the moment of the alpha emission.

In Figure 4.8, decay schemes of two alpha emitter nuclides (^{230}Th and ^{241}Am) are shown. Similar schemes are constructed for all radioactive nuclides. All important information on the nuclides (parent and daughter nuclides), the mechanism of the decay, and the half-life of the parent nuclide can be found. In addition, the ratio of the lines with different energy is given, and the spin and parity (+ or −) are also included.

Models describing the alpha decay postulate two stages of alpha emission: (1) the separation of the parent nuclide into the alpha particle and the daughter nuclide; (2) the penetration of the alpha particle through a potential barrier that is formed by the joint action of nuclear forces and a Coulomb (electrostatic) interaction of the alpha particle with the remaining portion of the nucleus (daughter nucleus; see Figure 4.9). The range of nuclear forces is very short (see Section 2.2), and at greater distances, the Coulomb interaction is determining. As seen previously, alpha particles have two positive charges. Since the daughter nucleus is also positive, the alpha particle and the daughter nucleus repulse each other. The energy

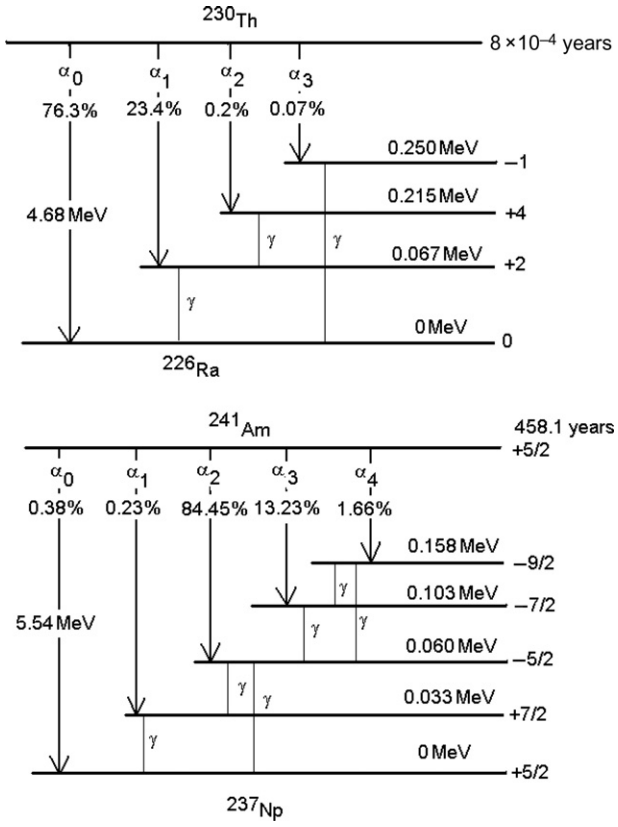

Figure 4.8 Decay scheme of alpha-emitting nuclides (^{230}Th and ^{241}Am).

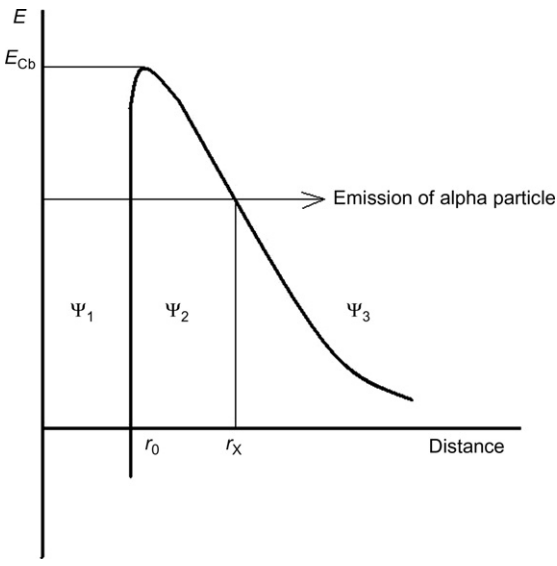

Figure 4.9 Potential barrier against alpha emission. The center of the nucleus is in the origin, Ψs are the wave function at the different spaces, E_{Cb} is the Coulomb repulsion energy, r_0 is the radius of the nucleus, r_x is the outer wall of the Coulomb barrier, and the emitted alpha particle is outside this barrier.

of the repulsion between the alpha particle and the daughter nuclide (the height of the potential barrier) is:

$$E_{\mathrm{Cb}} = \frac{2Ze^2}{r_0} \tag{4.83}$$

where E_{Cb} is the height of the potential barrier, Z is the atomic number, and r_0 is the Coulomb radius. E_{Cb} can be determined experimentally in nuclear reactions with charged particles. It is about 20−25 MeV. The energy of the alpha radiation, however, is about 4−9 MeV. According to classical physics, the kinetic energy of the alpha particles is too low to penetrate the potential barrier. Therefore, alpha decay cannot be interpreted by classical physics. The problem of alpha decay can be solved by quantum physics, assuming the wave- particle dual nature. This means that each particle can be described by a wave function, an energy, a linear moment, and a direction of which is the same as those of the particle.

The total energy of the wave or the particle is:

$$E = h\nu \tag{4.84}$$

where ν is the frequency.

The moment of the wave function (g) is:

$$g = hk = h\frac{1}{\lambda} = \frac{h\nu}{c} \tag{4.85}$$

where λ is the wavelength of the alpha particle, its reciprocal (k) is the wave number, and c is the velocity of light in a vacuum.

The intensity of the wave is:

$$I = (\Psi)^2 \tag{4.86}$$

where Ψ is the probability amplitude of the wave function.

The kinetic energy of the particle at a place with U potential can be expressed by the difference between the total energy and the potential energy:

$$E_{\mathrm{kin}} = E - U = \frac{1}{2}mv^2 = \frac{g^2}{2m} \tag{4.87}$$

From here,

$$g = \sqrt{2m(E-U)} = hk \tag{4.88}$$

The probability amplitude of the alpha particle is found as follows:

In the nucleus:

$$\Psi_1 = B_1\, \mathrm{e}^{2\pi \mathrm{i}(\mathrm{k}_1 r - \nu_1 t)} \tag{4.89}$$

At the place with U potential of the barrier:

$$\Psi_2 = B_2 \, \mathrm{e}^{2\pi \mathrm{i}(\mathrm{k}_2 r - \nu_2 t)} \tag{4.90}$$

and over the barrier (outside the nucleus):

$$\Psi_3 = B_3 \, \mathrm{e}^{2\pi \mathrm{i}(\mathrm{k}_3 r - \nu_3 t)} \tag{4.91}$$

As a consequence of Eq. (4.88), k is an imaginary number if the potential U is greater than the total energy of the particle (E). When the imaginary k is multiplied by 2πi as in the power, the power of Eq. (4.91) will be a real number. Therefore, the alpha particles can be present outside the nucleus.

The wave functions defined in Eqs. (4.89)−(4.91) can be summarized in the Schrödinger equation. An approximate solution of the Schrödinger equation for the alpha radiation is discussed here.

When the rate of the alpha particle in the nucleus is v, the number of collisions on the potential barrier in 1 s is n_c:

$$n_\mathrm{c} = \frac{v}{2r_0} \tag{4.92}$$

where r_0 is the radius inside the nucleus where the nuclear field is homogeneous. The number of hits can be given by means of the de Broglie wavelength (λ) of the particle:

$$\lambda = \frac{h}{mv} \approx 2r_0, \quad \text{from here } v = \frac{h}{2mr_0} \tag{4.93}$$

When substituting the rate (v) into Eq. (4.92), we obtain:

$$n_\mathrm{c} = \frac{h}{4mr_0^2} \tag{4.94}$$

The ratio of the probability amplitude of the alpha particle existing outside and inside the nucleus is:

$$\frac{|\Psi_3|^2}{|\Psi_1|^2} \tag{4.95}$$

The decay constant is given as the product of the number of collisions and the ratio of the probability amplitude as follows:

$$\lambda = \frac{h}{4mr_0^2} \frac{|\Psi_3|^2}{|\Psi_1|^2} \tag{4.96}$$

When substituting Eqs. (4.89) and (4.91) into Eq. (4.96) and integrating the Schrödinger equation from r_0 to r_x, we obtain:

$$\lambda = \frac{h}{4mr_0^2} \exp\left\{ -\frac{2\pi}{h} \int_{r_0}^{r_x} \sqrt{2m\frac{2(Z-2)[e]^2}{r} - E} \right\} \mathrm{d}r \tag{4.97}$$

The approximate solution of Eq. (4.97) for heavy nuclei is:

$$\log \lambda = 20.47 - 1.191 \times 10^9 \frac{Z-2}{v} \frac{1}{\sqrt{E}} + 4.084 \times 10^6 \sqrt{Z-2} \times \sqrt{r_0} \tag{4.98}$$

In this way, the decay constant (λ) is obtained in seconds. Equation (4.98) is formally similar to the Geiger−Nuttall rule.

The radius of the nucleus (r_0 in Eq. (4.98)) calculated from the decay constant is always smaller than the radius calculated from the alpha backscattering. For example, the radius of ^{238}U is 9.5×10^{-15} m calculated from the decay constant and 4×10^{-14} m from alpha backscattering. The differences originate in a different place than the location of the collision of the alpha particles: in the case of alpha decay, the alpha particles collide at the inner side of the potential barrier, while in the case of backscattering, alpha particles collide at the outer side of the potential barrier.

4.4.2 Beta Decays

Beta decays take place when the ratio of protons and neutrons is not optimal. Beta decays tend to allow the nucleus to approach the optimal proton/neutron ratio. When there are too many neutrons related to the protons, negative beta decay occurs; when there are too many protons related to the neutrons, positive beta decay takes place. As a result of beta decays, the mass number of the atoms remains the same, but the atomic number changes: the atomic number increases in the negative beta decay and decreases in the positive beta decay, respectively. Besides the beta particle, another particle is also emitted: antineutrino in the negative beta decay and neutrino in the positive beta decay.

$$\text{Negative beta decay:} \quad {}^{A}_{Z}M \rightarrow {}^{A}_{Z+1}M + \beta^- + \overline{\nu} \tag{4.99}$$

$$\text{Positive beta decay:} \quad {}^{A}_{Z}M \rightarrow {}^{A}_{Z-1}M + \beta^+ + \nu \tag{4.100}$$

In Eqs. (4.99) and (4.100), β^- are β^+ are the negative and positive beta particles, i.e., electrons and positrons. It is important to note that the term "beta particles" means only electrons (positive or negative) emitted from nuclei. Electrons emitted from the extranuclear shell are called "electrons" and designed by e^-.

Similar to alpha decay, the emitted energy of beta decays can be calculated from the rest masses of the parent and daughter nuclide plus the emitted particles:

$$\text{Negative beta decay:} \quad E = ({}^{A}_{Z}M - {}^{A}_{Z+1}M)\ 931\ \text{MeV} \tag{4.101}$$

$$\text{Positive beta decay:} \quad E = ({}^{A}_{Z}M - {}^{A}_{Z-1}M - 2m_e)\ 931\ \text{MeV} \tag{4.102}$$

The rest mass of the neutrino can be ignored because its rest mass is about 10,000 times lower (150 eV at most) than the rest mass of the electron (0.51 MeV). As seen in Eqs. (4.101) and (4.102), besides the differences between the rest masses of the parent and daughter nuclides, there are differences between the rest masses of two electrons since the increase of the atomic number in the negative beta decay requires the uptake of another electron, while the decrease of the atomic number in the positive beta decay causes the emission of another electron. This means that positive beta decay can take place only if the rest mass of the parent nuclide is at least two electron masses (1.02 MeV) heavier than the rest mass of the daughter nuclide.

Since the radioactive decay always releases energy (in the exothermic process), it takes place only if the rest mass of the parent nuclide is greater than the rest mass of the daughter nuclide + the emitted particle(s). (As mentioned previously, the rest mass of the neutrino can be ignored.) For negative beta decay, this can be expressed as:

$${}^{A}_{Z}M - Zm_e > {}^{A}_{Z+1}M - (Z+1)m_e + m_e \tag{4.103}$$

Similarly, for positive beta decay:

$${}^{A}_{Z}M - Zm_e > {}^{A}_{Z-1}M - (Z-1)m_e + m_e \tag{4.104}$$

The solution of Eqs. (4.103) and (4.104) is:

$${}^{A}_{Z}M > {}^{A}_{Z+1}M \tag{4.105}$$

$${}^{A}_{Z}M > {}^{A}_{Z-1}M + 2m_e \tag{4.106}$$

As seen in Eqs. (4.105) and (4.106), the differences in the rest masses give discrete values for the emitted energy. The spectrum of the beta radiation, however, is continuous (Figure 4.10), and the calculated energy is equal to the maximum energy. (The electrons with discrete energy are emitted from the electron shells.)

The continuous beta spectra can be interpreted by the two emitted particles, the beta particle and the neutrino. The energy of beta decay is divided into two parts: both beta particles and neutrinos have some energy. The emission of two particles explains the changes of the spin of the nucleus as a result of the decay: the spin of the nucleus changes by 1, the spin of both beta particle and neutrino is 1/2 (see Table 2.3).

Figure 4.10 General shape of beta spectra: the number of beta particles with a given energy ($N(E)$) versus beta energy (E).

The elementary process of the beta decay can be described as follows:
Negative beta decay:

$$n \rightarrow p^+ + \beta^- + \overline{\nu} \tag{4.107}$$

Positive beta decay:

$$p^+ \rightarrow n + \beta^+ + \nu \tag{4.108}$$

It is important to note that the processes in Eqs. (4.107) and (4.108) do not mean the free nucleons, but bound in the nucleus. Since the rest mass of the neutron is larger than the rest mass of the proton, the difference of masses in the process of Eq. (4.107) produces energy. The negative beta decay is obviously exothermic. In positive beta decay, however, a proton is transformed to a neutron. This requires energy because of the differences between the rest masses (1.3 MeV; see Table 2.1), which is provided by the decrease of the mass of the nucleus. In addition, the emittion of the positron requires more 0.51 MeV energy, which is also to be provided by the decrease of the mass of the nucleus. The sum of the two energies is 1.8 MeV.

The neutrino emitted in the beta decays cannot be detected directly because it is neutral and its rest mass is very small. However, because of the conservation of linear momentum at beta decay, the momentum vectors (i.e., the pathways of the particles) of the daughter nuclide and the beta particle should be at an angle of 180°. However, as photographed in a cloud chamber in the beta decay of ^{6}He by Csikai and Szalay in 1957 (Figure 4.11), another particle (neutrino) has to be released during the decay as well.

The antineutrino can be detected using the following reaction:

$$p + \overline{\nu} \rightarrow n + \beta^+ \tag{4.109}$$

Since the cross section of the reaction (4.109) is very low (as discussed in Chapter 6), the high flux of antineutrinos is required similar to those present in nuclear reactors. When an aqueous solution of $CdCl_2$ is placed into a nuclear

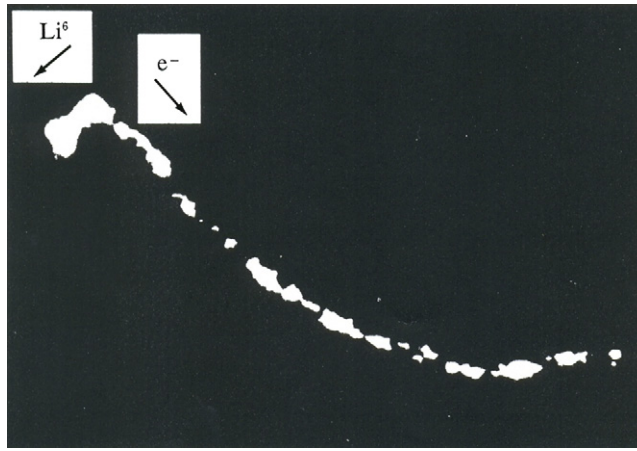

Figure 4.11 Cloud chamber photograph of the decay of ^{6}He to ^{6}Li. The angle of the tracks of the ^{6}Li and the beta particle (e^{-}) is $<180^{\circ}$, proving the emission of a third particle, antineutrino.
Source: Reprinted from Csikai (1957), with kind permission of Società Italiana di Fisica.

reactor, antineutrinos react with the protons of water in the reaction (4.109). The two products, namely, the positive beta particle and the neutron, can be detected simultaneously in the following way. The positive beta particles and electrons are annihilated, and as a result, photons of 0.51 MeV are emitted (see Section 5.3.3). The neutrons are thermalized in a few microseconds and initiate the nuclear reaction ^{113}Cd(n,γ)^{114}Cd. The gamma photons emitted in this nuclear reaction of ^{113}Cd follow the emission of the photons with 0.51 MeV after a few microseconds. The two photons can be detected by coincidence measurements.

In beta decays, the nuclei usually emit one beta particle. However, two beta particles are emitted in a single process in some cases. This process is called double beta decay. Theoretically, two types of double beta decays can exist: in the first, two beta particles and two neutrinos are emitted [$\beta\beta(\nu\nu)$], in the other, only two beta particles (no neutrinos) are formed [$\beta\beta(0\nu)$]. In the first case, the two neutrinos annihilate each other; and in the second, the emitted neutrino is absorbed by another one.

Decay products of the double beta decay [$\beta\beta(\nu\nu)$] (by extraction of crypton and xenon from very old selenium and tellurium minerals) in geological samples were detected in 1950. Under laboratory conditions, double beta decay was observed in 1986 when the double beta decay of ^{82}Se was measured:

$$^{82}\mathrm{Se} \rightarrow {}^{82}\mathrm{Kr} + 2\mathrm{e}^{-} + 2\nu \tag{4.110}$$

In the laboratory experiments, 1.1×10^{20} years was obtained for the half-life of the double beta decay of ^{82}Se. This value is similar to the results obtained in geochemical measurements.

More than 60 naturally occurring isotopes are capable of undergoing double beta decay. Only 10 of them were observed to decay via the two-neutrino mode: ^{48}Ca, ^{76}Ge, ^{82}Se, ^{96}Zr, ^{100}Mo, ^{116}Cd, ^{128}Te, ^{130}Te, ^{150}Nd, and ^{238}U.

The neutrinoless double beta decay [$\beta\beta(0\nu)$] has not been demonstrated beyond any doubt.

4.4.3 Electron Capture

In this process, the nucleus captures an electron from an inner electron shell (K or L shell) resulting in the following transition:

$$p^+ + e^- \rightarrow n + \overline{\nu} \tag{4.111}$$

The process is characterized as electron capture, EC decay, or EX decay. EC decay is energetically more desirable than positive beta decay since there is no beta particle emission in EC decay. The neutrinos formed in the electron capture are monoenergetic.

The electron capture is always followed by the emission of electromagnetic radiation because the orbital vacancy results in an excited electron state. When the vacancy in the K shell is filled with an electron from an outer, mainly L, shell, the difference between the K and L binding energies is emitted as characteristic X-ray radiation. It is emphasized here that the high-energy electromagnetic radiation is called "gamma radiation" if it is the result of nuclear transition, while if the source of the radiation is the transition of electrons between the extranuclear orbitals, it is called an "X-ray."

Instead of X-ray radiation, the excitation energy can be transferred to another electron, which is then ejected from the atom. This second ejected electron is called an Auger electron. In this process, the produced nucleus has more than one positive charge, so it can react easily with other substances. The probability of the Auger effect decreases as the atomic number increases. As a result, the ratio of the gamma photons and the Auger electrons depends on the atomic number: for light elements, the Auger electrons are significant, while for heavy elements, the characteristic X-ray is dominant (Figure 4.12).

Furthermore, the electrons captured from the K and L shells, on their pathway toward the nucleus, lose their energy in the nuclear field. This process results in the emission of X-ray radiation called inner *Brehmsstrahlung*, the spectrum of which is continuous. Thus, as a result of electron capture, both characteristic and continuous X-ray radiations are emitted.

The electron capture results in excited nuclei. This excitation energy may be lost through either the emission of gamma photons or the transition of the excitation energy to an electron on the atomic orbital (mainly a K electron) of the same atom, followed by an electron emission. The latter process is called "internal conversion," and the emitted electrons are conversion electrons. The kinetic energy of the conversion electron is equal to the energy of the gamma quantum reduced by

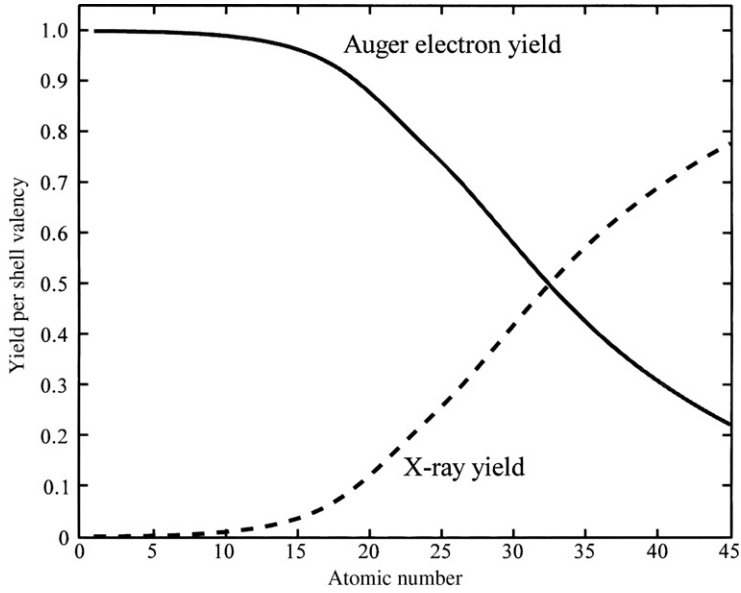

Figure 4.12 The relative yield of X-ray fluorescence photons and Auger electrons for the K shell. Similar curves can be constructed for the L and M transitions. Auger transitions (continuous curve) are more probable for lighter elements, while X-ray yield (dotted curve) becomes dominant at higher atomic numbers.

the binding energy of the electron. This means that the conversion electrons, similar to Auger electrons, have discrete energy.

In some cases, the energy of the electron capture can be measured by using the cyclic process, as shown by the following:

$$^{244}\mathrm{Am} \xrightarrow{\mathrm{EC}} {}^{244}\mathrm{Pu} \tag{4.112}$$

$$^{240}\mathrm{Np} \underset{523\,\mathrm{MeV}}{\overset{\alpha}{\leftarrow}} {}^{244}\mathrm{Am}$$

$$\beta^{-}\ \mathbf{0.36}\,\mathrm{MeV}\uparrow \qquad \downarrow \Delta E_{EC}\ ?$$

$$^{240}\mathrm{U} \underset{4.65\,\mathrm{MeV}}{\overset{\alpha}{\leftarrow}} {}^{244}\mathrm{Pu}$$

4.4.4 Proton and Neutron Decay

Proton decay can take place after positive beta radiation of the light elements, which is followed by proton emission. For example,

$$^{21}\mathrm{Mg} \xrightarrow{\beta^{+}} {}^{21}\mathrm{Na} \xrightarrow{p^{+}} {}^{20}\mathrm{Ne} \tag{4.113}$$

Neutron decay, or delayed neutron decay, may occur when a negative beta decay followed by neutron emission takes place. Neutron decay can be observed for the heavier nuclides too. For example,

$$^{17}\mathrm{N} \xrightarrow{\beta^+} {}^{17}\mathrm{O}^* \xrightarrow{\mathrm{n}} {}^{16}\mathrm{O} \tag{4.114}$$

Some fission products emit negative beta particles as well as neutrons, for example,

$$^{87}\mathrm{Br} \xrightarrow{\beta^-} {}^{87}\mathrm{Kr}^* \xrightarrow{\mathrm{n}} {}^{86}\mathrm{Kr} \tag{4.115}$$

$$^{127}\mathrm{I} \xrightarrow{\beta^-} {}^{137}\mathrm{Xe}^* \xrightarrow{\mathrm{n}} {}^{136}\mathrm{Xe} \tag{4.116}$$

These isotopes are significant in the neutron flux of nuclear reactors, especially when the power is decreasing.

4.4.5 Spontaneous Fission

Similar to alpha decay, spontaneous fission takes place with heavy nuclides. The nucleus is split into two smaller nuclei, assuming that the sum of the mass of the daughter nuclides and the emitted neutrons, if any, is less than the mass of the parent nuclide. The energy of spontaneous fission can be calculated from the decrease of the mass:

$$E = 931\ \mathrm{MeV}({}^{A}_{Z}M - {}^{A1}_{Z1}M - {}^{A2}_{Z2}M - xm_n) \tag{4.117}$$

E has to be greater than zero, which is principally valid at about $A > 80$, as shown by the positive slope of Figure 2.2. However, spontaneous fission requires activation energy; therefore, it is characteristic of thorium and the heavier nuclides. Spontaneous fission was discovered by Petrzsak and Flerov in 1940, shortly after the discovery of neutron-induced fission by Otto Hahn (1939).

$${}^{A}_{Z}M \rightarrow {}^{A1}_{Z1}M + {}^{A2}_{Z2}M + xn \tag{4.118}$$

For spontaneous fission, the $\log \lambda$ versus Z^2/A function for the isotopes of a given element shows a maximum curve (Figure 4.13). The ratio Z^2/A is called the "fissionability parameter" because the liquid drop model (discussed in Section 2.5.1) predicts that the probability of fission should increase with this ratio. The composition of the fission products is similar for both spontaneous and neutron-induced fission (see Figure 6.4).

4.4.6 Isomeric Transition (IT)

As a result of radioactive decay, the nuclei of the daughter nuclides can be in an excited state. The excited nucleus may return to a lower excited state or ground state emitting photons with a characteristic energy. These photons are called

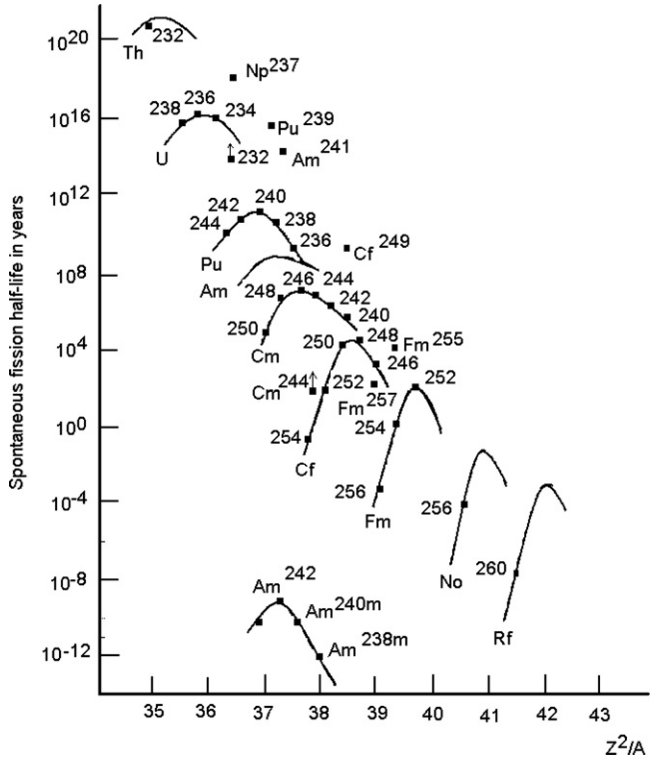

Figure 4.13 Log λ versus Z^2/A function for the spontaneous fission of isotopes of an element with an even mass number.
Source: Reprinted from Choppin and Rydberg (1980), with permission from Elsevier.

"gamma photons" or "gamma radiation." Thus, gamma radiation is not independent; it always follows another radioactive decay process. The time between the original radioactive decay and the gamma photons can range from minutes to years. This process is called "isomeric transition"; the excited state of the nucleus is known as a "metastable state." About 150 isomer pairs are known. An empirical relation between the mean lifetime (τ) and the radiation energy (E) has been found on the basis of the change in the spin (ΔJ):

$$\Delta J = 2 \log \tau = 4 - 5 \times \log E \tag{4.119}$$

$$\Delta J = 3 \log \tau = 17.5 - 7 \times \log E \tag{4.120}$$

$$\Delta J = 4 \log \tau = 27.7 - 9 \times \log E \tag{4.121}$$

In Eqs. (4.119)–(4.121), energy and mean lifetime are expressed in keV and seconds, respectively.

As an example of the isomer transition, let us discuss the ^{137}Cs isotope. ^{137}Cs itself is a beta emitter, while its daughter nuclide is ^{137m}Ba (m means the metastable, excited

state). The daughter nuclide, ^{137m}Ba, transforms into ^{137}Ba by emitting a gamma photon. The energy of the gamma photon is 662 keV. ^{137}Cs is frequently used to calibrate spectrometers; however, gamma photons are emitted by ^{137m}Ba, not directly by ^{137}Cs.

4.4.7 Exotic Decay

During exotic decay, the spontaneous emission of nuclei takes place. For example,

$$^{222}\mathrm{Ra} \rightarrow {}^{208}\mathrm{Pb} + {}^{14}\mathrm{C} \tag{4.122}$$

$$^{223}\mathrm{Ra} \rightarrow {}^{209}\mathrm{Pb} + {}^{14}\mathrm{C} \tag{4.123}$$

$$^{230}\mathrm{Th} \rightarrow {}^{206}\mathrm{Hg} + {}^{24}\mathrm{Ne} \tag{4.124}$$

$$^{232}\mathrm{U} \rightarrow {}^{208}\mathrm{Pb} + {}^{24}\mathrm{Ne} \tag{4.125}$$

Exotic decays are very rare, so they are difficult to observe. In the case of the ^{223}Ra isotope, for example, the probability of the decay (4.123) is about 10^{11} times lower than the probability of the alpha decay. The emitted nuclei are very stable, having closed nucleon shells.

Further Reading

Burshop, E.H.S. (1952). *The Auger Effect and Other Radiationless Transitions*. Cambridge University Press, Cambridge.

Csikai, J. (1957). Photographic evidence for the existence of the neutrino. *Il nuove cimento* 5:1011−1012.

Choppin, G.R. and Rydberg, J. (1980). *Nuclear Chemistry, Theory and Applications*. Pergamon Press, Oxford.

Friedlander, G., Kennedy, J.W., Macias, E.S. and Miller, J.M. (1981). *Nuclear and Radiochemistry*. Wiley, New York, NY.

Haissinsky, M. (1964). *Nuclear Chemistry and its Applications*. Addison-Wesley, Reading, MA.

Kullerud, K. 2003. The Rb-Sr method of dating. <http://ansatte.uit.no/kku000/webgeology/webgeology_files/english/rbsr.html.> (accessed 24.03.12.)

National Nuclear Data Center, 2010. List of Adopted Double Beta (ββ) Decay Values. <http://www.nndc.bnl.gov/bbdecay/list.html.> (accessed 24.03.12.)

Lagoutine, F., Ciursol, N. and Legrand, J. (1983). *Table de Radionucleîdes*. Comissirait á l'Energie Atomique, France.

Lieser, K.H. (1997). *Nuclear and Radiochemistry*. Wiley-VCH, Berlin.

McKay, H.A.C. (1971). *Principles of Radiochemistry*. Butterworths, London.

Perkins, D.H. (2000). *Introduction to High Energy Physics*. 4th edition. Cambridge University Press, Cambridge.

Spalding, K.L., Buchholz, B.A., Bergman, L.-E., Druid, H. and Frisén, J. (2005). Age written in teeth by nuclear tests. A legacy from above-ground testing provides a precise indicator of the year in which a person was born. *Nature* 437:15.

5 Interaction of Radiation with Matter

5.1 Basic Concepts

As discussed in Chapter 1, radioactivity was first detected when radiation interacted with material on photographic plates. Further studies of radioactivity have indicated that radiation may interact with matter in many other ways. The ionizing effect of radiation has been recognized very early. It has also been observed that the degree of the ionization strongly depends on the type of radiation. Rutherford called the radiation with the smallest range "alpha radiation," the radiation with intermediate range "beta radiation," and the radiation with the highest range "gamma radiation." The radiation causes transitional or permanent physical and chemical changes in the molecules that interact with the radiation.

For the interpretation of these interactions, let us look at how energy transitions from radiation to matter and the ensuing changes. To do this, both particles (radiation) and their interactions with matter have to be classified. The particles can be classified on the basis of their characteristic properties, the charge and rest mass. Accordingly, there are charged and neutral particles, and heavy and light particles (Table 5.1).

As seen in Table 5.1, the particles, especially their rest mass, cover a large range, and as such, they can participate in various interactions depending on which part of a substance they interact with and on the mechanism type of the interaction. For example, the reaction of radiation with matter can involve the electron orbitals, the nuclear field, and the nucleus. The particles can partially or totally transfer their energy to matter, can be absorbed, or can be scattered elastically or nonelastically. Furthermore, as a consequence to the interaction, the matter undergoes excitation or ionization, or nuclear resonance or nuclear reactions can be induced. The interactions between radiation and matter may be strong, intermediate, or weak. All these possibilities are summarized in Figure 5.1.

In Figure 5.1, the first three branches show what can happen to the radiation, and the last three branches indicate the changes that they induce in matter. This classification also allows quantitative characterization of the changes that result from the interaction. The changes in the particles of radiation can be mathematically described, assuming that the number of interactions (ν) is proportional to the

Nuclear and Radiochemistry. DOI: http://dx.doi.org/10.1016/B978-0-12-391430-9.00005-6

Table 5.1 Classification of Particles

Charged Particles		Neutral Particles	
Heavy	**Light**	**Heavy**	**Light**
p	β^-	n	γ
D	Electron		X-ray
T	β^+		ν
α			
Heavy ions without electrons			

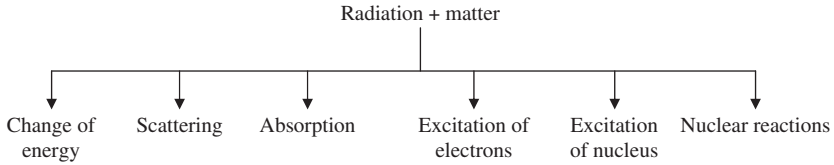

Figure 5.1 Interaction of radiation with matter.

number of particles (n) introduced at a distance x into a substance with ρ atomic density:

$$\nu = \sigma(E) n \rho x \tag{5.1}$$

The cross section ($\sigma(E)$) is the probability of the interactions of the particle with the substance. The value of the cross section depends on the energy of the particle. Equation (5.1) is valid only if the thickness of the layer of the matter (ρx) is so thin that the energy of the particle does not change significantly during the transition through distance x, i.e., $\sigma(E)$ is constant.

The number of particles decreases when they transit trough thickness dx of a substance:

$$\frac{\mathrm{d}n}{\mathrm{d}x} = -\sigma(E) n \rho \tag{5.2}$$

When at $x = 0$, $n = n_0$, the solution of Eq. (5.2) is:

$$n = n_0 \, \mathrm{e}^{-\sigma(E)\rho x} \tag{5.3}$$

Equation (5.3) is the general equation of the absorption of radiation. A special form of this equation is known as the Lambert−Beer law, and it describes the absorption of light photons.

Table 5.2 Interactions of Alpha Particles with Matter

Reacting Particles and Fields	Changes	
	In Radiation	**In Matter**
Orbital electron	*Bremsstrahlung*, absorption	Excitation, ionization, chemical change
Nuclear field	Scattering, *Bremsstrahlung*, absorption	
Nucleus	Nuclear reaction	New nucleus, chemical change

Source: Adapted from Kiss and Vértes (1979), with permission from Akadémiai Kiadó.

The number of particles left as a result of the interactions is expressed by:

$$n_0 - n = n_0[1 - \exp^{(-\sigma(E)\rho x)}] \tag{5.4}$$

The change that happens in the substance as a result of the interaction with radiation will be discussed in the sections dealing with the reactions induced by the different types of radiations Sections 5.1–5.5. Also, the nuclear reactions will be discussed separately in Chapter 6.

5.2 Interaction of Alpha Particles with Matter

One of the most important heavy-charged particles is the alpha particle. As demonstrated by Rutherford, the alpha particle is the nucleus of a helium atom. The energy of alpha particles formed in alpha decay is in the range of 4–10 MeV.

Alpha particles can interact with orbital electrons, which leads to ionization or other chemical changes; with the nuclear field, where they can be scattered; or with the nucleus initiating nuclear reactions (Table 5.2).

5.2.1 Energy Loss of Alpha Particles

The alpha particles can transfer some of their energy and momentum to the orbital electrons, and their velocity decreases. The energy and momentum transfer can be understood as follows. Let us define a Cartesian coordinate system (Figure 5.2), the horizontal axis (x) of which coincides with the pathway of the alpha particle. In such a system, the electron that participates in the interaction is on the perpendicular axis (y), and the origin of the two axes is where the observation takes place.

During the journey from $-\infty$ to $+\infty$, the alpha particle transfers p momentum to the electron at distance b. Momentum is a vector with x- and y-components:

$$p_x = \int_{-\infty}^{+\infty} F_x \, \mathrm{d}t \tag{5.5}$$

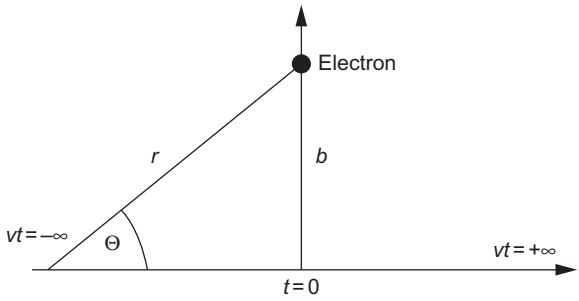

Figure 5.2 The pathway of the alpha particle next to the electron.

$$p_y = \int_{-\infty}^{+\infty} F_y \, \mathrm{d}t \tag{5.6}$$

where F is the electrostatic force between the alpha particle and the electron in the directions of the x- and y-axis, respectively. The electrostatic force acting between two charged particles can be described by the Coulomb law:

$$F = \frac{Ze^2}{r^2} \tag{5.7}$$

$$F_x = \frac{Ze^2}{r^2}\cos\Theta \quad \text{and} \quad F_y = \frac{Ze^2}{r^2}\sin\Theta \tag{5.8}$$

Z means the charge of the alpha particle, $Z = 2$. As seen in Figure 5.2:

$$r = \frac{b}{\sin\Theta} \tag{5.9}$$

By substituting Eq. (5.9) into Eq. (5.8), we obtain:

$$F_x = \frac{Ze^2}{b^2}\sin^2\Theta\cos\Theta \quad \text{and} \quad F_y = \frac{Ze^2}{b^2}\sin^3\Theta \tag{5.10}$$

The variable t of Eqs. (5.5) and (5.6) can be expressed by using an angle Θ:

$$\mathrm{tg}\,\Theta = -\frac{b}{v_\alpha t} \tag{5.11}$$

$$t = -\frac{b}{v_\alpha}\mathrm{ctg}\,\Theta \tag{5.12}$$

$$\mathrm{d}t = \frac{b}{v_\alpha}\frac{1}{\sin^2\Theta}\mathrm{d}\Theta \tag{5.13}$$

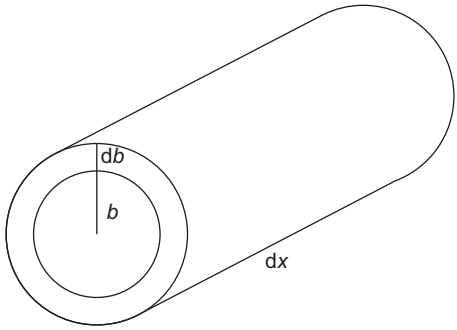

Figure 5.3 A cylinder shell surrounding the pathway of an alpha particle.

By substituting Eqs. (5.10) and (5.13) into Eqs. (5.5) and (5.6), we obtain the following:

$$p_x = \int_0^{\pi} \frac{Ze^2}{bv_\alpha} \cos\Theta \, \mathrm{d}\Theta = \frac{Ze^2}{bv_\alpha} [-\sin\Theta]_0^{\pi} = 0 \tag{5.14}$$

$$p_y = \int_0^{\pi} \frac{Ze^2}{bv_\alpha} \sin\Theta \, \mathrm{d}\Theta = \frac{Ze^2}{bv_\alpha} [\cos\Theta]_0^{\pi} = \frac{Ze^2}{bv_\alpha} (-1 - 1) = -\frac{2Ze^2}{bv_\alpha} \tag{5.15}$$

This means that the alpha particle transfers momentum to an electron as expressed by Eq. (5.15), and the electron moves in the y direction. The kinetic energy transferred to the electron (E_e) is:

$$E_e = \frac{p_y^2}{2m_e} = \frac{2Z^2e^4}{m_e b^2 {v_\alpha}^2} \tag{5.16}$$

where m_e is the rest mass of the electron.

Equation (5.16) gives the energy, which the alpha particle transfers to one electron. During its pathway, however, the alpha particle can interact with many electrons and can transfer energy to them. Therefore, the energies transferred to each electron have to be summed up. The moving alpha particle is surrounded by a cylindrical shell, the volume of which is $2\pi b \times \mathrm{d}b \times \mathrm{d}x$ (Figure 5.3). If the number of atoms with the Z' atomic number in a unit volume is n, the total energy transferred to the electrons is:

$$-\mathrm{d}E = E_e n Z' 2\pi b \, \mathrm{d}b \, \mathrm{d}x = \frac{4\pi Z^2 e^4}{m_e {v_\alpha}^2} n Z' \frac{1}{b} \mathrm{d}b \, \mathrm{d}x \tag{5.17}$$

$$-\frac{\mathrm{d}E}{\mathrm{d}x} = \frac{4\pi Z^2 e^4}{m_e {v_\alpha}^2} n Z' \int_{b_{\min}}^{b_{\max}} \frac{\mathrm{d}b}{b} \tag{5.18}$$

In Eq. (5.18), b_{min} and b_{max} are the minimal and maximal radius of the cylinder, inside which the alpha particle can interact with the electrons.

$$-\frac{dE}{dx} = \frac{4\pi Z^2 e^4 n}{m_e v_\alpha^2} Z' \ln \frac{b_{max}}{b_{min}} \tag{5.19}$$

The value of b_{min} can be determined from the maximal energy transferred to the electron. This value can be calculated from the conservation of momentum (Eq. (5.20)) and energy (Eq. (5.21)):

$$m_\alpha v_\alpha = m_\alpha v'_\alpha + m_e v_e \tag{5.20}$$

$$\frac{m_\alpha v_\alpha^2}{2} = \frac{m_\alpha v'^2_\alpha}{2} + \frac{m_e v_e^2}{2} \tag{5.21}$$

The left and right sides of Eqs. (5.20) and (5.21) give the momentum and energy before and after the energy transfer, respectively. The rate of the electron (v_e) can be expressed by means of Eqs. (5.20) and (5.21):

$$v_e = \frac{2v_\alpha}{1 + \frac{m_e}{m_\alpha}} \approx 2v_\alpha \tag{5.22}$$

Since the mass of the electron is much smaller than the mass of the alpha particle, the denominator of Eq. (5.22) tends toward the value 1. The maximal energy transferred to the electron is:

$$E_{max} = 2m_e {v_\alpha}^2 \tag{5.23}$$

By substituting Eq. (5.23) into Eq. (5.16), we obtain:

$$b_{min} = \frac{Ze^2}{m_e {v_\alpha}^2} \tag{5.24}$$

The value of b_{max} can be obtained from the distance where the electrostatic potential is a multiplied by the ionization and excitation potential (I):

$$b_{max} = \frac{Ze^2}{aI} \tag{5.25}$$

By substituting Eqs. (5.24) and (5.25) into Eq. (5.19), the energy transferred in a unit pathway can be given as follows:

$$-\frac{dE}{dx} = \frac{4Z^2 e^4 \pi n}{m_e v_\alpha^2} Z' \ln \frac{m_e v_\alpha^2}{aI} \tag{5.26}$$

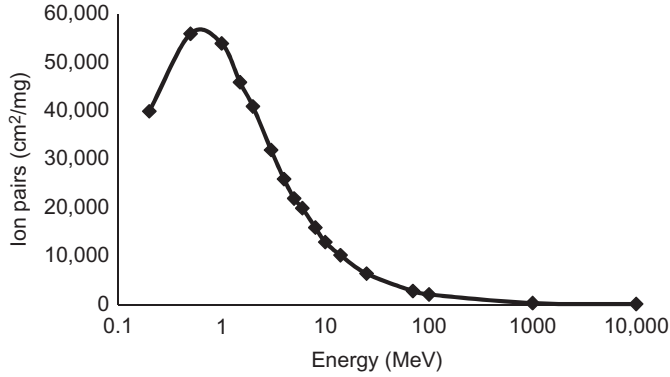

Figure 5.4 Specific ionization of alpha particles in air.

When the velocity of the electron is very high, the relativistic mass increase has to be taken into account. In this case, the Bethe-Bloch formula is obtained:

$$-\frac{\mathrm{d}E}{\mathrm{d}x} = \frac{4Z^2e^4\pi n}{m_\mathrm{e}v_\alpha^2}Z'\left[\ln\frac{2m_\mathrm{e}v_\alpha^2}{I} - \ln\left(1-\frac{v^2}{c^2}\right) - \frac{v^2}{c^2}\right] \tag{5.27}$$

As seen in Eqs. (5.26) and (5.27), the energy transferred to the electrons is inversely proportional to the square of the velocity of the alpha particle (v_α^2); in other words, it is inversely proportional to the kinetic energy. Accordingly, we can observe the broadening of the tracks of the alpha particles in cloud chamber photographs due to the higher energy transfer at the later part of the pathway (Figure 5.7). The energy transfer ends when the alpha particle loses all its energy and transforms to a neutral helium atom as in Rutherford's experiment (discussed in Section 4.4.1). The ionization effect of the alpha particles of various energies is shown in Figure 5.4. At the same time as the ionization, the alpha particles take up electrons and lose their positive charge. The relative charge of the alpha particles as a function of the alpha energy is plotted in Figure 5.5. When the alpha particles lose their total energy, they lose their charge as well and produce neutral helium atoms.

During its passage through a substance, alpha particles lose energy until the energy becomes close to zero. The distance to this point is called the "particle range." The range (R) of the alpha radiation depends on the energy of the radiation and the composition of the matter. The range is usually expressed compared to the range in dry air (1 bar, 15°C) (R_0):

$$R = \frac{\rho_\mathrm{air}}{\rho}\sqrt{\frac{A}{A_\mathrm{air}}}R_0 \tag{5.28}$$

The range of alpha particles in air is several centimeters. In a more condensed medium, however, it is much lower: alpha radiation is absorbed by a sheet of paper or the dead, upper layer of the human skin.

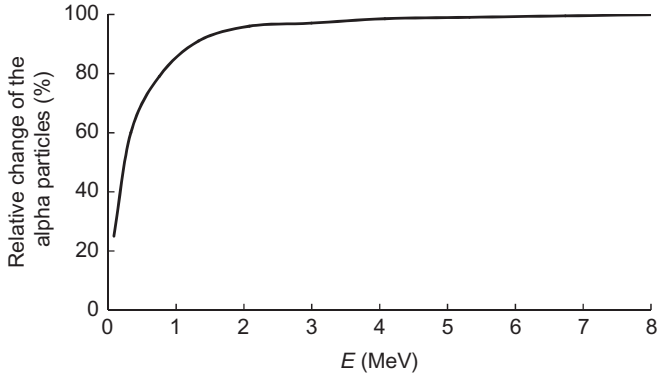

Figure 5.5 The relative charge of alpha particles as a function of alpha energy.

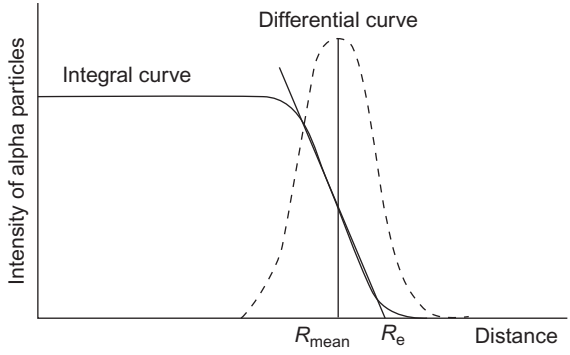

Figure 5.6 Determination of the range of alpha particles from the intensity−distance curve.

The stopping power of the alpha radiation is the energy loss per unit distance ($-dE/dx$), whose dimension is MeV/m. Since the stopping power relates to distance, it is called "linear stopping power." If it is divided by the atomic density, the atomic stopping power is obtained, whose dimension is MeV × m^2/atom.

The relative stopping power (S) of the alpha radiation is the ratio of ranges in air and another medium:

$$S = \frac{R_0}{R} \tag{5.29}$$

The range of the alpha particles can be determined from the intensity−distance curve (Figure 5.6). The mean range (R_{mean}) is the point at which the number of alpha particles decreases into the half, i.e., the range at the inflexion point of the intensity−distance curve. The extrapolated range (R_e) is determined by the extrapolation of the decreasing branch of the intensity−distance curve.

The range and the linear pathway of the alpha particles can be seen in cloud chamber photographs (Figure 5.7).

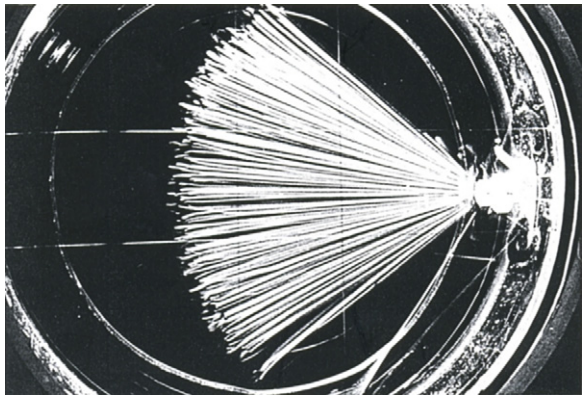

Figure 5.7 Cloud chamber photograph of the pathway of alpha particles. (Thanks to Prof. Julius Csikai, Department of Experimental Physics, University of Debrecen, Hungary, for the photograph.)

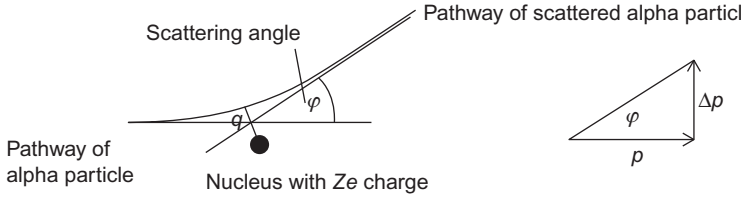

Figure 5.8 The pathway of an alpha particle next to a nucleus with *Ze*.

5.2.2 Backscattering of Alpha Particles

As discussed in Section 2.2.2, Geiger and Mardsen, led by Rutherford, studied the absorption of alpha radiation in thin gold foil (about 5×10^{-7} m thick). They observed that most of the alpha particles passed through the gold foil without being deflected. However, a very small number of alpha particles bounced back; i.e., they were deflected to 180°. Since the mass of the alpha particles is relatively great, the phenomenon was interpreted on the assumption that most of the space surrounding the atoms was empty; most of the alpha particles could pass through here. Only a few alpha particles were deflected at high angles. This is possible only if there is enormous repulsion between the alpha particles and the deflecting part of the atom. Since the alpha particles are positive, the enormous repulsion proves that the positive charge is found in a very small area of the atom. This means that the entire positive charge and mass are concentrated in this small area of the atom, which is called the nucleus.

When approaching a nucleus, the alpha particles follow a hyperbolic pathway with nucleus in one of the focuses of the hyperbola (Figure 5.8). For the alpha particle, the conservation of both the energy and the momentum applies. Assuming that the Coulomb law is applicable at small distances ($<10^{-10}$ m):

$$\frac{1}{2}m_\alpha v_0^2 = \frac{1}{2}m_\alpha v^2 + \frac{Ze \times 2e}{q} \tag{5.30}$$

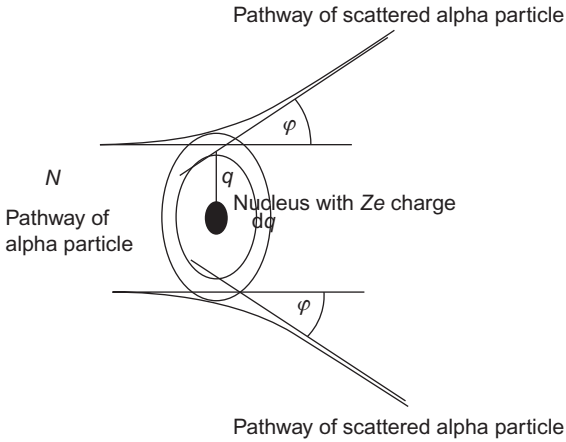

Figure 5.9 The scattering of an alpha beam with N flux on a nucleus with a Ze charge.

where m_α is the mass of the alpha particle, v_0 and v are the velocity of the alpha particle before and after the scattering, Ze is the charge of the nucleus, $2e$ is the charge of the alpha particle, and q is the distance of the nucleus from the original pathway of the alpha particle or, in other words, the collision parameter (Figure 5.8).

The angle of the deflection of the alpha particle is φ. As seen in Figure 5.8, the momentum of the original alpha particles and the change of momentum as a result of scattering can be expressed as:

$$\text{tg}\ \varphi = \frac{\Delta p}{p} = \frac{F\Delta t}{p} = \frac{2Ze^2}{q^2}\frac{2q}{v_0}\frac{1}{p} = \frac{4Ze^2}{qv_0p} \tag{5.31}$$

$\Delta p = F\Delta t$ has been discussed already in Eqs. (5.5) and (5.6) in Section 5.2.1. At small deflections (around 0 and π), tg $\varphi \approx$ tg $\varphi/2$. From here:

$$\text{tg}\frac{\varphi}{2} = \frac{4Ze^2}{qv_0p} \tag{5.32}$$

When the flux of the irradiation alpha beam is N, the number of alpha particles deflected by one scattering atom is (Figure 5.9):

$$\mathrm{d}N = 2\pi q\ \mathrm{d}q\ N \tag{5.33}$$

The ratio of $\mathrm{d}N/N = 2\pi q\ \mathrm{d}q$ is called the "differential scattering cross section." Assuming that the thickness of the scattering layer d, the number of the atoms in a unit volume n, and each alpha particle are scattered by only one nucleus:

$$\mathrm{d}N_\varphi = nd2\pi q\ \mathrm{d}q\ N \tag{5.34}$$

The ratio $dN_\varphi/N = nd2\pi q\, dq\, N$ is the macroscopic scattering cross section. By expressing q and dq by the angle φ and substituting into Eq. (5.34), after equivalent mathematical transformation, we obtain:

$$N_\varphi = \frac{NndZ^2e^4}{m_\alpha^2 v_0^4} \frac{1}{\sin^4 \frac{\varphi}{2}} \tag{5.35}$$

As seen in Eq. (5.35), the ratio of N_φ to N at a constant angle φ depends on the atomic number and the number of particles in a unit volume.

In addition to the number of deflected alpha particles at a given angle, the energy of the deflected alpha particles depends on the quality of the deflecting atoms:

$$E_\varphi = E_\alpha \left(\frac{\frac{4}{A}\cos\varphi + \sqrt{1 - \left(\frac{4}{A}\right)^2 \sin^2\varphi}}{1 + \frac{4}{A}} \right)^2 \tag{5.36}$$

where E_φ and E_α are the energy of the deflected and the original alpha particles and A is the mass number.

One of the main results of the alpha backscattering studies was the experimental determination of the charge of the nuclei, which provides a confirmation about the position of the elements in the periodic table; that is, the atomic number is the number of positive charges. First, Rutherford determined the atomic number of gold, and later Chadwick measured the atomic number of copper, silver, and platinum in 1920.

The atomic number of hydrogen is 1, and its nucleus contains one positive charge, meaning that the nucleus of hydrogen is a proton. The determination of the charges in the nucleus of helium (which is 2) was also significant: the nuclei of helium are alpha particles.

The other important observation was that the alpha particles can get as close as 10^{-14} m to the center of the scattering atom; at this distance, only the Coulomb repulsion acts between the alpha particles and the center of the atoms. By substituting the momentum of the alpha particle, $p = m_\alpha \times v_0$, into Eq. (5.32), we obtain $\mathrm{tg}\frac{\varphi}{2} = \frac{4Ze^2}{qm_\alpha {v_0}^2}$.

From this expression, the distance of the closest approach (q) for the alpha particles at a given angle for the different elements can be determined. This value indicates the upper limit of the radius of the nuclei. Similar data for other elements are summarized in Table 5.3.

As seen in Table 5.3, the alpha scattering experiments show that the radius of the nuclei can be about 10^4 times smaller than the radius of the atoms ($\approx 10^{-10}$ m). The radius of the proton is about 1.3×10^{-15} m. Therefore, the alpha backscattering studies proved Rutherford's assumption that almost the entire positive charge and mass is concentrated on the small space of the atom, that is in the nucleus. The residual volume of the atoms is filled with electrons. Since electrons were found to be

Table 5.3 Radii of Several Nuclei on the Basis of the Alpha Backscattering Expression (Eq. 5.32)

Atom	^{238}U	^{197}Au	^{107}Ag	^{63}Cu	^{195}Pt
$r \times 10^{14}$ m	4.0	3.1	2.0	1.2	3.0

even smaller than nucleons, this means that the atom consists of mostly empty space. This model of the atoms is the Rutherford model or planetary model, which became as the quantitative starting point for the term "chemical elements" in the twentieth century.

The alpha backscattering studies have analytical importance too. Equations (5.35) and (5.36) show that the number and energy of the scattered alpha particles at a given angle depend on the atomic (Z) number, mass number (A), and quantity of elements (n). This means that the deflection of the alpha particles can be applied to qualitative and quantitative analysis of surface layers. The thickness of the layer depends on the range of the alpha particles. The alpha backscattering spectra of an oxide layer produced on SiC are shown in Figure 5.10.

5.3 Interaction of Beta Radiation with Matter

The transformation of the nuclei and the electron orbitals may result in electron emission. As discussed in Section 4.4.2, the negative or positive particles (namely, electrons or positrons following the transformation of the nuclei) are called negative or positive beta radiation, respectively, and they have continuous spectra. The transformation of the atomic orbital can also produce electrons, as discussed in Section 4.4.3. These electrons, such as Auger and conversion electrons, have discrete energy. In addition, electromagnetic radiation can produce photo, Compton, and pair electrons, as discussed in Section 5.4.

The rest mass of the beta particle is 0.51 MeV, which is much less than the rest mass of the alpha particle. Therefore, at the same energy of the radiation, the velocity of the beta particle is much higher than that of the alpha particle. Because of the high velocity, the relative increase in the mass often has to be taken into account.

When beta radiation interacts with matter, the electrons in the matter may get excited or ionized, and the direction of the pathway of the beta particle may change as a result of elastic and inelastic collisions. In addition, the kinetic energy is partly or totally transmitted to the matter. When the beta particles interact with the nuclear field, *Bremsstrahlung* is emitted, which has a continuous spectrum. The inner *Bremsstrahlung* has been discussed in Section 4.4.3.

The beta particles can be scattered and absorbed, eventually losing all their energy (Table 5.4).

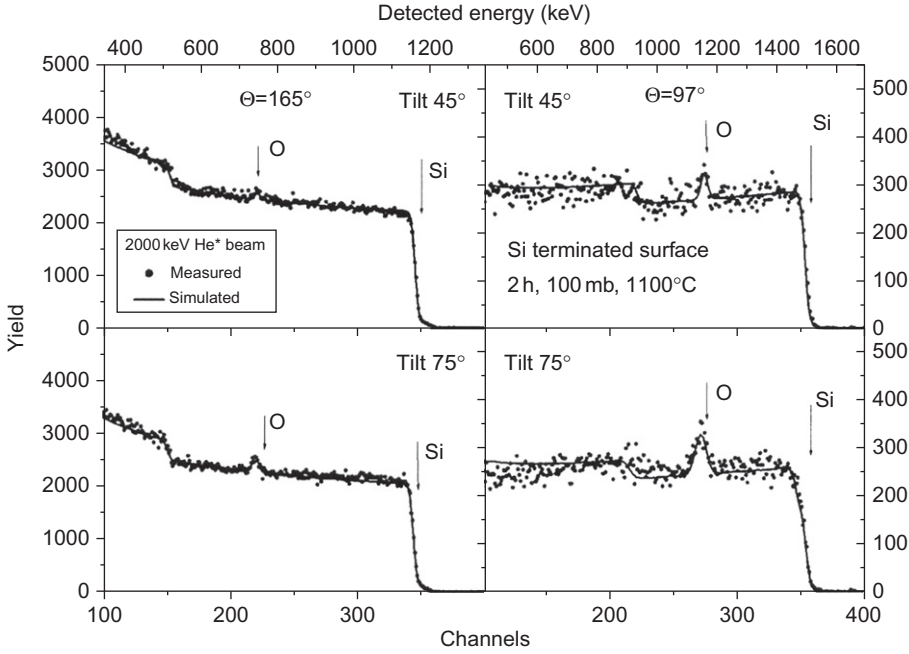

Figure 5.10 Measured and simulated RBS spectra taken on oxidized SiC at scattering angles of 165° and 97°. Each sample was measured at least at two different tilt angles. For the composition, Si:O ratio of 1:2 was determined for each sample. The arrows represent the surface positions of the elements. (Thanks to Dr. E. Szilágyi, KFKI Research Institute for Particle and Nuclear Physics, Budapest, Hungary, for the spectra.)
Source: Reprinted from Szilagyi et al. (2008), with permission of the American Institute of Physics.

Table 5.4 Interaction of Beta Particles with Matter

Reacting Particles and Fields	**Changes**	
	In Radiation	**In Matter**
Orbital electron	*Bremsstrahlung*, scattering, absorption	Excitation, ionization, chemical change
Nuclear field	*Bremsstrahlung*, scattering, absorption	
Nucleus	No interaction	

Source: Adapted from Kiss and Vértes (1979), with permission from Akadémiai Kiadó.

5.3.1 Interaction of Beta Particles with Orbital Electrons and the Nuclear Field

The transmitted energy of the beta particles to orbital electrons depends on the energy of the beta particle. The expressions describing the transmitted energy are different whether the velocity of the beta particle is below or above the velocity of light in a vacuum.

At $E_\beta < m_e c^2$ (E_β is the energy of the beta particle), the energy used up for ionization is:

$$-\left(\frac{dE}{dx}\right)_{ion} = \frac{4\pi e^4 n}{m_e v_\beta^2} Z' \ln \frac{1.66 m_e v_\beta^2}{2I} \tag{5.37}$$

Equation (5.37) is similar to Eq. (5.26), indicating that the ionization is similar for both alpha and beta particles. The numerical factors signify the differences in the size of the alpha and beta particles.

At $E_\beta > m_e c^2$, the energy used up for ionization is:

$$-\left(\frac{dE}{dx}\right)_{ion} = \frac{2\pi e^4 n}{m_e c^2} Z \ln\left(\frac{E^3}{2 m_e c^2 I^2} + \frac{1}{8}\right) \tag{5.38}$$

Equation (5.38) takes into consideration the relative mass increase because of the high energy of the beta particle.

The decrease of the energy of the beta particles as a result of ionization is shown in Figure 5.11.

Some of the beta particles interact with the nuclear field, producing *Bremsstrahlung*. As discussed previously, *Bremsstrahlung* is a continuous X-ray. The energy of beta particles producing *Bremsstrahlung* can be expressed as:

$$-\left(\frac{dE}{dx}\right)_{X\text{-ray}} = \frac{4Z^2 e^2 n}{137 m_e^2 c^4} (E + m_e c^2)\left[\ln \frac{2(E + m_e c^2)}{m_e c^2} - \frac{1}{3}\right]' \tag{5.39}$$

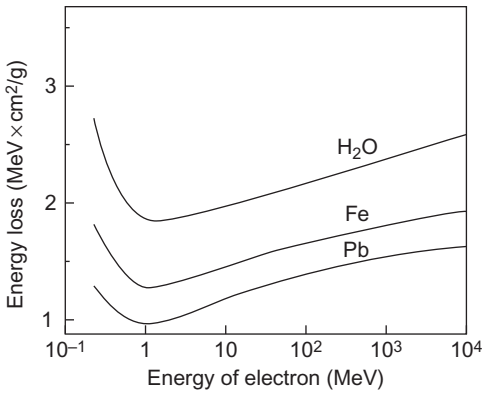

Figure 5.11 Specific energy loss of beta particles versus energy for different absorbers.
Source: Adapted from Kiss and Vértes (1979), with permission from Akadémiai Kiadó.

The total energy loss of the beta particle is the sum of the energies transmitted to orbital electrons (ionization) and producing *Bremsstrahlung* (X-rays):

$$\left(\frac{\mathrm{d}E}{\mathrm{d}x}\right)_{\mathrm{tot}} = \left(\frac{\mathrm{d}E}{\mathrm{d}x}\right)_{\mathrm{ion}} + \left(\frac{\mathrm{d}E}{\mathrm{d}x}\right)_{\mathrm{X\text{-}ray}} \tag{5.40}$$

The ratio of the energies producing X-rays and ionization is expressed as follows:

$$\frac{\left(\frac{\mathrm{d}E}{\mathrm{d}x}\right)_{\mathrm{X\text{-}ray}}}{\left(\frac{\mathrm{d}E}{\mathrm{d}x}\right)_{\mathrm{ion}}} \approx \frac{EZ}{800} \tag{5.41}$$

where E is the energy of the beta particle, and Z is the atomic number of the absorber.

5.3.2 Cherenkov Radiation

Cherenkov radiation (also spelled Cerenkov or Čerenkov) is an electromagnetic radiation emitted when a beta particle passes through a dielectric medium at a speed greater than the velocity of light in that medium. It was discovered by Cherenkov in 1934, when he studied the radiation of radium salts in an aqueous solution. The experience was interpreted by I.M. Frank and I.E. Tamm. The gamma radiation of radium produces many secondary electrons with high energy (e.g., Compton electrons, discussed in Section 5.4.3), which pass through the medium (water) polarizing the molecules and arranging the dipoles. After passing the beta particle, the molecules rapidly revert to their ground state, emitting electromagnetic radiation. When the velocity of the beta particle (v) is greater than the velocity of light in the given medium ($v > c/n$, where c is the velocity of light in vacuum, n is the refractive index of the medium), there is an angle (θ) where the waves of the electromagnetic radiation emitted at 0 and dt times interfere (Figure 5.12).

The angle of the interference is:

$$\cos\Theta = \frac{c}{nv} \tag{5.42}$$

For example, with water ($n = 1.337$):

$$\frac{c}{n} = \frac{3 \times 10^8}{1.337}\mathrm{m/s} \approx 2.2 \times 10^8\ \mathrm{m/s} \tag{5.43}$$

This velocity is equal to 0.26 MeV. Therefore, to have Cherenkov radiation, the beta particles must have at least 0.26 MeV. In practice, however, to be observed easily, beta energies must be above $\sim$0.5 MeV.

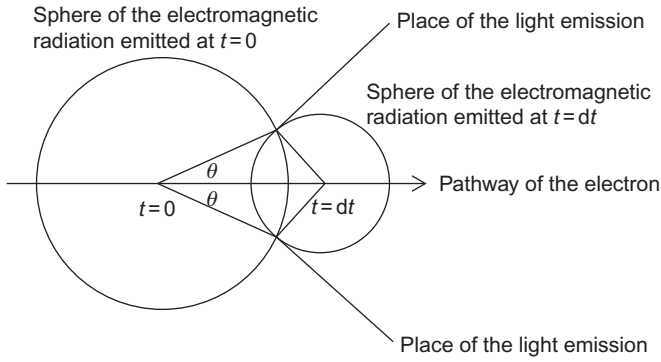

Figure 5.12 Formation of Cherenkov radiation.

The relation of the intensity ($I(\nu)$) and the frequency (f) of the Cherenkov radiation can be expressed as:

$$I(\nu) = \frac{2\pi e^2}{c^2} v \left[1 - \frac{c^2}{n^2 v^2}\right] f \tag{5.44}$$

The maximal intensity is:

$$I_{\max} = \frac{2\pi e^2}{c^2} \left[1 - \frac{1}{n^2}\right] f \tag{5.45}$$

This means that the intensity is proportional to the frequency; therefore, the Cherenkov radiation is blue.

This interaction of the beta radiation can be applied to the direct measurement of the beta radiation by light detectors, for example, by photo multipliers. Cherenkov light can be observed in the nuclear reactors.

5.3.3 Annihilation of Positrons

During β^+-decay, positrons are emitted. The positron is the antiparticle of the electron, and therefore it is unstable. Its half time is the time of thermalization, which means that the time required for the velocity of the positron decreases to zero. It is about 10^{-10} s. If the positron encounters an electron in this interval, the two particles (electron and positron) transform to electromagnetic radiation, gamma photons. The process is called "annihilation." The rest mass of the positron (β^+-particle) is 0.51 MeV, equal to the rest mass of the electron, so 2×0.51 MeV energy is emitted in the annihilation process. Usually, two gamma photons with 0.51 MeV energies are emitted at an angle of 180°. The probability of the formation of two photons is about 90%. (This process is applied in the PET (Section 12.6)). In about 10% of the annihilation process, only one photon with 1.02 MeV is formed.

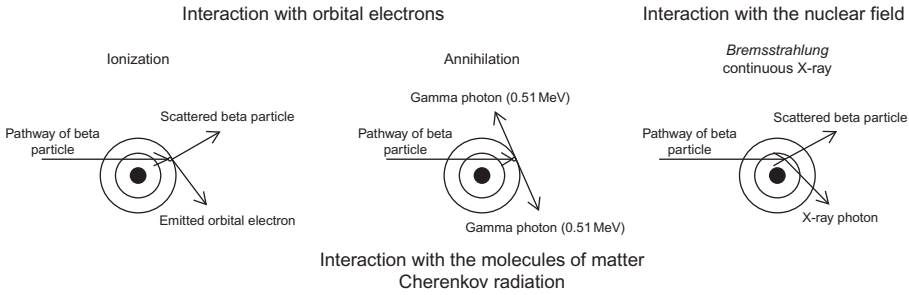

Figure 5.13 Summary of interaction of beta particles with matter.

In some cases, three photons are emitted, and the total energy of them is also 1.02 MeV. The positive beta decay can be detected easily through the detection of the gamma photons with 0.51 MeV.

It is interesting to mention here that before the total thermalization, the positron can interact with an electron, constructing a short-life light element, positronium, whose nucleus is the positron. Positronium can be treated as an atom with an atomic number of zero.

Positronium has two forms: *ortho*- and *para*-positronium, depending on the spins of the positron and electron. In *ortho*-positronium, the spins are parallel; the lifetime in a vacuum is 1.4×10^{-7} s. In *para*-positronium, the spins are antiparallel; the lifetime in a vacuum is 1.25×10^{-10} s. In other media, the chemical reactions (addition, substitution, oxidation, and reduction) decrease the lifetime; thus, the kinetics of chemical reactions can be studied by measuring the lifetime of positronium.

5.3.4 Absorption of Beta Radiation

As a result of the interactions of matter, beta particles can totally lose their energy and absorb into matter. This process is called "real absorption of the beta radiation." However, during the transmission of beta particles through any substance, the intensity (I) of the beta radiation can also decrease as a result of other processes (e.g., by scattering). These processes have been discussed previously and summarized in Figure 5.13. Usually, all decreases in intensity are treated as absorption, regardless of the underlying cause of the decreases.

Quantitatively, the absorption of beta radiation can only be described with difficulty due to the continuous nature of the beta spectra. This means that the energy of beta particles when entering matter can range from zero to the maximum energy of the beta spectrum. Therefore, the expressions describing the beta absorption are usually empirical. It is interesting, however, that the empirical equation of beta absorption (Eq. (5.46)) is similar to the general equation of the absorption of radiation (Eq. (5.3)):

$$I = I_0 \, e^{-\mu(E)l} \tag{5.46}$$

where I_0 and I are the intensities of the beta radiation before and after the transmission through the matter, l is the thickness of the absorber, and $\mu(E)$ is the linear absorption coefficient; its dimension is reciprocal length (e.g., mm^{-1}, cm^{-1}, m^{-1}). The value of the linear absorption coefficient depends on both the energy of the radiation and the atomic number and density of the absorber. By introducing the mass absorption coefficient, it can be avoided to determine the linear absorption coefficient for all maximal beta energies and for all substances. For this purpose, the linear absorption coefficient in the exponent of Eq. (5.46) is divided and multiplied by the density of the absorber (ρ). Note that the density is the ratio of the mass and volume ($\rho = m/V = m/(l \times S)$):

$$I = I_0 \, \mathrm{e}^{-\frac{\mu(E)}{\rho}\frac{m}{l \times S}l} \tag{5.47}$$

where m and S are the mass and the surface area of the absorber, respectively. $\frac{\mu(E)}{\rho} = \mu$ is the mass absorption coefficient, and its dimension is surface area/mass. Since $l/l = 1$, the mass/surface area (m/S) remains in the exponent of Eq. (5.47). This quantity describes the mass of the absorber on a unit surface area; it is called "surface density" (d); its dimension is mass/surface area (e.g., mg/cm^2). This leads to:

$$I = I_0 \, \mathrm{e}^{-\mu d} \tag{5.48}$$

The relation of the mass absorption coefficient and the maximum beta energy ($E_{\beta max}$) and the atomic number of the absorber (Z) can be approximated by empirical equations. When $Z < 13$:

$$\mu = \frac{35Z}{M_a E_{\beta max}^{1.14}} \tag{5.49}$$

When $Z > 13$:

$$\mu = \frac{7.7Z^{0.31}}{E_{\beta max}^{1.14}} \tag{5.50}$$

In Eq. (5.47), M_a is the relative atomic mass of the absorber. For compounds and mixtures, the mass absorption coefficient can be calculated by the mass absorption coefficients of the components, taking into consideration their mass ratio (w):

$$\mu = \sum_{i \to 1}^{n} w_i \mu_i \tag{5.51}$$

As seen in Eq. (5.48), the absorption of continuous beta radiation can be described by an exponential equation. However, the monoenergetic (> 0.2 MeV)

electron radiations (e.g., conversion electrons) show the linear absorption curve as a function of surface density. Below 0.2 MeV, the absorption curve of the monoenergetic electron deviates more or less from linearity.

To characterize the absorption of the beta radiation (exponential law, Eq. (5.48)), the half-thickness of the absorber ($d_{1/2}$) is defined. This is the thickness where the intensity of the beta radiation decreases by half:

$$d_{1/2} = \frac{\ln 2}{\mu} \tag{5.52}$$

As seen in Section 5.2.1, alpha radiation has a well-defined range (R). However, the range of beta radiation can be described only by empirical formulas at different maximal beta energies, such as:

$$R = \frac{1}{1.500} E_{\max}^{\frac{5}{3}}, \quad E_{\max} < 0.2 \text{ MeV} \tag{5.53}$$

$$R = 0.15\, E_{\max} - 0.0028, \quad 0.03 < E_{\max} < 0.15 \text{ MeV} \tag{5.54}$$

$$R = 0.407\, E_{\max}^{1.38}, \quad 0.15 < E_{\max} < 0.8 \text{ MeV} \tag{5.55}$$

$$R = 0.524\, E_{\max} - 0.133, \quad E_{\max} > 0.8 \text{ MeV} \tag{5.56}$$

$$R = 0.571\, E_{\max} - 0.161, \quad E_{\max} > 1 \text{ MeV} \tag{5.57}$$

In Eqs. (5.53)–(5.57), the dimensions of range and energy are g/cm^2 and MeV, respectively.

Cloud chamber photographs show the differences in the pathways of the beta and alpha particles (Figure 5.7 shows the alpha track, and Figure 5.14 shows the alpha and beta tracks). Since alpha particles are much heavier than beta particles/electrons, the pathway of alpha particles is linear. Beta particles, however, tend to deviate more or less, depending on their energy. The interaction of gamma radiation with matter will be discussed later (in Section 5.4); for now, just note that gamma radiation produces secondary electrons, the tracks of which will be shown in the later discussion.

In the presence or two or more beta emitters, Eq. (5.48) consists of several members:

$$I = I_{10}\, \mathrm{e}^{-\mu_1 d} + I_{20}\, \mathrm{e}^{-\mu_2 d} + \cdots + I_{n0}\, \mathrm{e}^{-\mu_n d} \tag{5.58}$$

This means that the absorption of each beta radiation has to be taken into account separately. The mass absorption coefficients and the range of some beta emitters as a function of maximal beta energy are plotted in Figure 5.15. These data are widely applied in the characterization of beta absorption and the planning of shielding against radiation. However, Eqs. (5.49) and (5.50) show that the mass

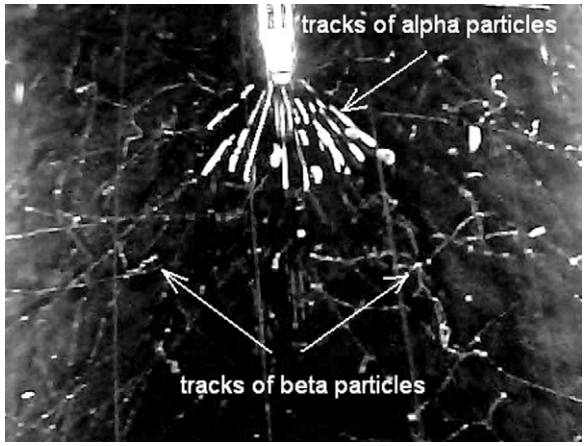

Figure 5.14 Cloud chamber photograph of the pathway of alpha and beta particles. (Thanks to Dr. Péter Raics, Department of Experimental Physics, University of Debrecen, Hungary, for the photograph.)

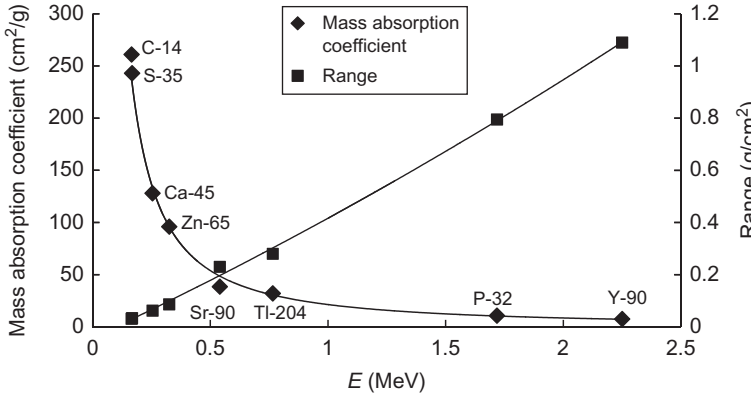

Figure 5.15 The mass absorption coefficients and ranges versus maximal beta energy.

absorption coefficients depend on the atomic number. Therefore, at $Z > 13$, the mass absorption coefficients calculated on the basis of Eq. (5.50) are about twice as high as the data in Figure 5.15. It should be noted, however, that the plan of shielding uses the principle of the so-called conservative estimation, which means that the plans consider the worst scenario. Therefore, the application of the lower mass absorption coefficient is permitted or even can be desirable.

5.3.5 Self-Absorption of Beta Radiation

In a sample containing the beta emitter, the beta particles can also be absorbed by the sample itself in a process called "self-absorption." The precise and accurate measurement of the samples containing beta emitters requires taking into consideration the effect of self-absorption, except when the sample is "infinitely thin." In every other case, the radioactive intensities measured for the same radioactivity

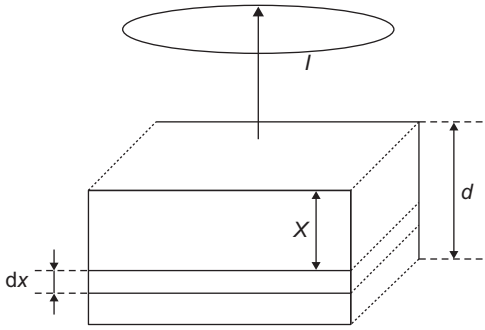

Figure 5.16 Study of self-absorption of beta radiation.

depend on the thickness of the sample, the quantity of the carrier (an excess of inactive atoms of the same elements in the same chemical state), or an inactive matrix (every other substance). In some cases, the molecule itself containing the radioactive isotope can absorb a part of the beta radiation. In solutions, the solvent can absorb the radiation to such a high degree that it becomes impossible to measure the activity. For this reason, beta emitters are usually measured in the solid phase. (It is important to note here that there is a special technique for the measurement of beta emitters, namely, the liquid scintillation technique, which utilizes this absorption. It will be discussed in Section 14.2.1.)

When the beta energy is low (so-called weak beta, e.g., ^{14}C, ^{35}S), the self-absorption is significant at thin layers. However, it cannot be ignored at high beta energies, either, especially when the sample is thick because of the presence of the inactive matrix. Depending on the quantity of inactive matrix, the measured intensity of the same radioactive substance can differ.

The effect of self-absorption can be corrected in two ways: the method of constant activities for high beta energies, and the method of constant specific activities for low beta energies. In the method of constant activities, the intensity is extrapolated for the infinitely thin layer, while in the method of constant specific activities, the intensity is measured at the so-called saturated thickness ($>10 \times d_{1/2}$). The two methods of the correction of self-absorption are discussed as follows.

In the method of constant activities, the total radioactivity of the sample is constant and the quantity of the matrix changes. The samples are arranged as shown in Figure 5.16.

The thickness of the sample is d (g cm^{-2}), and the total intensity of the radiation (the intensity without matrix) is I_0. From here, the intensity of the radiation in a unit thickness is I_0/d. Consider a dx elementary thickness at a distance x from the upper surface of the sample; the intensity in this elementary thickness is $I_0\,\mathrm{d}x/d$. Passing through the distance x, the radiation is absorbed and the intensity decreases. The intensity reaching the upper surface (dI) is expressed by the radiation absorption law (Eq. (5.48)):

$$\mathrm{d}I = \frac{I_0}{d}\exp(-\mu x)\mathrm{d}x \tag{5.59}$$

where μ is the mass absorption coefficient.

By integrating Eq. (5.59) for the total thickness of the sample (d), we obtain the total intensity reaching the surface:

$$I = \frac{I_0}{\mu d}[1 - \exp(-\mu d)] \tag{5.60}$$

If the intensities of samples with constant radioactivity in different quantities of matrix are measured, the intensity decreases as the quantity of the matrix, i.e., the thickness of the samples increases. The I_0 can be obtained by extrapolating to zero thickness. It can be done graphically or by a parameter-estimating computer program from the I versus d function. The measurements can be done up to 1−2 half-thickness (Figure 5.17).

For thin layers (up to the 30% of the half-thickness), I_0 can be determined by the series expansion of Eq. (5.60):

$$I = I_0\left(1 - \frac{1}{2}\mu d\right) \tag{5.61}$$

In the method of constant specific activities, the characteristic properties of self-absorption (mass absorption coefficient and half-thickness) can be determined as follows. Samples with different thickness are produced from a substance having the same specific activity. In this case, the intensity of a unit thickness is defined as I_0 (its dimension is intensity/surface density). The intensity reaching the surface decreases because of the absorption as described by the radiation absorption law (Eq. (5.48)): $I_0 \exp(-\mu d)$. The total intensity reaching the surface is:

$$I = \int_0^d I_0 \exp(-\mu x)\mathrm{d}x = \frac{I_0}{\mu}[1 - \exp(-\mu d)] \tag{5.62}$$

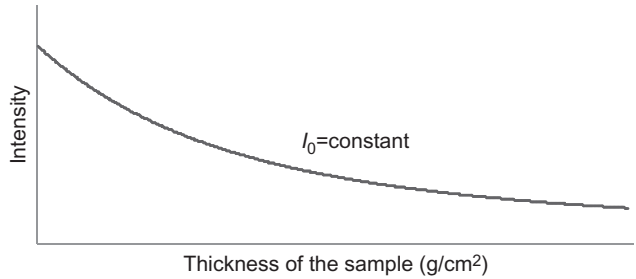

Figure 5.17 Intensity as a function of the thickness of a sample in cases of constant total activity.

Since

$$\frac{I_0}{\mu} = \text{constant} = I_\infty \tag{5.63}$$

from Eq. (5.62), we obtain the following:

$$I = I_\infty [1 - \exp(-\mu d)] \tag{5.64}$$

where I_∞ is the intensity at the saturation thickness. This is the maximal intensity, which does not increase even if the thickness increases. The intensity as a function of the thickness is shown in Figure 5.18.

In the method of constant specific activities, the half-thickness can be defined ($d_{1/2}$) as:

$$d_{1/2} = \frac{\ln 2}{\mu} \tag{5.65}$$

The half-thickness can be determined from Eq. (5.64) graphically or by a parameter-estimating computer program.

The method of constant specific activities can be used if the thickness is at least 7−10 times greater than the half-thickness. In this case, the specific intensities of the samples can be compared since they are proportional to the radioactivity.

5.3.6 Backscattering of Beta Radiation

The beta particles may scatter both on the orbital electrons and in the nuclear field. Since the beta particles are much lighter than the alpha particles, the degree of the scattering of the beta particles is much higher than that of the alpha particles, resulting in very important measuring and analytical consequences.

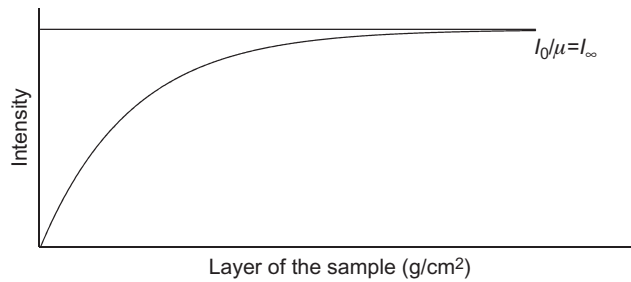

Figure 5.18 Intensity as a function of thickness in the method of constant specific activities.

The backscattering of the beta radiation as a function of the thickness of the scattering medium can be described as follows. Let us take a beta emitter on the bottom of a ring of lead-shielding, and a scattering medium with d thickness and arrange them as illustrated in Figure 5.19.

Then let us irradiate the surface area (F) of the medium with a beta radiation with I_0 intensity. Because of the absorption of the beta radiation, the intensity decreases when passed through a distance x, and the intensity reaching the dx unit thickness is:

$$\mathrm{d}I_x = I_0\, \mathrm{e}^{-\mu x} \tag{5.66}$$

Let ν be the ratio of beta particles that are backscattered from the dx thickness:

$$\nu\, \mathrm{d}I_x\, \mathrm{d}x = \nu\, I_0\, \mathrm{e}^{-\mu x}\, \mathrm{d}x \tag{5.67}$$

The backscattered beta particles are absorbed again when returned through the x thickness. Therefore, the intensity of the backscattered beta particles reaching the surface (F) can be expressed again by the absorption law. The energy of the backscattered beta particles may be lower than the energy of the original beta particles, so the values of the mass absorption coefficients may be different when the beta particles pass in (μ_{in}) or out (μ_{out}). In backscattering studies, the resultant effect of the two mass absorption coefficients is observed, so we can assume that $\mu_{\mathrm{in}} + \mu_{\mathrm{out}} = \mu_{\mathrm{b}}$:

$$\mathrm{d}I = \nu I_0\, \mathrm{e}^{-(\mu_{\mathrm{in}}+\mu_{\mathrm{out}})x}\, \mathrm{d}x = \nu I_0\, \mathrm{e}^{-\mu_{\mathrm{b}}x}\, \mathrm{d}x \tag{5.68}$$

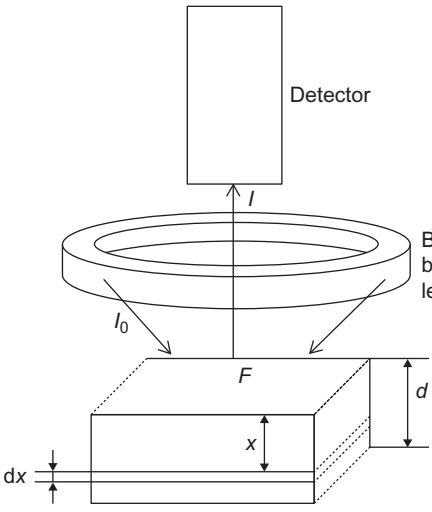

Figure 5.19 Study of backscattering of beta radiation.

The total backscattered intensity can be obtained by the integration of Eq. (5.68) for the total thickness (d):

$$I = \int_0^d \mathrm{d}I = \frac{\nu}{\mu_\mathrm{b}} I_0 \left[1 - \mathrm{e}^{-\mu_\mathrm{b} d}\right] \tag{5.69}$$

As seen from Eq. (5.69), the backscattered intensity tends to a limit as a function of the thickness. This limit for the infinite thickness of the sample is:

$$I_\infty = I_0 \frac{\nu}{\mu_\mathrm{b}} \tag{5.70}$$

The backscattering of beta radiation can be characterized by the backscattering coefficient (Rf):

$$Rf = \frac{I_\infty}{I_0} \tag{5.71}$$

Rf can also be expressed in percent.

The energy of the backscattered beta particles is less than the energy of the original particles (Figure 5.20).

Similar to Eq. (5.65), the half-thickness of the backscattered beta radiation can be defined. The backscattered intensity of beta radiation of aluminum, zinc, and lead is shown in Figure 5.21 as a function of the half-thickness. As seen, the backscattered intensity depends on the atomic number of the scattering media.

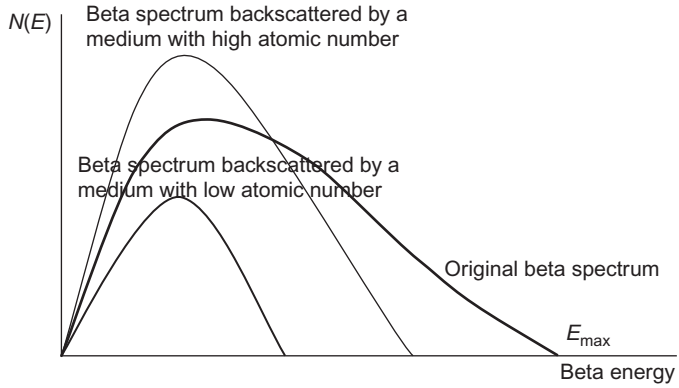

Figure 5.20 The energy of the backscattered beta particles for different scattering media.

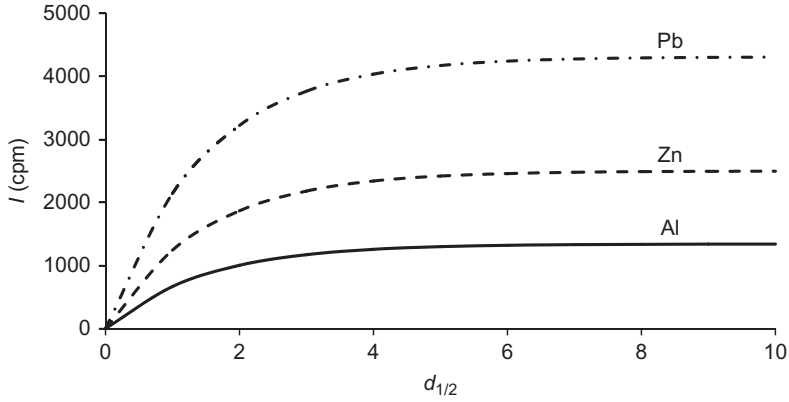

Figure 5.21 Backscattered intensity of beta radiation of aluminum, copper, and lead as a function of half-thickness.

Table 5.5 Constants of the Müller Formula for Backscattering of Beta Radiation

Period	*Z*	*a*	*b*	*R*
II	2–10	1.2311	−2.157	0.3–10.2
III	10–18	0.96731	0.476	10.2–17.9
IV	18–36	0.68582	5.556	17.9–30.3
V	36–54	0.34988	17.664	30.3–36.6
VI	54–86	0.26225	22.396	36.6–45

Source: Adapted from Müller (1957), with permission from the American Chemical Society.

The values of *Rf* and the atomic number (*Z*) are in strict correlation. The backscattered intensity, or *Rf* versus *Z* function, cannot be calculated exactly; empirical correlations are usually applied. One of them is as follows:

$$I_{\infty\omega} = k_1 Z^{k_2} \tag{5.72}$$

where $I_{\infty\omega}$ is the scattered intensity at an angle, $k_1 = 0.0415\ I_{\infty\omega}/2\pi$ and $k_2 = 2/3$.

Another *Rf* versus *Z* function is the so-called Müller formula:

$$R = aZ + b \tag{5.73}$$

where *a* and *b* are constants for the elements in a given period of the periodic table (Table 5.5). Hydrogen is a special element; it can be fitted into the system by a hypothetical atomic number, which is −7.434. This can be explained by the fact that the ratio of nucleons to electrons is usually 2, while in the case of hydrogen, this ratio is only 1.

Equations (5.73) and (5.74) are also valid for compounds and mixtures if the mean atomic number is applied. The mean atomic number can be defined as:

$$\overline{Z} = \frac{\sum_{i=1}^{n} n_i A_i Z_i}{\sum_{i=1}^{n} n_i A_i} = \sum_{i=1}^{n} x_i Z_i \tag{5.74}$$

where Z_i is the atomic number of the constituents, n_i is the number of the atoms, A_i is the mass of the atoms, and x_i is the mass ratio of the ith atom in the compound or mixture.

Equations (5.73) and (5.74) can also be applied for solutions; the Rf versus x_i function is linear. Therefore, the Rf versus x_i function is suitable for the concentration measurement of solutions. In addition, by extrapolating the Rf versus x_i function to $x_i = 1$, the backscattering coefficient (Rf) of the pure solid substance is obtained.

In conclusion, the measurements of the backscattered intensities of beta radiation give information on:

1. The thickness of the scattering matter or the thickness of thin layers on a thick plate (Section 11.3.4).
2. The mean atomic number.
3. The concentration of solutions.

5.4 Interaction of Gamma Radiation with Matter

The gamma radiation (gamma photon) is very different from alpha and beta radiation. The most important difference is that it has no charge or mass. It forms during the transition of nucleons between the shells in the nuclei, and their energy is in a very broad range. As discussed previously, the gamma photons are always emitted from the nuclei, whereas the photons emitted by the inner electron orbitals are called "X-ray photons." However, both gamma and X-ray radiations are electromagnetic radiation, so their interactions with matter can be treated together.

The gamma and X-ray photons usually have intermediate interactions with matter. The interactions are summarized in Table 5.6 and Figure 5.22. The dominant type of the interaction is strongly affected by the energy of gamma photons. Depending on the energy, the gamma photos can interact with the orbital electrons, the nuclear field, and the nucleus. The cross section of the interactions (the absorption coefficient, in other words) also depends on the atomic number of the substance.

It is important to emphasize that one of the most important interactions is the scattering of the gamma photons. Depending on the energy, different scattering phenomena can be observed, namely, Rayleigh, Thompson, and Compton

Table 5.6 Interaction of gamma (X-ray) Radiation with Matter

Reacting Particles and Fields	Absorption	Scattering	
		Elastic/Coherent	**Inelastic/ Incoherent**
Orbital electron	Photoelectric effect $\sigma \sim Z^4$	Rayleigh scattering $\sigma \sim Z^2$ Thomson scattering $\sigma \sim Z$	Compton scattering $\sigma \sim Z$
Nuclear field	Pair formation $\sigma \sim Z^2$		
Nucleus	Nuclear reaction with gamma photon (γ,n); (γ,p) $\sigma \sim Z$ Resonance absorption, Mössbauer effect	(γ,γ) nuclear reaction $\sigma \sim Z$	(γ,γ') nuclear reaction

Source: Adapted from Kiss and Vértes (1979), with permission from Akadémiai Kiadó.

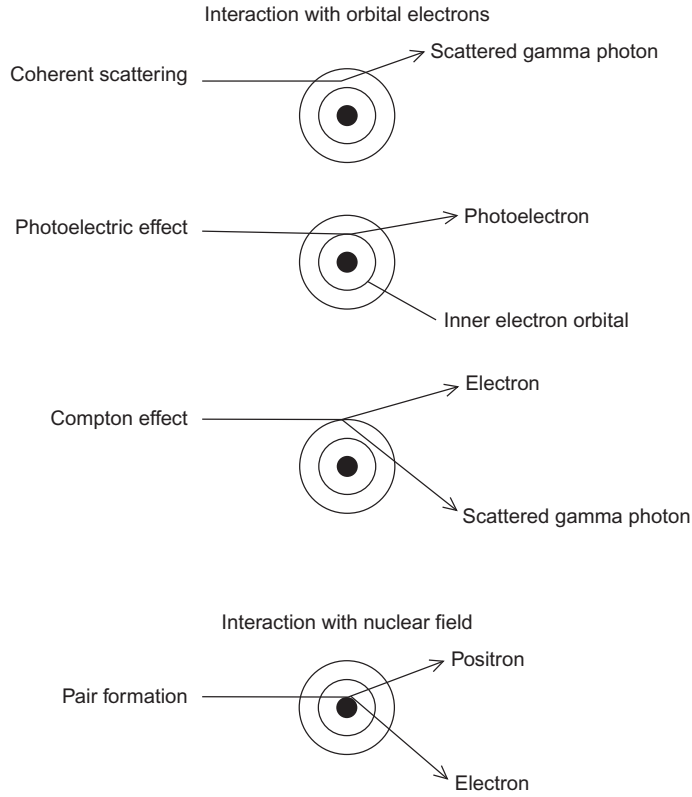

Figure 5.22 Interactions of gamma photons with the different constituents of matter.
Source: Reprinted from Choppin and Rydberg (1980), with permission from Elsevier.

scattering in the interaction with the orbital electrons, and the (γ,γ) and (γ,γ') nuclear reactions in the nuclei. In addition, gamma photons do not cause direct ionization; only the secondary electrons forming in the interactions of gamma radiation with matter can produce ions.

5.4.1 Rayleigh Scattering

At gamma energy below ~100 keV, the gamma photons are scattered on heavy elements (or their compounds) at small angles. The electromagnetic field of the gamma radiation polarizes the orbital electrons (i.e., induces dipoles), resulting in the emission of secondary radiation in the total space (in 4π spatial angle). The wavelength of the scattered radiation remains the same, i.e., the scattering is elastic or coherent.

5.4.2 Thomson Scattering

Thompson scattering can be observed in the case of both X-ray and gamma radiation. The wavelength of the scattered radiation does not change (elastic scattering). The phenomenon, similarly to Rayleigh scattering, has been interpreted by J.J. Thomson, using the classical theory of the scattering of electromagnetic radiation. The Rayleigh and Thomson scattering show differences in the cross section versus atomic number function (Table 5.6).

5.4.3 Compton Scattering

The classical theory of the scattering of electromagnetic radiation is valid only when $h\nu \ll mc^2$, i.e., at small energies. At higher energies, the wavelength of the scattered radiation changes: the frequency of gamma photons decreases, meaning that gamma energy is lost. This is called "inelastic" or "incoherent" scattering. This process was first studied by Compton.

The process is interpreted as follows. The gamma photons with $h\nu$ energy encounter an electron. By inelastic collision, part of their energy is transferred to the electron and the direction of the pathway of the gamma photon changes. The process can be described quantitatively by assuming a coordinate system, the x-axis of which is the direction of the pathway of the gamma photon; the y-axis is perpendicular to the x-axis. The electron is placed where the axes intersect, in the origin (Figure 5.23). The energy of the gamma photon before and after the collision with the electron is $h\nu$ or $h\nu'$. The energy of the electron before and after the collision is m_0c^2 and mc^2, respectively. m_0 is the rest mass of the electron; m is the mass of the moving electron. Before the collision, the momentum of the gamma photon is $h\nu/c$ in the direction of the x-axis, and zero in the direction of the y-axis. The momentum of the electron before the collision is equal to zero in both directions of the coordinate system. After the collision, the electron gains momentum, which is $p_e \cos\varphi$ in the direction of the x-axis and $p_e \sin\varphi$ in the direction of the y-axis.

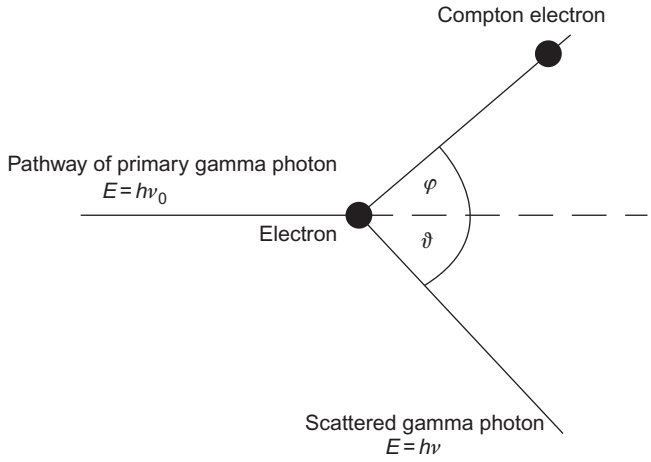

Figure 5.23 Compton scattering.

By applying the conservation of energies and momentums for the collision of the electron and the gamma photon, we can define the equations as follows:

$$h\nu_0 = h\nu + E_c \tag{5.75}$$

$$\frac{h\nu_0}{c} = \frac{h\nu}{c}\cos\vartheta + p_e \cos\varphi \tag{5.76}$$

$$0 = \frac{h\nu}{c}\sin\vartheta - p_e \sin\varphi \tag{5.77}$$

$$E_c = mc^2 - m_0c^2 \tag{5.78}$$

The relation between the rest mass of the electron and the mass of the moving electrons (m_0 and m) is:

$$m = \frac{m_0}{\sqrt{1 - \frac{v^2}{c^2}}} \tag{5.79}$$

where c is the velocity of light in a vacuum, and v is the velocity of the electron. By substituting Eq. (5.79) into Eq. (5.78), we obtain:

$$E_c = m_0c^2\left(\frac{1}{\sqrt{1 - \frac{v^2}{c^2}}} - 1\right) \tag{5.80}$$

The momentum of the electron (p_e) can be expressed as:

$$p_e = mv = \frac{m_0 v}{\sqrt{1-\frac{v^2}{c^2}}} = \frac{m_0 c \frac{v}{c}}{\sqrt{1-\frac{v^2}{c^2}}} \tag{5.81}$$

The momentum of the electron (p_e) can also be expressed from Eqs. (5.76) and (5.77):

$$p_e^2 = \left(\frac{h\nu_0}{c}\right)^2 + \left(\frac{h\nu}{c}\right)^2 - 2\left(\frac{h\nu_0}{c}\right)\left(\frac{h\nu}{c}\right)\cos\vartheta \tag{5.82}$$

In addition, p_e^2 can be obtained by means of Eqs. (5.78), (5.80), and (5.81), using $E = h\nu$. By equivalent mathematical transformation, we obtain the following:

$$\left(\frac{h\nu_0}{m_0c^2}\right) + \left(\frac{h\nu}{m_0c^2}\right) - 2\frac{h\nu_0 h\nu}{(m_0c^2)^2}\cos\vartheta = \left(\frac{h\nu_0}{m_0c^2} - \frac{h\nu}{m_0c^2} + 1\right) - 1 \tag{5.83}$$

and

$$\nu_0 - \nu = \frac{h\nu_0\nu}{m_0c^2}(1-\cos\vartheta) \tag{5.84}$$

By multiplying Eq. (5.84) by the Planck constant (h), we obtain the following:

$$h\nu_0 - h\nu = \frac{h\nu_0 h\nu}{m_0c^2}(1-\cos\vartheta) = E_0 - E = \frac{E_0 E}{0.51}(1-\cos\vartheta) \tag{5.85}$$

In this equation, m_0c^2 means the energy equivalent of the rest mass of the electron; i.e., 0.51 MeV.

The change of the energy of the primary gamma photon can be obtained using Eq. (5.85):

$$\Delta E = \frac{E_0^2(1-\cos\vartheta)}{E_0(1-\cos\vartheta)+0.51} \tag{5.86}$$

As seen from Eq. (5.86), the energy of the photon as a result of Compton scattering depends on the energy of the primary photon ($h\nu_0$) and on the angle. The highest change of the gamma energy can be observed at 180°; the energy does not change at 0° (no scattering). Compton scattering has an important effect on the gamma spectra (see Section 14.2.1 and Figure 14.5).

5.4.4 The Photoelectric Effect

The gamma photons can transfer energy to the orbital electrons. The electron is emitted as a photoelectron of a certain kinetic energy:

$$E_k = h\nu_0 - E_b \tag{5.87}$$

where E_k is the kinetic energy of the photoelectron, E_b is the binding energy of the electron, and $h\nu_0$ is the energy of the gamma photon before the interaction. Because of the great differences between the masses of the atom and the emitted electron, the energy of recoiling can be ignored in Eq. (5.87). The process is called the "photoelectric effect"; it can be observed when the energy of the gamma photon is similar to the binding energy of the electron. For this reason, high-energy gamma photons usually do not induce the photoelectric effect. The low-energy gamma photons have an energy that is closest to the binding energy of the K and L electrons, so the emission of photoelectrons from the K and L orbitals is the most likely.

The emission of the photoelectron results in the formation of an excited electron state because when one electron is missing from the inner shell of the atom, a vacancy is formed. This excited state can relax in two ways. One way is that an electron in outer orbitals moves into the inner orbital to fill the vacancy, emitting the excess energy between the orbitals as a characteristic X-ray photon. The wave number of the X-ray photon (ν^*) can be calculated by the Moseley law:

$$\nu^* = Ry(Z-1)^2\left(\frac{1}{n^2} - \frac{1}{m^2}\right) \tag{5.88}$$

where Ry is the Rydberg constant, Z is the atomic number, and n and m are the main quantum numbers of the electron orbitals. This process forms the basis of the X-ray fluorescence analysis.

The other way is the emission of low-energy Auger electrons (as discussed in Section 4.4.3). This process is called the Auger effect (Figure 5.24). For light elements, the emission of Auger electrons is the preferred result, while in the case of heavier elements, the emission of X-ray photons is more preferable. The two processes, the emission of X-ray photons and Auger electrons, continue until the atom reaches its ground-state energy. All the photoelectrons, Auger electrons, and X-ray photons intensively ionize the atoms of the absorber. This is a secondary ionization effect.

The cross section of the photoelectric effect (σ_f), or the absorption coefficient of the photoelectronic effect (μ_f), can be given by a rude empirical formula:

$$\sigma_f = \text{constant}\frac{Z^{4.1}}{E_\gamma^3} \tag{5.89}$$

where E_γ is the energy of the gamma and X-ray photons. Equation (5.89) expresses the fact that the probability of the emission of photoelectrons increases as the atomic number increases and the energy of the gamma photons decreases.

The photoelectric effect produces photoelectrons, characteristic X-ray photons, and Auger electrons. The measurements of the energy and intensity of these radiations are used in different analytical techniques. The measurement of the photoelectrons gives information on the chemical environment of the atoms in a substance (high-resolution beta spectroscopy or photoelectron spectroscopy). The quality and

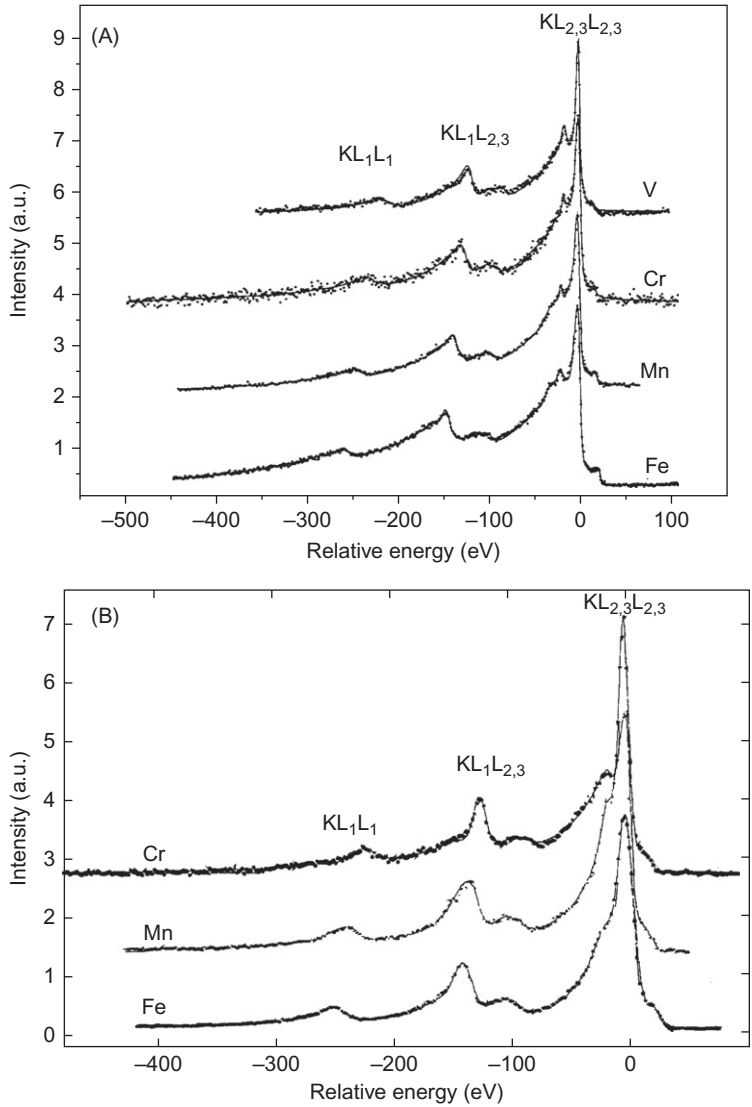

Figure 5.24 (A) Comparison of the measured photoexcited V, Cr, Mn, and Fe KLL Auger spectra. (B) Comparison of the Cr, Mn, and Fe KLL Auger spectra obtained following electron capture. The sign KLL means that the photoelectric effect produces the vacancy on the K shell, it is filled from the L shell, and the Auger electron also is emitted from the L shell. The indexes 1−3 mean the subshells of the L shell. (Thanks to Dr. László Kövér, Institute of Nuclear Research, Hungarian Academy of Sciences, Debrecen, Hungary, for the figure.)
Source: Reprinted from Némethy et al. (1996), with permission from Elsevier.

quantity of the elements of a substance can be determined by the measurement of the characteristic X-ray photons (X-ray fluorescence spectroscopy, as discussed in Section 10.2.3.1). Auger electron spectroscopy (AES) can be used for the analysis of surface layers.

5.4.5 Pair Formation

When the energy of the gamma photon ($h\nu$) is higher than the energy equivalent with the rest mass of two electrons ($2m_0c^2$), the gamma photon can transform into an electron and a positron when it passes the nuclear field. This process is called "pair formation," the reverse process of annihilation (as discussed in Section 5.3.3). On the basis of the conservation of energy:

$$h\nu = m_0c^2 + E_{e^-} + m_0c^2 + E_{e^+} \tag{5.90}$$

where E_{e^-} and E_{e^+} are the kinetic energy of the electron and the positron, respectively.

The cross section of the pair formation can be described as:

$$\sigma_p = KZ^2 f(E_\gamma) \tag{5.91}$$

where $f(E_\gamma)$ is a factor depending on the energy of the gamma radiation, Z is the atomic number of the interacting substance (absorber), and K is constant. As seen, the cross section of the pair formation increases as the gamma energy and the atomic number increase.

5.4.6 Total Absorption of Gamma Radiation

In the previous sections (Sections 5.4.1–5.4.5), the different interactions (namely, coherent and incoherent scattering), photoelectric effect, and pair formation of the gamma radiation have been discussed. As seen, the cross sections, or the absorption coefficients of all these interactions depends on the energy of gamma radiation and the atomic number of the absorber. The cross sections versus energy or atomic number functions are significantly different for the different processes. The total absorption of the gamma radiation is the sum of the different interactions, expressed by the cross sections:

$$\mu = \mu_{\text{Rayleigh}} + \mu_{\text{Thomson}} + \mu_{\text{photoelectric}} + \mu_{\text{Compton}} + \mu_{\text{pair}} \tag{5.92}$$

The absorption law (Eq. (5.3)) for the gamma radiation can be expressed as:

$$I = I_0\, e^{-\mu x} \tag{5.93}$$

Equation (5.93) can be transformed to mass absorption coefficients, as is done in the case of beta radiation (see Section 5.3.4).

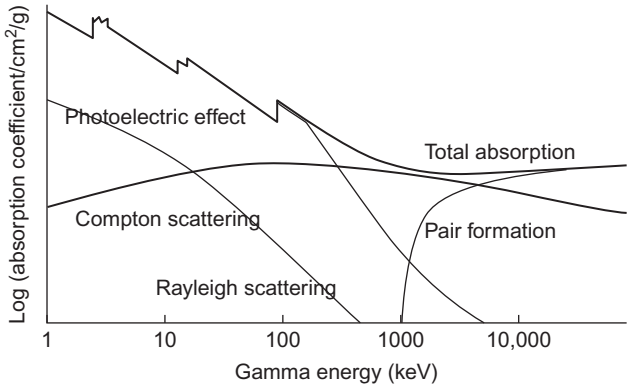

Figure 5.25 The scheme of the total absorption of gamma radiation as a function of gamma energy.

The scheme of the total absorption of gamma radiation as a function of the gamma energy is shown in Figure 5.25.

As seen in Figure 5.25, the mass absorption coefficients of the individual interactions show the range of gamma energy that is characteristic of the given interaction. The mass absorption coefficient of the total absorption (μ) as a function of gamma energy shows a minimum: the mass absorption coefficient decreases until the gamma energy exceeds 1.02 MeV; it is the start of the pair formation.

In Figure 5.26, the mass absorption coefficient for different gamma energies as a function of the atomic number of the absorbers is shown.

5.4.7 Resonance Absorption of Nuclei and the Mössbauer Effect

As discussed in Chapter 2, the nucleons can be in different energy states in the nucleus (see the explanation of the shell model in Section 2.2.2). Therefore, the nucleons may be in excited states as a result of different nuclear processes. The excitation energy can produce the emission of a nucleon or radiation. The emission of a nucleon takes place in the nuclear reactions (Chapter 6), for example, in the (γ,n) nuclear reactions. As discussed in Section 4.4.6, the nuclei of the daughter nuclides can be in an excited state due to a radioactive decay. The excited nucleus may return to a lower excited state or ground state, emitting gamma photons with a characteristic energy.

The gamma photons can excite another nucleus. The cross section of this excitation process may be high when the energy of the gamma photon and the excitation energy of the nucleons are very close, for example, when the structure of the emitting and absorbing nuclei is similar, such as in the case of isobars, isotopes, or isoton nuclei. This process is called "nuclear resonance absorption."

At first sight, the resonance absorption seems to be simple. However, the recoil of the nuclei during the emission and absorption reduces the energy of the gamma

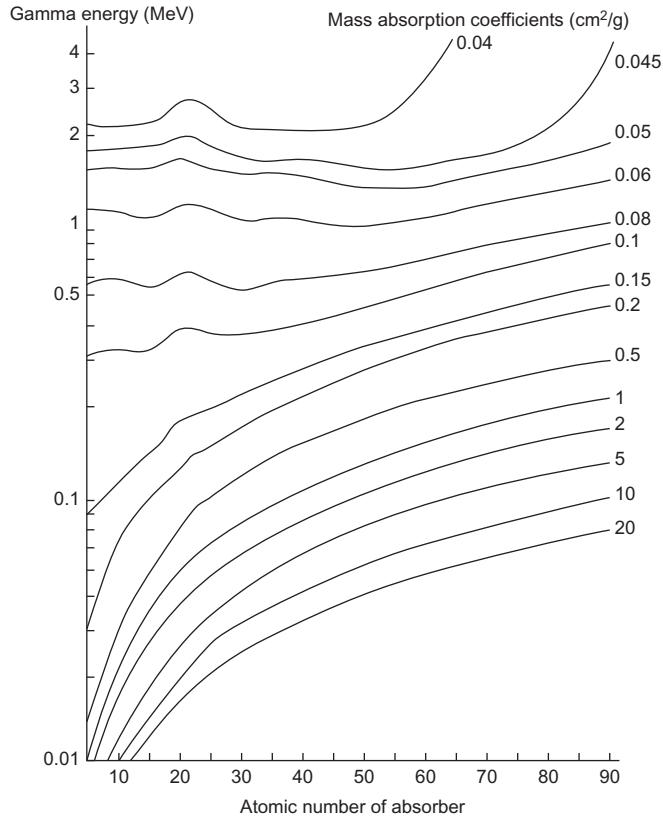

Figure 5.26 The mass absorption coefficient for different gamma energies as a function of the atomic number of the absorbers.

photons (E_0). The loss of energy (E_R) can be calculated using the principle of the conservation of momentum:

$$-Mv = \frac{E_0}{c} \tag{5.94}$$

where M is the mass of the nucleus, v is the velocity of the nucleus after the emission of the gamma photon, and c is the velocity of light in a vacuum. By expressing the velocity of the nucleus after the emission of gamma photon, we obtain:

$$v = -\frac{E_0}{Mc} \tag{5.95}$$

The kinetic energy of the recoiled nucleus can be given as:

$$E_R = \frac{1}{2}Mv^2 = \frac{E_0^2}{2Mc^2} \tag{5.96}$$

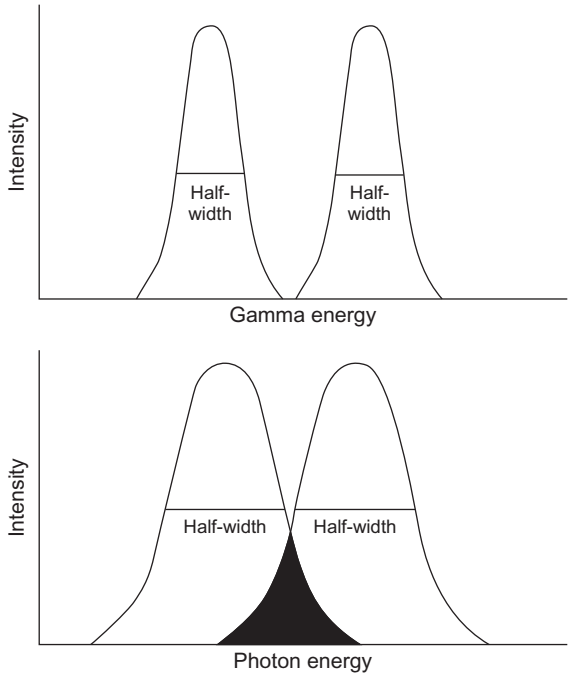

Figure 5.27 Overlapping of absorption (left) and emission (right) photons. (A) In the case of gamma radiations, the lines do not overlap because of the high energy of recoil. (B) The overlapping of the emission and absorption lines at electron transmissions (optical spectra).

Besides the energy loss at the emission, gamma photons lose energy again when absorbed in the nucleus of the absorber. Therefore, the energy of the gamma photon (E) after the absorption is:

$$E = E_0 - 2E_R \tag{5.97}$$

As a result of the recoils of the two nuclei, the gamma photon does not have enough energy to excite the nucleus of the absorber. However, resonance absorption can take place even if the gamma lines are so broad that the emission and absorption lines overlap (Figure 5.27).

The natural width of the lines (Γ) can be calculated by the Heisenberg uncertainty principle:

$$\Gamma\tau = \frac{h}{2\pi} \tag{5.98}$$

where τ is the lifetime of the excited state. In nuclear processes, this lifetime is about 10^{-9}–10^{-7} s, so the natural line width is very small (Figure 5.27, A). Furthermore, the atoms that are emitting radiation have different velocities because of the thermal movement. So, the frequency of each emitted photons (ν) is shifted by the Doppler effect, depending on the velocity (v) of the atom relative to the observer:

$$\nu = \nu_0\left(1 \pm \frac{v}{c}\right) \tag{5.99}$$

where ν_0 is the frequency of the gamma photons when there is no difference in the velocities. Therefore, there is still some possibility of resonance absorption. As the temperature increases, the line width and the probability of the resonance absorption increase.

^{191}Os isotope (half-life, 15 days) emits beta particles, producing an ^{191m}Ir isotope. This excited nuclide falls into its ground state (^{191}Ir) in 4.9 s, emitting gamma photons with 129 keV energy. Meantime, the nuclear spin decreases from +5/2 to +3/2. Mössbauer performed absorption experiments with this gamma radiation and iridium foil in 1958 and discovered the recoil-free resonance absorption of nuclei. Because he wanted to avoid resonance absorption, he did the experiments at very low temperatures. The unexpected result was that the resonance absorption increased enormously. At the first approximation, it is interpreted by the increased rigidity of the structure of the crystal lattice at low temperatures; i.e., the whole crystal can be considered to be a "recoiled atom." So, the mass of the crystal can be substituted as M into Eqs. (5.95) and (5.96). As a result, the velocity and the energy of the recoiled atom will be negligible.

The recoil-free resonance absorption of nuclei can be used in the study of chemical states because the oxidation state and the chemical environment influence the energy state of the nucleus via the electrostatic interactions between the electrons and the nucleus. This change, called an "isomer shift" or a "chemical shift," is by 7−8 orders of magnitude smaller than the characteristic energies of the nuclear processes. Therefore, a very small change of the very high energies has to be measured. The isomer shift is measured using the Doppler effect: the resonance absorption is created by the relative movement of the sample (absorber) and the gamma radiation source. The relative velocity of the sample and the radiation source corresponds to the degree of the isomer shift, and its dimension is measured in cm/s or mm/s (for example). This small velocity correlates with the small differences of the gamma energies caused by the different oxidation state or chemical environment of the Mössbauer nuclide in the absorber. The most important Mössbauer nuclides are ^{57}Fe, ^{119}Sn, ^{121}Sb, ^{151}Eu, ^{191}Ir, ^{195}Pt, ^{197}Au, and ^{237}Np.

The practical importance of the Mössbauer effect comes from the fact that one of the natural isotopes of iron, Fe-57 isotope, is a Mössbauer nuclide. The gamma radiation source is Co-57 (with a half-life of 9 months), the gamma radiation of 0.0144 MeV of which can excite the Fe-57 isotope. The decay scheme of Co-57 is shown in Figure 5.28.

The isomer shift of the different oxidation states of iron is illustrated in Figure 5.29 by the example of Fe(III) and Fe(II) fluorides. Figure 5.30 shows the Mössbauer spectrum of clay containing iron species.

As seen in Figure 5.29, the iron(III) in FeF_3 is in a symmetrical environment and the electron configuration is $3d^5$, indicating high spin and the presentation of a singlet. The chemical environment of iron(II) in FeF_2 is asymmetrical, with $3d^6$ configuration. The asymmetrical environment interacts with the electric quadrupole moment of the nucleus, resulting in the presentation of a doublet. At low temperatures, an inner magnetic field is formed, causing magnetic splitting (the Zeeman effect) with a sextet in the spectrum.

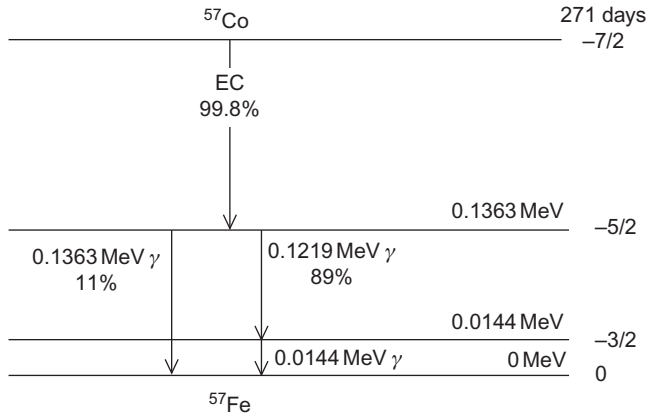

Figure 5.28 Decay scheme of Co-57.

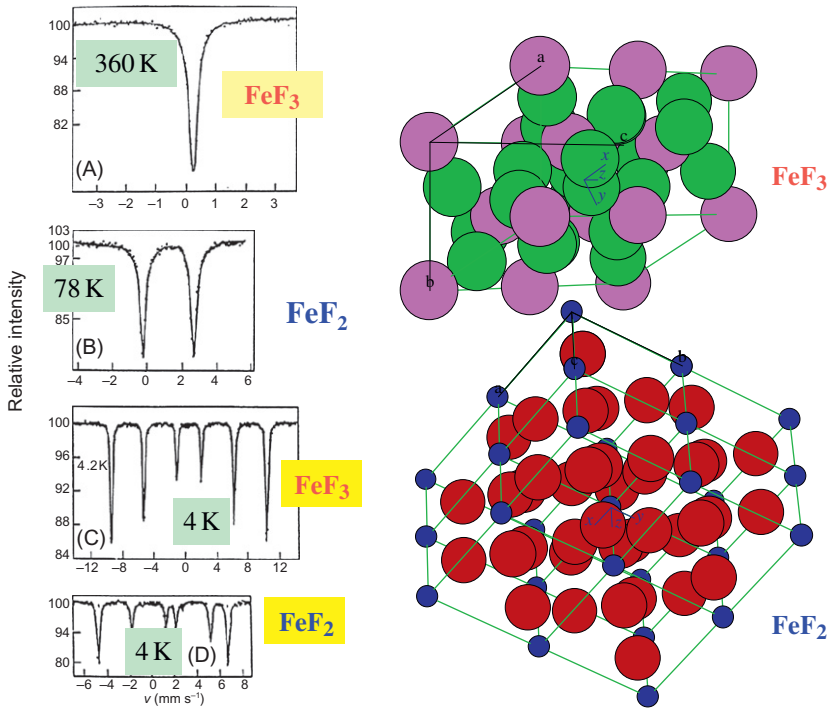

Figure 5.29 The Mössbauer spectrum of an iron(III) and iron(II) in fluorides spectrum. A: spectrum of iron(III) fluoride at 360 K; B: spectrum of iron (II) fluoride at 78 K; C: spectrum of iron(III) fluoride at 4.2 K; D: spectrum of iron(II) fluoride at 4 K. (Thanks to Prof. Ernő Kuzmann, Chemical Research Center, Budapest, Hungary, for the picture.)

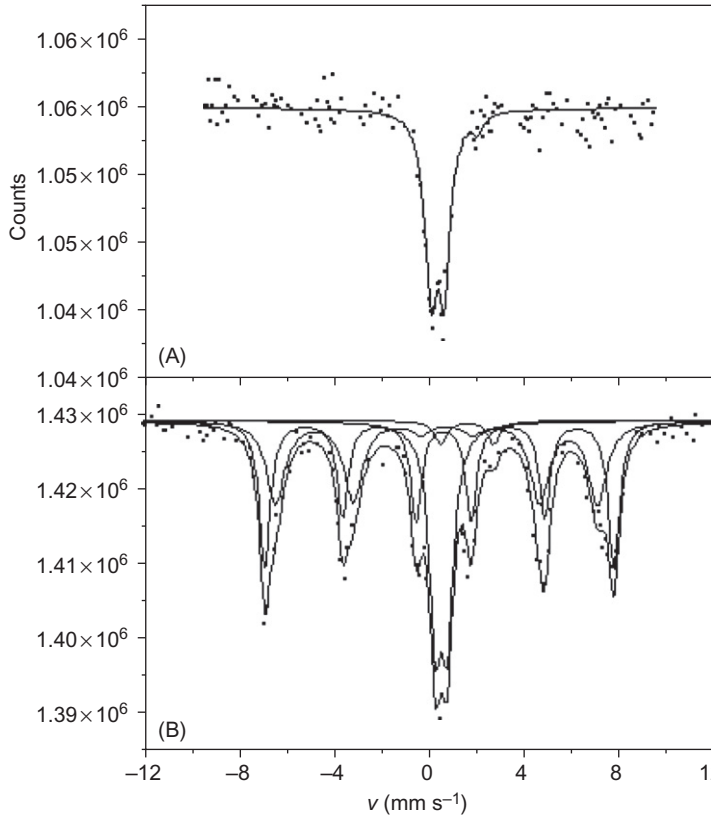

Figure 5.30 The Mössbauer spectrum of Bentonite clay at 74 K before (A) and after (B) treatment with $FeCl_3$ solved in acetones. (A) shows the +2 and +3 oxidation states of iron in Bentonite. The sextet in (B) refers to the formation of a magnetic phase.
Source: Reprinted from Komlósi et al. (2006), with permission from Springer.

Figure 5.30 illustrates the Mössbauer spectrum of bentonite clay at 74 K before (A) and after (B) treatment with $FeCl_3$ solved in acetones. Segment (A) shows the +2 and +3 oxidation states of iron in bentonite. The sextet in Figure 5.30B refers to the formation of a magnetic phase.

5.5 Interaction of Neutrons with Matter

As mentioned several times previously (Chapter 2), the neutrons are the basic particles of nuclei. They can be present as free neutrons as a result of neutron decay (see Section 4.4), but it is a very rare phenomenon. Neutrons, however, can be produced by nuclear reactions (Chapter 6) and can be widely used in different scientific and practical applications. Thus, in this chapter, the basic concepts of the interactions of neutrons with matter will be discussed.

5.5.1 Discovery of Neutrons

Since neutrons have no charge, detecting them is difficult. For this reason, neutrons were discovered relatively late, although Rutherford had postulated their existence in 1920.

In 1930, during the study of the energy levels of nuclei, Bothe and Becker irradiated beryllium with alpha particles and observed the emission of radiation with a very long range and high energy (5 MeV). Since the energy levels of nuclei were studied, the emitted radiation was supposed to be gamma radiation of beryllium. This experiment was repeated in 1932 by Irene Curie and Frederic Joliot-Curie; however, they detected the emitted radiation by other techniques and found that the energy of the radiation was much higher than what was given by Bothe and Becker. Similarly, Chadwick measured energy readings that were as high as 50 MeV. As a consequence, Chadwick stated that if the energy of the "gamma" radiation of the beryllium depends on the detection method, it cannot be "gamma" radiation, or at least another particle must be emitted besides gamma radiation. In addition, Chadwick postulated that the long-range radiation should consist of neutral particles that transfer energy only by colliding with nuclei. These particles were called "neutrons."

Chadwick measured the rest masses of the neutrons by elastic collision with hydrogen and nitrogen nuclei and found that the ratio of the neutron to the hydrogen nucleus (proton) is about 1.1:1.

5.5.2 Production of Neutrons

Neutrons can be produced in different ways:

- In neutron sources.
- In neutron generators.
- In nuclear reactors.
- By nuclear spallation.

In neutron sources, neutrons are mostly produced by (α,n) nuclear reactions (as discussed in Section 6.2.3). The alpha particles are obtained from an alpha emitter radioactive isotope such as Ra-226, Pu-239, or Po-210. These isotopes are mixed with a light element (the binding energy of neutron is relatively low), mainly by beryllium. The neutrons are produced in the reaction as follows:

$$^{9}\mathrm{Be}(\alpha, \mathrm{n})^{12}\mathrm{C} \tag{5.100}$$

The neutron yield of these neutron sources is 10^6-10^8 neutrons/s.

The radium–beryllium (RaBe) neutron source has undesirably high gamma radiation, and therefore it is no longer used.

Neutrons can be produced by the spontaneous fission of ^{252}Cf. The yield of the commercial ^{252}Cf neutron sources is about 10^7-10^9 neutrons/s.

Neutrons can be produced by (γ,n) nuclear reactions (see Section 6.2.2). Gamma photons can initiate nuclear reactions if their energy is higher than the binding energy of the target nucleus. For example, the ^{24}Na isotope has high-energy gamma photons. The gamma photons can initiate nuclear reactions with deuterium, lithium, beryllium, and boron. For example:

$$\mathrm{Be}(\gamma, \mathrm{n})^{8}\mathrm{Be} \tag{5.101}$$

$$^{2}\mathrm{H} + \gamma \rightarrow \mathrm{n} + \mathrm{p}^{+} \tag{5.102}$$

Therefore, when a salt containing an ^{24}Na isotope is dissolved in heavy water (D_2O), a mobile neutron source can be produced (as described in Section 6.2.2).

In neutron generators, the isotopes of hydrogen are used in nuclear reactions. Mostly deuterium, tritium nuclei, or the mixture of these nuclei are accelerated in linear accelerators, and the metal hydride target containing deuterium, tritium, or both is bombarded by the accelerated nuclei. The nuclear reactions (described further in Section 6.2.4) are:

$$^{2}\mathrm{H} + {}^{3}\mathrm{H} \rightarrow {}^{4}\mathrm{He} + \mathrm{n} \tag{5.103}$$

$$^{2}\mathrm{H} + {}^{2}\mathrm{H} \rightarrow {}^{3}\mathrm{He} + \mathrm{n} \tag{5.104}$$

The energy of the neutrons produced in neutron generators is about 14 MeV. The yield of the neutron is about 10^8-10^9 neutrons/s.

Neutrons can be produced in cyclotrons by (p,n) nuclear reactions. For this reaction, lithium or beryllium is used as target material.

The neutron production in nuclear reactors will be discussed in detail in Section 6.2.1 and Chapter 7. Thus, it is not detailed here; we will just mention that in the fission reaction, high-energy gamma photons are also produced, which initiate the reaction (5.102). This reaction produces extra neutrons, which affects the neutron balance of the nuclear reactors.

The greatest neutron yields can be obtained by nuclear spallation. Spallation is a nuclear reaction in which photons or particles with high energy (e.g., protons with GeV) hit a nucleus, resulting in the emission of many other particles (such as neutrons or light nuclei) or photons. The target is a heavy element (e.g., mercury, tungsten, or lead). Recently, there are only a few spallation neutron sources all over the world.

The lifetime of free neutrons is short; they transform into protons, beta particles with 0.728 MeV, and antineutrinos.

$$^{1}_{0}\mathrm{n} \xrightarrow[10.25\ \mathrm{min}]{} {}^{1}_{1}\mathrm{p} + \beta^{-}_{0.782\ \mathrm{MeV}} + {}^{0}_{0}\overline{\nu} \tag{5.105}$$

The half-life of the reaction is 10.25 min.

5.5.3 Interaction of Neutrons with Matter

The most important characteristics of neutrons have been mentioned in previous chapters (Chapter 2); thus, they are summarized only briefly here. The rest mass of a neutron is 1.0086 amu, and it has no net charge. However, it consists of one up quark and two down quarks, so a neutron has magnetic momentum.

The de Broglie wavelength (Eq. (4.93)) of neutrons is about 10^{-10} m, which is in the range of the atoms. Therefore, neutrons can be applied for analytical purposes on a molecular scale.

Neutrons are classified according to their kinetic energy as follows:

- $\approx$ meV: cold neutrons
- $<$0.1 eV: thermal neutrons
- 0.1−100 eV: slow neutrons
- 100 eV−100 keV: neutrons with intermediate energies and epithermal neutrons
- $>$100 keV: fast neutrons.

The interaction of a neutron with matter is determined by the properties mentioned previously and the energy of the neutron. The most important interactions are summarized in Table 5.7.

As seen in Table 5.7, the important interactions of neutrons with matter are nuclear reactions and the scattering phenomena, including elastic and inelastic scattering. The tracks of protons thrown by neutrons emitted in a PuBe neutron sources are shown in Figure 5.31.

Having no charge, neutrons can be captured easily by the different atomic nuclei. All elements, except for helium, have isotopes reacting with neutrons. This is used for radionuclide productions (as discussed in Chapter 8). Some nuclei, such as boron, cadmium, and dysprosium, have an extremely high cross section for neutron captures. The nuclear reactions with neutrons will be discussed in detail in Section 6.2.1.

The neutrons play an essential role in the production of nuclear energy: the (n,f) reaction of ^{235}U is the basic reaction (see Chapter 7 for more detail). The inelastic scattering of neutrons causes the neutrons to lose energy, which is an essential

Table 5.7 Interactions of Neutrons with Matter

Reacting Particles and Fields	Changes	
	In Radiation	**In Matter**
Orbital electron	No interaction	
Magnetic field of unpaired electrons	Elastic scattering, inelastic scattering	Excitation or magnetic relaxation
Nuclear field	No interaction	
Nucleus	Nuclear reaction, elastic scattering, inelastic scattering	New nucleus, chemical change—excitation or magnetic relaxation

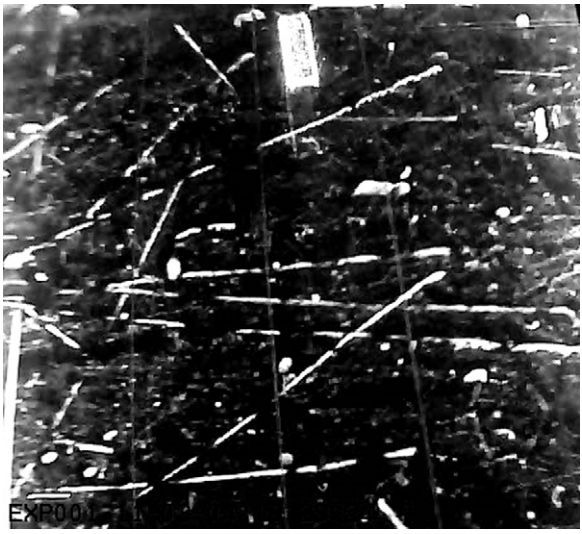

Figure 5.31 Cloud chamber photograph of the tracks of protons (long linear pathways) thrown by neutrons emitted in PuBe neutron source. The short thick lines are the pathways of alpha particles emitted by plutonium in the neutron source. (Thanks to Dr. Péter Raics, Department of Experimental Physics, University of Debrecen, Hungary, for the photograph.)

condition in the operation of nuclear reactors (see Table 7.2). The energy production reaction is regulated by nuclear reactions with a high cross section (as discussed in Section 7.1.1.6).

Neutrons can be applied in the different fields of natural sciences:

- In physics, the statistical physical systems, the magnetic structure, and dynamic of solids can be studied. The elementary particles composing neutrons (quarks, pions, and gluons) have significant effects on many physical properties of nuclei, such as radioactive decay, magnetic momentum, and electric dipole momentum.
- In material science, the substances used in magnetoelectronics (magnetic sensors, hard discs, spin valves, etc.) can be investigated. The imaging procedures, neutron radiography, and tomography are also important (see Section 10.2.2.3).
- In chemistry, each substance containing hydrogen can be studied. The transition between phases on a molecular scale (e.g., liquids and glasses) can be examined. Neutrons can assist in the molecular design and the production of materials with improved performance in the different fields of chemistry (nanocomposites, implants, drugs, catalysts, etc.). Neutrons are especially important in biological, biotechnological, and medical studies because the dynamics of the atoms and molecules and the changes in the structure of the biological molecules can be studied by neutron scattering methods (see Section 10.2.2.4).
- In energy production: the possibilities of the safe storage of hydrogen as an energy carrier (metal hydrides and ionic compounds of the lighter elements) can be studied by neutron scattering (see Section 10.2.2.4). In addition, a large portion of natural gas exists as methane−water clathrates in the shallow earth, which means that there are enormous energy resources. Methane, however, can release from the clathrate, increasing the greenhouse effect. For this reason, it is important to understand the structural and dynamical properties of these substances.
- In geology, the study of the structure and dynamics of minerals and magmas under the Earth's mantle can assist the causes that are responsible for geohazards such as earthquakes and volcanic eruptions.

- In archeology, neutron activation (see Section 10.2.2.1) and neutron scattering/diffraction (see Section 10.2.2.4) provide information on the chemical composition and technological procedures of ancient artifacts.

The analytical applications of the nuclear reaction and scattering of neutrons will be discussed in Section 10.2.2. The activation analytical methods are based on the nuclear reactions with the isotopes of all elements except helium. The scattering methods are based on the interaction of the neutrons with the nuclei and the magnetic field of matter, providing information on both the nuclei and the magnetic field.

Further Reading

Bothe, W. and Becker, A. (1930). Künstliche Erregung von Kern-Strahlen. *Z. Phys.* 66:289−306.

Chadwick, J. (1932). The existence of a neutron. *Proc. R. Soc. A* 136:692−708.

Choppin, G.R. and Rydberg, J. (1980). *Nuclear Chemistry, Theory and Applications*. Pergamon Press, Oxford.

Curie, I. and Joliot, F. (1932). The emission of high energy photons from hydrogenous substances irradiated with very penetrating alpha rays. *Comptes. Rendus.* 194:273−275.

Friedlander, G., Kennedy, J.W., Macias, E.S. and Miller, J.M. (1981). *Nuclear and Radiochemistry*. Wiley, New York, NY.

Haissinsky, M. (1964). *Nuclear Chemistry and its Applications*. Addison-Wesley, Reading, MA.

Kiss, I. and Vértes, A. (1979). *Magkémia (Nuclear Chemistry)*. Akadémiai Kiadó, Budapest, Hungary.

Komlósi, A., Kuzmann, E., Homonnay, Z., Nagy, N.M., Kubuki, S. and Kónya, J. (2006). Effect of $FeCl_3$ and aceton on the structure of Na-montmorillonite studied by Mössbauer and XRD measurements. *Hyperfine Interact.* 166:643−649.

Lagoutine, F., Ciursol, N. and Legrand, J. (1983). *Table de radionucleîdes*. Comissirait á l'Energie Atomique, France.

Lieser, K.H. (1997). *Nuclear and Radiochemistry*. Wiley-VCH, Berlin.

McKay, H.A.C. (1971). *Principles of Radiochemistry*. Butterworths, London.

Müller, R.H. (1957). Interaction of beta particles with matter. *Anal. Chem.* 29:969.

Némethy, A., Kövér, L., Cserny, I., Varga, D. and Barna, P.B. (1996). The KLL and KLM Auger spectra of 3d transition metals, Z=23–26. *J. Electron Spectrosc. Relat. Phenom.* 82:31−40.

Szilágyi, E., Petrik, P., Lohner, T., Koós, A.A., Fried, M. and Battistig, G. (2008). Oxidation of SiC investigated by ellipsometry and Rutherford backscattering spectrometry. *J. Appl. Phys.* 104:014903.